

# What Is the Covalency of Hydrogen Bonding?

Sławomir Janusz Grabowski<sup>\*,†,‡</sup>

<sup>†</sup>Kimika Fakultatea, Euskal Herriko Unibertsitatea and Donostia International Physics Center (DIPC) P.K. 1072, 20080 Donostia, Euskadi, Spain

<sup>‡</sup>IKERBASQUE, Basque Foundation for Science, 48011, Bilbao, Spain

## CONTENTS

1. Introduction	2597
2. Geometrical Parameters of Hydrogen Bonding	2598
3. Hydrogen-Bond Energy	2600
4. Quantum Theory of "Atoms in Molecules" in Analysis of Hydrogen Bonding	2604
5. Interrelations between QTAIM and the Interaction Energy Components	2611
6. Covalency of Different Types of Hydrogen Bonds	2614
7. Summary	2620
Author Information	2621
Biography	2621
Acknowledgment	2621
References	2621

## 1. INTRODUCTION

Hydrogen bonding is an important interaction playing a key role in chemical, physical, and biochemical processes.<sup>1–4</sup> One can mention numerous examples such as the role of hydrogen bonding in enzymatic catalysis,<sup>5,6</sup> arrangement of molecules in crystals,<sup>7,8</sup> crystal engineering,<sup>9</sup> proton transfer reactions,<sup>10,11</sup> and also its important role in life processes.<sup>12,13</sup> Hence, its nature is often the subject of investigations and polemics.

One of the first definitions of hydrogen bonding was formulated by Pauling who stated that<sup>14</sup> "under certain conditions an atom of hydrogen is attracted by rather strong forces to two atoms, instead of only one, so that it may be considered to be acting as a bond between them. This is called the hydrogen bond". Pauling also pointed out that the hydrogen atom is situated only between the most electronegative atoms and it usually interacts much stronger with one of them. The latter interaction is a typical covalent bond (A–H). The interaction between hydrogen and another electronegative atom is much weaker and mostly electrostatic in nature; it is a nonbonding interaction (H···B). This system is often designated as A–H···B where the B-center (acceptor of proton) should possess at least one lone electron pair;<sup>14</sup> A–H is called the proton-donating bond. Pauling stated that sometimes the H···B interaction possesses characteristics of the covalent bond. The [FHF]<sup>–</sup> ion is an example where the proton is inserted between two negative fluorine ions, accurately in the middle of the F···F distance. Hence, both H···F interactions are equivalent. This is in line with an early conclusion of Lewis that "an atom of hydrogen may at times be attached to two electron pairs of two different atoms"<sup>15</sup> and with the statement of Latimer and Rodebush that "the hydrogen nucleus held by two octets constitutes a

weak bond".<sup>16</sup> The latter statements correspond to recent studies on proton bound homodimers, that is, systems where the proton is inserted between two closed-shell moieties and where it often interacts equivalently with both of them. Chan and co-workers analyzed recently what factors determine whether the proton-bound homodimer has a symmetric or an asymmetric hydrogen bond.<sup>17</sup> In the other study, it is discussed what conditions should be fulfilled for the proton situated accurately in the midpoint of the donor–acceptor distance.<sup>18</sup> The high level calculations up to CCSD(T)/6-311++(3df,3pd)//CCSD/6-311++(3df,3pd) were performed on the [FHF]<sup>–</sup> ion and systems with O–H···O or N–H···N hydrogen bonds. The latter study is supported by the experimental X-ray and neutron diffraction data because there are numerous crystal structures with short O–H···O hydrogen bonds and the proton situated in the central position or nearly so.<sup>18</sup> Also recently, homogeneous and heterogeneous short and strong hydrogen bonds (SSHBs) as well as the proton bound homodimers were analyzed theoretically at MP2/aug-cc-pVDZ + diffuse(2s,2p) level.<sup>19</sup>

Among various topics, the matter was raised if hydrogen bonding is an electrostatic or covalent interaction.<sup>20,21</sup> The following question arises: what does the covalency of hydrogen bonding mean? The decomposition of the interaction energy is useful to analyze hydrogen bonding and particularly to answer the latter question. One of the first decomposition schemes introduced is one of Morokuma and Kitaura,<sup>22</sup> where the interaction energy is calculated within the Hartree–Fock one-electron approximation and it is decomposed into the following components: the exchange energy,  $E_{\text{EX}}$  (arising from repulsive forces), and the other components, which might be a result of attractive forces: the polarization energy,  $E_{\text{PL}}$ , the charge transfer energy,  $E_{\text{CT}}$ , and the electrostatic energy,  $E_{\text{ES}}$ . If a method is applied where the correlation of electrons is taken into account, then the correlation energy may be included.<sup>23,24</sup> One of the most important attractive components of the correlation energy is the dispersive energy.<sup>25</sup> Different H-bonded systems were analyzed early by Umeyama and Morokuma who stated that: "The energy components are strongly distance dependent. At a relatively small separation, ES, CT, and PL can all be important attractive components, competing against a large EX repulsion. At larger distances for the same complex the short-range attractions CT and PL are usually unimportant and ES is the only important attraction."<sup>26</sup> One can see that the "covalency of interaction" may be connected with short H···B distances where terms other than the electrostatic attractive one are important.

Received: October 24, 2007

Published: February 15, 2011

It was pointed out that the electron transfer from the acceptor to the proton-donating bond is characteristic for hydrogen bonding.<sup>27</sup> This transfer is greater for stronger interactions. Desiraju claimed that stronger hydrogen bonds are characterized by considerable charge transfer energy, whereas weaker hydrogen bonds are electrostatic in nature.<sup>28</sup> It was found recently that the delocalization (approximately both  $E_{CT}$  and  $E_{PL}$  terms if one refers to the Kitaura–Morokuma partitioning) and the electrostatic interaction energy,  $E_{ES}$ , are the most important attractive terms for hydrogen-bonding interactions.<sup>29</sup> If the interaction strength increases, then the  $H \cdots B$  distance shortens and also the ratio between delocalization and electrostatic interaction energy terms increases.<sup>29</sup> Gilli and co-workers pointed to the so-called resonance-assisted hydrogen bonds (RAHBs) where the enhancement of hydrogen-bond strength is the result of  $\pi$ -electron delocalization.<sup>30,31</sup> The authors stated that RAHBs are often strong and covalent in nature; similarly, charge-assisted hydrogen bonds (CAHBs) are often classified as strong hydrogen bonds.

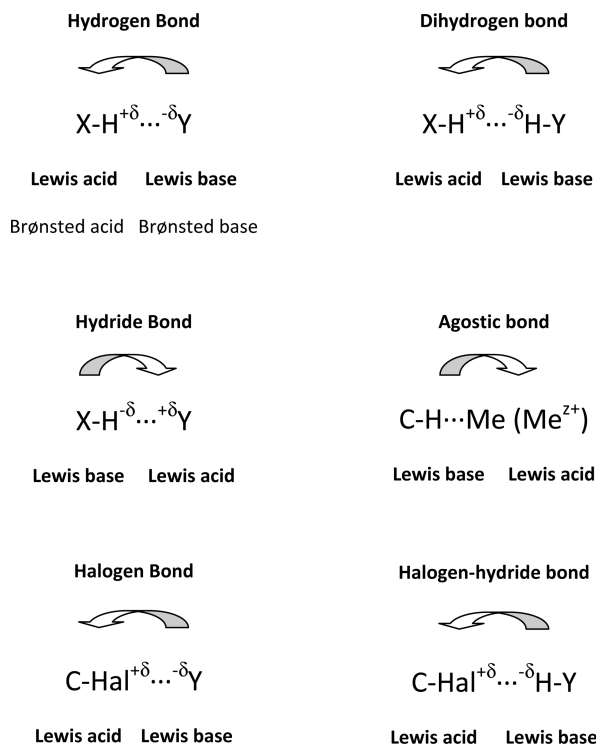
There are different definitions of hydrogen bonding; thus, in numerous studies the classification of any interaction considered may be equivocal. For example, numerous  $C-H \cdots B$  interactions were classified as hydrogen bonds.<sup>21,32,33</sup> However, they could not be classified as hydrogen bonds if the Pauling definition of hydrogen bonding is applied because carbon is not an electronegative atom. There are the other examples; in the mid-1990s an interaction named as dihydrogen bond (DHB) was detected and analyzed.<sup>34</sup> Since then, the number of studies concerning DHB systems has increased rapidly; such systems were analyzed both experimentally<sup>35</sup> and theoretically.<sup>36,37</sup> It seems that the definition of hydrogen bonding introduced very early by Pimentel and McClellan covers a broad range of interactions.<sup>21</sup> The authors stated that:

“A H bond exists between a functional group  $A-H$  and an atom or a group of atoms  $B$  in the same or a different molecule when

- there is evidence of bond formation (association or chelation),
- there is evidence that this is new bond linking  $A-H$  and  $B$  specifically involves the hydrogen atom already bonded to  $A$ .”

Thus, all kinds of hydrogen bonding mentioned above are covered by this definition, among them dihydrogen bonds and  $C-H \cdots B$  interactions. However, it is not precisely defined what is “evidence of bond formation”; additionally, according to this definition, the so-called inverse hydrogen bonding or hydride bonding<sup>38,39</sup> is also classified as hydrogen bonding. The latter interaction is characterized by the existence of the negatively charged hydrogen atom inserted between two electropositive atoms; thus, it seems that it is not the kind of hydrogen bonding. Similarly, the so-called agostic interaction is not classified as hydrogen bonding either because it was shown that this interaction possesses characteristics of hydride bonding.<sup>39</sup> On the other hand, dihydrogen bond may be classified as hydrogen bonding; this will be explained in detail in the next sections. Such considerations depend on the kind of definition applied.

Chart 1 presents different types of interactions, not only hydrogen bonds but also such interactions that are in nature similar to hydrogen bonding. All interactions presented may be classified as Lewis acid–Lewis base ones,<sup>40</sup> and all of them are represented in crystal structures of organic and organometallic compounds. It was pointed out in early studies<sup>41</sup> that hydrogen

Chart 1.<sup>a</sup>

<sup>a</sup>Reprinted with permission from ref 40. Copyright 2006 American Chemical Society.

bonding may be treated as the Brønsted acid–Brønsted base interaction. The transfer of electron charge (Chart 1, arrows) from the Lewis base to the Lewis acid is one of the characteristics attributed to hydrogen bonding.<sup>27</sup> The Natural Bond Orbitals method (NBO)<sup>42,43</sup> shows that for typical hydrogen bonding, a two-electron  $n_B \rightarrow \sigma_{AH}^*$  intermolecular donor–acceptor interaction exists where electron density from the lone pair  $n_B$  of the Lewis base  $B$  delocalizes into the unfilled  $\sigma_{AH}^*$  antibonding orbital of the Lewis acid. The  $n_B \rightarrow \sigma_{AH}^*$  orbital overlap is characteristic for hydrogen-bonding interaction.<sup>20,42,43</sup> There are other methods to analyze intra- and intermolecular interactions; the Quantum Theory of “Atoms in Molecules” (QTAIM)<sup>44–47</sup> is one of the approaches often applied to analyze the electron charge distribution for the hydrogen-bonded systems.

It was pointed out in numerous studies that the short and strong hydrogen bonds (SSHBs) have a partly covalent character,<sup>48</sup> similarly to low barrier hydrogen bonds (LBHBs).<sup>49</sup> Is the covalent character attributed to weaker hydrogen bonds? This matter was considered in recent studies,<sup>50</sup> but it was also pointed out early by Pauling who even proposed how to estimate the covalency for hydrogen bonds existing in ice.<sup>14</sup> These topics are discussed in this Review, not only for typical Pauling-type hydrogen bonds but also for the other interactions often classified as hydrogen bonds.

## 2. GEOMETRICAL PARAMETERS OF HYDROGEN BONDING

The dependence between the strength of hydrogen bonding and the  $H \cdots B$  distance is often discussed, especially for  $O-H \cdots O$  systems.<sup>30</sup> However, such a relationship is only a rough

one even if  $\text{H}\cdots\text{O}$  distances concern similar species immersed into similar environments, in other words, if the considered sample of  $\text{O}-\text{H}\cdots\text{O}$  systems is homogeneous.<sup>51</sup> The estimation of hydrogen-bonding strength on the basis of distances is not possible for a heterogeneous sample, especially if hydrogen bonds differ in the type of proton donor and/or proton acceptor. In view of the above difficulties, such ideas as the bond order<sup>52,53</sup> or the other ones allow one to unify interactions to estimate their strength even if different pairs of atoms are considered. The bond number connected with interatomic distance seems to be good to introduce a measure of strength for nonbonding contacts including hydrogen bonds. The bond number was introduced early by Pauling for interatomic distances observed in metals.<sup>54</sup> The distance–bond number relationship is expressed by the following equation:

$$r_n - r_s = \Delta r = -c \log n \quad (1)$$

where  $r_n$  and  $r_s$  designate bond lengths, the given one with the bond number equal to  $n$ , and a single, reference one with the bond number equal to 1.  $c$  is the constant that varies depending on the nature of atoms involved in the interaction. Most often this constant is calculated from the symmetrical systems. Thus, the  $\text{A}-\text{H}\cdots\text{B}$  ( $\text{A} = \text{B}$ ) system with the centric position of proton is taken into account. Then, for such a system, we have two equivalent half-bonds, and further one can estimate the value of  $c$ :

$$r_{1/2} - r_s = -c \log 1/2 \quad (2)$$

For the  $\text{O}-\text{H}\cdots\text{O}$  system with the proton situated in the middle of the  $\text{O}\cdots\text{O}$  distance, the following  $\text{O}\cdots\text{O}$  distances, 2.44 Å<sup>55</sup> and 2.4 Å,<sup>30</sup> were taken into account, leading to the corresponding half-bond lengths. Thus, one can see that the reference interatomic distance choice is arbitrary, and this concerns the half-bond as well as the single bond.

The bond number may be understood as the fraction of electron pair participating in the atom–atom contact, and the logarithmic relation expressed by eq 1 is a consequence of the exponential character of intermolecular forces. Hence, one may say that for the proton–acceptor distance ( $\text{H}\cdots\text{B}$ ), the bond number,  $n$ , expresses the sharing of electrons in an interatomic region, in other words, the covalency of intermolecular interaction. It is not a new idea since Pauling used the concept of bond number to estimate the covalent contribution of intermolecular  $\text{H}\cdots\text{O}$  interactions to amount to 6% for the crystal structure of ice.<sup>14</sup>

Bürgi and Dunitz<sup>55,56</sup> adopted Pauling's relationship (eq 1) for triatomic systems with an additional assumption postulating that the sum of two bond numbers within the system considered is equal to unity, which leads to the equation:

$$10^{-\Delta r_1/c} + 10^{-\Delta r_2/c} = 1 \quad (3)$$

where  $\Delta r_1 = r_1 - r_s$  and  $\Delta r_2 = r_2 - r_s$  are bond length increases and correspond to  $r_1$  and  $r_2$  bond lengths within the considered system. Equation 3 is known as the bond number conservation (BNC) rule. A similar relation was introduced by Johnston<sup>57,58</sup> to describe the gas-phase reactions, and originally it was called the bond order conservation rule. BNC rule may be applied for hydrogen bonding.<sup>30,55,59</sup> It may be understood in the following way. If the  $\text{A}-\text{H}$  bond is not involved in any additional external interaction, then its bond number amounts to unity. If the  $\text{A}-\text{H}$  bond participates in the intermolecular interaction such as hydrogen bonding, then the  $\text{A}-\text{H}$  bond elongates, and consequently (eq 1) the bond number value decreases. In other words,

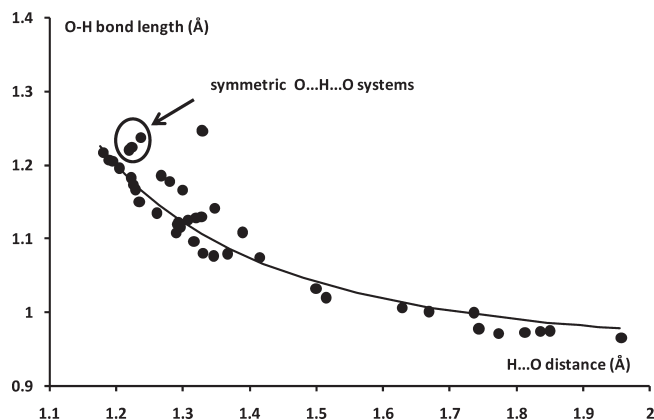


**Figure 1.** Relationship between the  $\text{H}\cdots\text{O}$  distance and  $\text{O}-\text{H}$  bond length (both in Å) for the accurate neutron diffraction results of  $\text{C}=\text{O}\cdots\text{H}-\text{O}-\text{C}$  systems. Three symmetric  $\text{O}\cdots\text{H}\cdots\text{O}$  systems with central position of the proton are shown; the solid line represents this relationship obtained from the bond number conservation rule.

the proton donating bond “loses its covalency” as a result of complexation. This loss is compensated by the  $\text{H}\cdots\text{B}$  contact where one can observe the sharing of electrons; a fractional part of the electron pair is expressed by the bond number. Hence, for the shorter  $\text{H}\cdots\text{B}$  contacts within the  $\text{A}-\text{H}\cdots\text{B}$  systems, there are longer  $\text{A}-\text{H}$  bonds. The latter relationship was analyzed for numerous samples taken from experimental measurements as well as from theoretical calculations.<sup>1,30,51,60–62</sup> It was found for the neutron diffraction results concerning various types of hydrogen bonds in crystals of organic and organometallic compounds.<sup>63</sup> The heteronuclear hydrogen bonds such as  $\text{N}-\text{H}\cdots\text{O}$ ,  $\text{O}-\text{H}\cdots\text{N}$ ,  $\text{O}-\text{H}\cdots\text{S}$ ,  $\text{S}-\text{H}\cdots\text{O}$ , and  $\text{N}-\text{H}\cdots\text{Cl}^-$  were considered.<sup>63</sup> Especially, there are numerous neutron diffraction results on  $\text{O}-\text{H}\cdots\text{O}$  systems and numerous studies concerning the relationships between geometrical parameters of these systems.<sup>64–67</sup>

The sample of  $\text{C}=\text{O}\cdots\text{H}-\text{O}-\text{H}$  systems is considered here, that is, systems containing the carbonyl group as a proton acceptor and the  $\text{O}-\text{H}$  proton-donating bond connected with carbon atom. The Cambridge Crystal Structure Database<sup>68</sup> was searched for such systems of neutron diffraction organic and organometallic crystal structures where  $R \leq 7\%$ , esd's for CC bonds  $\leq 0.005$  Å, and also only error free and no disorder structures were declared. Figure 1 presents the dependence between the  $\text{H}\cdots\text{O}$  distance and the  $\text{O}-\text{H}$  bond length for this sample; the line obtained from the bond number conservation rule is also given ( $r_0 = 0.957$  Å,  $r_{1/2} = 1.2$  Å). Weak  $\text{O}-\text{H}\cdots\text{O}$  hydrogen bonds are excluded because the  $\text{H}\cdots\text{O}$  distance was fixed to be less than 2 Å.

This relationship between the  $\text{H}\cdots\text{O}$  distance and the  $\text{O}-\text{H}$  bond length is well approximated by the monotonic function (eq 3; Figure 1) with a few exceptions only. For the shorter  $\text{H}\cdots\text{O}$  distances, there occurs a more meaningful elongation of the  $\text{O}-\text{H}$  bond; the shortest observed  $\text{H}\cdots\text{O}$  contacts are of about 1.2 Å. Further shortening of  $\text{H}\cdots\text{O}$  distance is not possible because it would be connected with longer  $\text{O}-\text{H}$  bond lengths than the corresponding  $\text{H}\cdots\text{O}$  contacts. However, the  $\text{O}-\text{H}\cdots\text{O}$  hydrogen bonds are possible where the elongation of  $\text{O}-\text{H}$  bond is connected with the elongation of  $\text{H}\cdots\text{O}$  contact. Three such cases were found for the sample considered. For these entries,  $\text{H}\cdots\text{O}$  and  $\text{O}-\text{H}$  interactions are equivalent because these



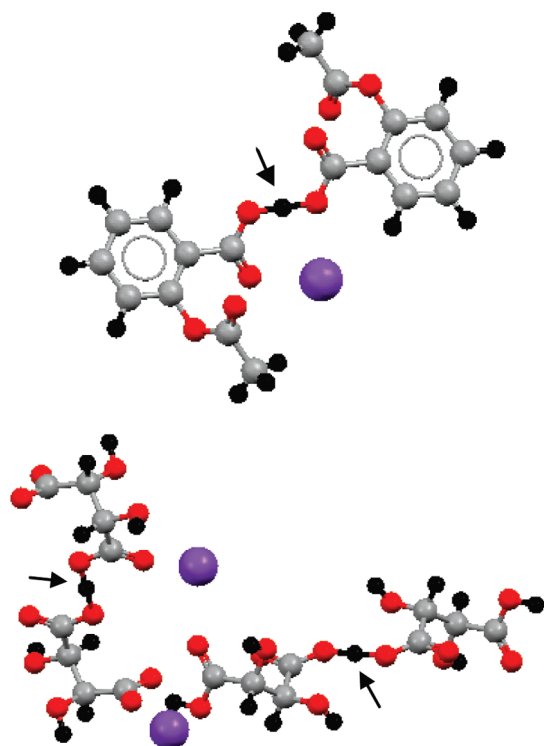


**Figure 2.** Fragments of crystal structures containing symmetric  $\text{O}\cdots\text{H}\cdots\text{O}$  systems designated in Figure 1. For the first crystal structure (KHDASL01 refcode), there is one symmetric  $\text{O}\cdots\text{H}\cdots\text{O}$  hydrogen bonding; for the second crystal structure (KHMTAR01 refcode), there are two such interactions, and those  $\text{O}\cdots\text{H}\cdots\text{O}$  systems are indicated by arrows; red circles, oxygen atoms; black, hydrogen; gray, carbon; violet, potassium ion.

distances are equal to each other. They amount to 1.22, 1.224, and 1.237 Å. The latter  $\text{O}\cdots\text{H}\cdots\text{O}$  systems may be classified as similar to the  $(\text{FHF})^-$  system where a very strong hydrogen bond occurs. One may say of such systems that the proton is inserted between two oxygen centers both possessing lone pairs of electrons. Thus, there is no diversity between  $\text{O}-\text{H}$  and  $\text{H}\cdots\text{O}$  because both are equivalent and both may be treated as interactions possessing the characteristics of the covalent bond. There are numerous such  $\text{O}\cdots\text{H}\cdots\text{O}$  systems known from the crystal structures with the proton situated exactly in the middle of the  $\text{O}\cdots\text{O}$  distance.<sup>18</sup> However, the sample analyzed here is only concerned with neutron diffraction results; thus, only two accurately determined crystal structures contain such systems (Figure 2). These are the crystal structures of potassium hydrogen bis(acetylsalicylate),  $\text{K}^+, \text{C}_{18}\text{H}_{15}\text{O}_8^-$ ,<sup>69</sup> and potassium hydrogen mesotartarate,  $\text{K}^+, \text{C}_8\text{H}_{11}\text{O}_{12}^-$ ;<sup>70</sup> the first one contains one type of  $\text{O}\cdots\text{H}\cdots\text{O}$  system with the central position of the proton, and the second structure contains two such systems (Figure 2).

The dependence between the  $\text{O}-\text{H}$  bond number ( $n_{\text{OH}}$ ) and the corresponding  $\text{H}\cdots\text{O}$  bond number ( $n_{\text{H}\cdots\text{O}}$ ) for the  $\text{C}=\text{O}\cdots\text{H}-\text{O}-\text{C}$  systems analyzed here is presented in Figure 3. This relationship may be interpreted in the following way. The bond number is the fraction of pair of electrons shared between atoms; thus, the shorter  $\text{H}\cdots\text{O}$  distance corresponds to the greater covalency contribution. Hence, even weak hydrogen bonds have the characteristics of covalent interaction because any atom–atom distance may be interpreted in terms of the bond number approach.

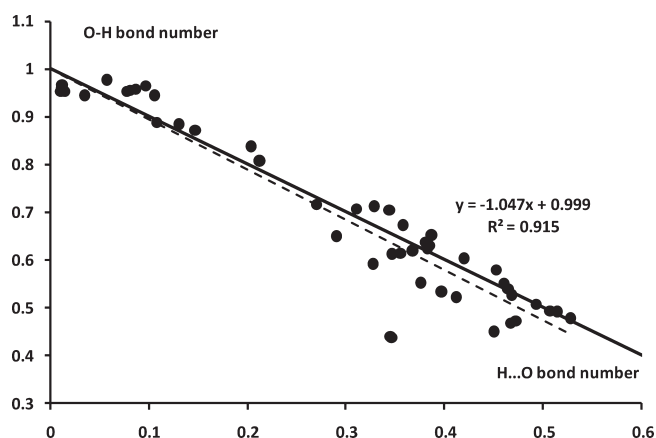


**Figure 3.** Relationship between the  $\text{H}\cdots\text{O}$  and  $\text{O}-\text{H}$  bond numbers of  $\text{O}-\text{H}\cdots\text{O}$  hydrogen bonds taken from accurate neutron diffraction results. The solid line corresponds to the bond number conservation rule, and the broken line represents the linear regression. The sample considered here is the same as that of Figure 1.

The linear correlation coefficient for this relation amounts to 0.957. The solid line in Figure 3 corresponds to the BNC rule ( $y = -x + 1$ ), and this model is in agreement with the experimental data for which the regression line is very close to the theoretical one (broken line in Figure 3,  $y = -1.047x + 0.999$ ).

There is another approach referring to the bond length, which also allows one to consider a broader spectrum of atom–atom interactions. It is the Bond Valence model (BV model).<sup>71–73</sup> The BNC rule and BV model were often applied in numerous investigations concerning interactions<sup>74–76</sup> and chemical reactions,<sup>77–79</sup> among the latter ones, proton transfer processes.<sup>80–83</sup>

The  $\text{A}-\text{H}\cdots\text{B}$  angle is another geometrical characteristic of hydrogen bonding. The hydrogen-bonded systems tend to linearity. This may be explained as a consequence of the maximal  $n_{\text{B}} \rightarrow \sigma_{\text{AH}}^*$  overlap.<sup>20</sup> Hence, if hydrogen bonding is stronger, thus the  $\text{A}-\text{H}\cdots\text{B}$  angle is closer to  $180^\circ$ . It was stated that for very strong hydrogen bonds, the  $\text{A}-\text{H}\cdots\text{B}$  angle range is  $175-180^\circ$ , for strong it is  $130-180^\circ$ , while for weak it is  $90-180^\circ$ .<sup>3</sup> This is supported by the crystal data taken from the Cambridge Structural Database (CSD);<sup>68</sup> for short  $\text{H}\cdots\text{O}$  contacts of  $\text{O}-\text{H}\cdots\text{O}$  interactions (strong hydrogen bonds), the angle range is narrower than for long such distances (weak hydrogen bonds). For  $\text{C}-\text{H}\cdots\text{O}$  interactions, a similar tendency is observed; however, no such short  $\text{H}\cdots\text{O}$  distances are observed as for  $\text{O}-\text{H}\cdots\text{O}$  hydrogen bonds. Thus, even for the shortest (C) $\text{H}\cdots\text{O}$  distances, the  $\text{C}-\text{H}\cdots\text{O}$  angle range is not as narrow as for the short (O) $\text{H}\cdots\text{O}$  distances.<sup>3</sup>

### 3. HYDROGEN-BOND ENERGY

It was shown in the previous section that the covalency of hydrogen bonding is related to the  $\text{H}\cdots\text{B}$  proton–acceptor distance. If that distance is expressed in terms of the Bond Valence (BV) model<sup>73</sup> or the bond number idea,<sup>54,55</sup> then it is possible to estimate “the degree of covalency”. However, these ideas are only approximate, having physical meaning only if one assumes that the bond number is understood as the fraction of electron pairs shared within the considered atom–atom region.<sup>54</sup> Therefore, the parameters better attributed to well-defined terms of physics, for example, the hydrogen-bond energy, should be taken into account to discuss the hydrogen-bonding



characteristics.<sup>84</sup> Desiraju claimed “Pronounced covalent character in a hydrogen bond is found only occasionally and that too in very strong bonds (energy range 20–40 kcal mol<sup>−1</sup>).”<sup>28</sup> However, it is proven in this Review that the covalent character is attributed to hydrogen-bonding interaction and it exists not only occasionally.

It is usually assumed<sup>85</sup> that if there is intermolecular hydrogen bonding between two species designated as R<sub>1</sub>–A–H and B–R<sub>2</sub>, then the energy of such an interaction may be expressed by eq 4.

$$\Delta E = E(R_1-A-H \cdots B-R_2) - E(R_1-A-H) - E(B-R_2) \quad (4)$$

There is stabilization of the R<sub>1</sub>–A–H $\cdots$ B–R<sub>2</sub> system connected with the H-bond formation; thus, the  $\Delta E$ -value is negative.<sup>86</sup> It is usually assumed that the hydrogen bonding is the most important and predominant interaction for two interacting species and the other interactions between them are meaningless. The  $\Delta E$  value is exactly the binding energy where all interactions leading to the stabilization of the complex are taken into account, not only the single A–H $\cdots$ B connection. The binding energy of the A $\cdots$ B complex is usually calculated according to the supermolecular approach,<sup>87,88</sup> eq 5.

$$E_{\text{bin}} = E_{A \cdots B}(A \cdots B)^{A \cup B} - E_{A \cdots B}(A)^A - E_{A \cdots B}(B)^B \quad (5)$$

The designations in parentheses correspond to systems in which energies are considered; the superscripts indicate the basis sets used for the corresponding systems, and the subscripts indicate the geometries optimized. The binding energy given by eq 5 is the difference between the energy of the A $\cdots$ B complex with the fully optimized geometry and the complex AUB basis set and the energies of A and B subsystems with geometries taken from the complex for which the energies are calculated within A and B monomers' basis sets. However, this approach (eq 5) does not take into account the deformation energy being the result of complexation. The deformation energy is positive because the isolated monomers involved in any stabilization interaction change their geometries and are taken out from minima. This energy is defined as follows:

$$E_{\text{def}} = E_{A \cdots B}(A)^A + E_{A \cdots B}(B)^B - E_A(A)^A - E_B(B)^B \quad (6)$$

The designations of eq 6 correspond to those of eq 5. Thus, one can obtain the binding energy where the deformation energy is taken into account ( $E_{\text{bin/def}}$ ).

$$\begin{aligned} E_{\text{bin/def}} &= E_{\text{bin}} + E_{\text{def}} \\ &= E_{A \cdots B}(A \cdots B)^{A \cup B} - E_A(A)^A - E_B(B)^B \end{aligned} \quad (7)$$

The other effect that should be taken into account to calculate the binding energy is the Basis Set Superposition Error (BSSE).<sup>89</sup> BSSE is more distinct for incomplete, unsaturated basis sets, and it may be explained as follows. For the complex, each monomer may compensate the basis set incompleteness using the basis function of its neighbor. Hence, the energy of the complex is lowered, and the H-bond energy (generally the binding energy) is overestimated (it is “more negative” than it should be). This effect decreases if the basis set applied is enlarged, and within the limits of the complete basis set, BSSE tends to zero.<sup>24,90</sup> However, it is not possible to use the large, saturated basis sets for large and complicated molecular systems as, for example, biochemically

active species because this requires considerable computational effort and the corresponding calculations are very time-consuming. Thus, for incomplete basis sets, a frequently applied approach to estimate the BSSE is the Counterpoise (CP) correction defined as:<sup>91</sup>

$$\begin{aligned} \Delta E_{\text{CP}} &= E_{A \cdots B}(A)^A + E_{A \cdots B}(B)^B - E_{A \cdots B}(A)^{A \cup B} \\ &\quad - E_{A \cdots B}(B)^{A \cup B} \end{aligned} \quad (8)$$

$\Delta E_{\text{CP}}$  is positive because the energy calculated at complex basis set (AUB) is lower than the energy calculated with the use of the monomer basis sets (A or B).<sup>89</sup> The correction introduced by Boys and Bernardi and expressed by eq 8 is most frequently applied. However, there are also other approaches that lead to the reduction of the basis set superposition error.<sup>92–96</sup> The other important correction often included in calculations is the so-called “zero point vibrational energy” (ZPVE).<sup>97,98</sup> Thus, there are the following important effects that should be taken into account to estimate the binding energy, particularly H-bond energy: the deformation energy, a physical effect being the result of complexation; ZPVE, the physical effect connected with vibrations in the ground state; and BSSE, the effect connected with computational limitations because the frequently applied basis sets are not saturated.

It was shown that the deformation of species forming hydrogen bonding increases if the strength of this interaction increases too.<sup>99,100</sup> This was confirmed by the calculations performed on complexes connected by various types of hydrogen bonding.<sup>101</sup> MP2/6-311++G(d,p) calculations were performed on systems with such hydrogen bonds as O–H $\cdots$ O, O–H $\cdots$ N, F–H $\cdots$ O, F–H $\cdots$ N, and C–H $\cdots$ O, dihydrogen bonds, and very strong charge-assisted (F $\cdots$ H $\cdots$ F)<sup>−</sup> hydrogen bond was also included. Particularly, the following complexes were considered: (C<sub>2</sub>H<sub>2</sub>)<sub>2</sub>, FH $\cdots$ OCH<sub>2</sub>, NF<sub>3</sub>H<sup>+</sup> $\cdots$ HBeH, H<sub>3</sub>N $\cdots$ HF, NH<sub>4</sub><sup>+</sup> $\cdots$ HBeH, NH<sub>4</sub><sup>+</sup> $\cdots$ HBeF, (H<sub>2</sub>O)<sub>2</sub>, FH $\cdots$ C<sub>2</sub>H<sub>2</sub>, (FHF)<sup>−</sup>, FH $\cdots$ OH<sub>2</sub>, FH $\cdots$ HLi, HCCH $\cdots$ OH<sub>2</sub>, and HOH $\cdots$ NH<sub>3</sub>.<sup>101</sup> Figure 4 presents selected complexes of this sample.

Figure 5 shows, for this sample, the relationship between the proton–acceptor distance (H $\cdots$ B) and the binding energy. Open symbols represent the binding energies where the deformation energies are included, whereas closed ones correspond to the energies where the deformation is not taken into account. (F $\cdots$ H $\cdots$ F)<sup>−</sup> is designated by triangles; for this system, the deformation energy outweighs 20 kcal/mol. Squares correspond to dihydrogen-bonded systems; these are usually strong charge-assisted interactions. For these species, the deformation is also visible. The remaining complexes correspond to weaker interactions like C–H $\cdots$ O for the complex of water (proton acceptor) and acetylene (proton donor) or T-shaped dimer of acetylene. Figure 5 does not show open circles for such complexes because the deformation energies are very close to zero. If one assumes that the H $\cdots$ B distance roughly expresses the hydrogen-bond strength, then one can observe the more important deformation energy (expressed in Figure 5 by the displacement between open symbols and the corresponding closed ones) for stronger hydrogen bonds. Two species are significantly out of the range of the remaining ones; they are the (F $\cdots$ H $\cdots$ F)<sup>−</sup> system where the deformation energy is equal to 21.2 kcal/mol and the charge-assisted dihydrogen-bonded system of the F<sub>3</sub>NH<sup>+</sup> $\cdots$ HBeH complex where this energy is equal to 6.1 kcal/mol. For the other complexes, the deformation energy does not exceed 0.8 kcal/mol.

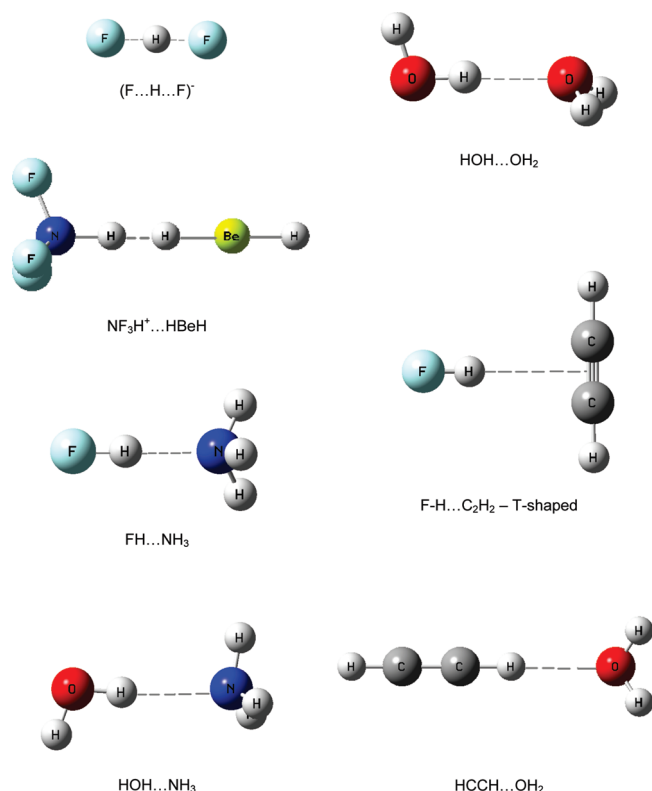


**Figure 4.** Selected systems of those presented in Table 1. Reprinted with permission from ref 101. Copyright 2005 Wiley Interscience.

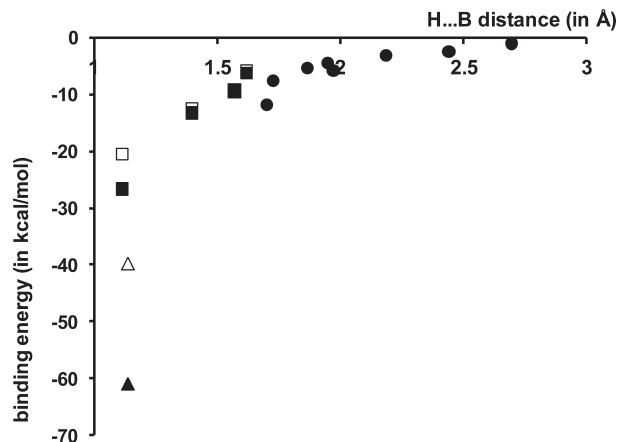


**Figure 5.** Relationship between the proton–acceptor distance (in Å) and the binding energy (kcal/mol) for complexes of Table 1. Squares correspond to the dihydrogen bonds, triangles to the  $(\text{FHF})^-$  system, and circles to the other complexes. Open symbols correspond to the binding energies calculated in such a way that the deformation energy is taken into account, and closed symbols correspond to supermolecular approach where deformation energy is not included. Reprinted with permission from ref 101. Copyright 2005 Wiley Interscience.

The decomposition of the interaction energy is a very useful tool to characterize hydrogen bonding. One of the first decompositions was that of Kollman and Allen.<sup>102,103</sup> However, the first approach that was commonly accepted and further applied was proposed by Morokuma and Kitaura.<sup>22,104,105</sup> The Hartree–Fock (SCF) interaction energy is decomposed here according to eq 9.

$$\Delta E_{\text{SCF}} = E_{\text{ES}} + E_{\text{EX}} + E_{\text{PL}} + E_{\text{CT}} + E_{\text{MIX}} \quad (9)$$

$E_{\text{ES}}$  designates the energy of interaction between the undistorted charge distributions of two interacting moieties, and this is called electrostatic interaction energy.  $E_{\text{PL}}$  is the energy of the distortion of charge distribution within monomers as an effect of complex formation, the polarization interaction energy.  $E_{\text{CT}}$  is the energy of charge transfer from one moiety to the other as an effect of complexation.  $E_{\text{EX}}$  is the exchange energy, which may be roughly defined as a result of the repulsion of electron clouds.  $E_{\text{MIX}}$  is the energy difference between SCF interaction energy and the above-mentioned four components, and it is usually named as “the coupling energy term”.  $E_{\text{EX}}$  is the repulsive interaction energy term, whereas the other terms,  $E_{\text{ES}}$ ,  $E_{\text{PL}}$ , and  $E_{\text{CT}}$ , are attractive interaction energy terms.

For methods including the correlation energy, for example, the MP2 method, the binding energy is expressed by eq 10.

$$\Delta E_{\text{MP2}} = \Delta E_{\text{SCF}} + E_{\text{CORR}} \quad (10)$$

The dispersion energy ( $E_{\text{DISP}}$ ) is one of the most meaningful attractive interaction energy components of the electron correlation energy,  $E_{\text{CORR}}$ . However,  $E_{\text{CORR}}$  and consequently  $E_{\text{DISP}}$  are not included in SCF binding energy. Hence, if one would like to include dispersion interaction energy, one should go beyond the Hartree–Fock method. Another inconvenience of the approach expressed by eq 9 is the  $E_{\text{MIX}}$  term, which does not have precise physical meaning because it is the result of poorly separated interaction energy.

There is another variation-perturbation approach where the starting wave functions of the subsystems are obtained in the dimer-centered basis set.<sup>106,107</sup> The results of that decomposition are presented in this Review. In the latter scheme, due to the full counterpoise correction, the total interaction energy as well as all of its components is free of basis set superposition error (BSSE). In this approach, the following interaction energy terms are obtained:

$$\Delta E = E_{\text{ES}}^{(1)} + E_{\text{EX}}^{(1)} + E_{\text{DEL}}^{(\text{R})} + E_{\text{CORR}} \quad (11)$$

where  $E_{\text{ES}}^{(1)}$  is the first-order electrostatic interaction energy term describing the Coulomb interaction of static charge distributions of both moieties within the complex;  $E_{\text{EX}}^{(1)}$  is the repulsive first-order exchange term resulting from the Pauli exclusion principle; and  $E_{\text{DEL}}^{(\text{R})}$  and  $E_{\text{CORR}}$  correspond to higher order delocalization and correlation components. The delocalization component contains all classical induction, exchange-induction, etc., from the second order up to infinity. For the approach expressed by eq 11, the delocalization interaction energy term  $E_{\text{DEL}}^{(\text{R})}$  roughly corresponds to  $E_{\text{CT}}$  and  $E_{\text{PL}}$  terms in eq 9. The  $E_{\text{DEL}}^{(\text{R})}$  term of the variation-perturbation approach (eq 11) is not partitioned because the charge transfer interaction energy is strongly basis set dependent, while the delocalization energy is much less sensitive to the basis sets effects.

The results of the Natural Bond Orbital (NBO), also presented in this Review, differ significantly from the other decomposition schemes. The disagreements between different approaches are connected with different treatments of orbital overlap,<sup>42,108–110</sup> which intrinsically affects how electron density is attributed to atomic centers; the Mulliken scheme is an example of the unrealistic overlap population division. In schemes based on the NBO method, the orbital overlap is removed at the atomic level because such approaches are formulated in the overlap-free domain of natural atomic orbitals (NAOs). This assures consistent charge assignments for further hybridization, bond formation, and intermolecular interactions, particularly

**Table 1. Binding Energies ( $\Delta E$ ) and Interaction Energy Terms (in kcal/mol) for H-Bonded Complexes<sup>a</sup>**

complex	$E_{H-L}^{(1)b}$	$E_{ES}^{(1)}$	$E_{EX}^{(1)}$	$E_{DEL}^{(R)}$	$\Delta E^{HF}$	$E_{CORR}$	$\Delta E$	$R_{H...B}$
HOH...OH <sub>2</sub>	−1.97	−8.75	6.78	−2.19	−4.16	−0.29	−4.46	1.950
HOH...NH <sub>3</sub>	−1.16	−12.09	10.92	−3.8	−4.96	−0.91	−5.87	1.974
FH...OCH <sub>2</sub>	−3.85	−8.87	5.02	−2.65	−6.5	1.06	−5.44	1.869
FH...OH <sub>2</sub>	−2.82	−14.23	11.41	−5.08	−7.9	0.21	−7.69	1.73
FH...NH <sub>3</sub>	−1.34	−22.47	21.13	−10.09	−11.43	−0.4	−11.83	1.703
(F...H...F) <sup>−</sup>	−4.22	−78.15	73.93	−63.92	−68.14	7.08	−61.05	1.138
HCCH...OH <sub>2</sub>	−1.4	−4.79	3.39	−1.06	−2.46	−0.01	−2.47	2.443
F−H...C <sub>2</sub> H <sub>2</sub> , T-shaped	0.1	−6.27	6.37	−2.82	−2.73	−0.46	−3.19	2.186
(C <sub>2</sub> H <sub>2</sub> ) <sub>2</sub> , T-shaped	0.08	−2.13	2.21	−0.54	−0.47	−0.59	−1.06	2.697
F−H...H−Li	−0.88	−19.27	18.39	−10.75	−11.64	−1.74	−13.37	1.399
NH <sub>4</sub> <sup>+</sup> ...HBeH	0.36	−8.62	8.98	−8.15	−7.79	−1.77	−9.57	1.571
NH <sub>4</sub> <sup>+</sup> ...HBeF	2.95	−4.26	7.2	−6.92	−3.97	−2.32	−6.28	1.62
NF <sub>3</sub> H <sup>+</sup> ...HBeH	15.58	−13.37	28.95	−38.69	−23.12	−3.63	−26.74	1.114

<sup>a</sup>The results obtained are at the MP2/6-311++G(d,p) level; the proton-acceptor ( $R_{H...B}$ ) distances (in Å) are also included. Results reprinted with permission from ref 101. Copyright 2005 John Wiley and Sons. <sup>b</sup>First-order Heitler–London energy term;  $E_{H-L}^{(1)} = E_{ES}^{(1)} + E_{EX}^{(1)}$ .

H-bond formation. In Morokuma-type decompositions, this is valid only in the long-range limit far beyond interatomic orbital interactions. For hydrogen-bonded systems, especially in the case of strong hydrogen bonds, the proton-acceptor distance is inside van der Waals contact, where atomic orbital overlap confuses assignments of atomic charge and consequently the electron transfer between monomers and the evaluation of  $E_{CT}$  term.

The other methods, like the Ziegler–Rauk approach,<sup>111</sup> Baerends–Bickelhaupt decomposition,<sup>112,113</sup> BLW,<sup>114–116</sup> or ALMO-EDA,<sup>117,118</sup> treat the overlap-density terms in different ways, but all differ significantly from the overlap-free NBO methods.

Table 1 presents the results of the decomposition of interaction energy (eq 11) for the same set of complexes as that presented in Figure 5. Additionally the first-order Heitler–London energy term,  $E_{H-L}^{(1)} = E_{ES}^{(1)} + E_{EX}^{(1)}$ , is included, as well as the Hartree–Fock interaction energy,  $\Delta E^{HF}$ . Generally, for the complexes presented in Table 1, the electrostatic interaction energy term is the most important attractive one. However, one can see that for some of the complexes, the Heitler–London interaction energy term is positive. This is observed for strong interactions, for such complexes as NH<sub>4</sub><sup>+</sup>...HBeH, NH<sub>4</sub><sup>+</sup>...HBeF, and F<sub>3</sub>NH<sup>+</sup>...HBeH where dihydrogen bonds exist. For the latter complex, the delocalization interaction energy term is the most important attractive one. Similarly, positive  $E_{H-L}^{(1)}$  appears for those complexes where  $\pi$ -electrons are the acceptor of proton in hydrogen bonds, that is, T-shaped complexes: dimer of acetylene, (C<sub>2</sub>H<sub>2</sub>)<sub>2</sub>, and F−H...C<sub>2</sub>H<sub>2</sub> complex.

Table 2 contains the interaction energy terms (eq 11) for complexes linked by intermolecular N−H...O, O−H...N, and O−H...O hydrogen bonds. These interactions are relatively strong because H-bond enhancement is observed for them as the result of  $\pi$ -electron delocalization. All these complexes optimized at the MP2/6-311++G(d,p) level are centrosymmetric dimers corresponding to minima.<sup>119–121</sup> The N−H...O bonds exist for formamide and its fluoro derivatives, whereas the O−H...N hydrogen bonds exist for their tautomeric forms. Formamides and their tautomers are related by the process of double proton transfer. Table 2 also contains results for centrosymmetric dimers of carboxylic acids: formic acid and acetic acid as well as the dimer of the pyrrole-2-carboxylic acid. Three configurations of the latter complex are considered. For two of

them, similarly as for formic and acetic acid dimers, the O−H...O hydrogen bonds exist, whereas for the third one, two related by symmetry N−H...O hydrogen bonds exist. Figure 6 presents a few species of the sample considered here, acetic acid dimer, formamide dimer, and its tautomeric form.

One can see that O−H...N are the strongest hydrogen bonds, the O−H...O interactions are weaker than the previous ones, and the N−H...O interactions are the weakest hydrogen bonds. The binding energies (each concerns two hydrogen bonds that are equivalent and related mutually by inverse center) collected in Table 2 show the above-mentioned relation. There are interesting relationships between the interaction energy terms. For the O−H...N systems, the Heitler–London energy is positive because the exchange energy outweighs the electrostatic energy term, while for the O−H...O hydrogen bonds  $E_{H-L}^{(1)}$  is close to zero. Figure 7 shows the relationship between the Heitler–London energy,  $E_{H-L}^{(1)}$ , and the delocalization interaction energy. For the weakest N−H...O hydrogen bonds, the Heitler–London energy is negative. The latter complexes do exist at longer distances where delocalization is not so important but electrostatic energy is sufficient to overcome the exchange repulsion. These results confirm the unique role of the delocalization (or charge transfer) interaction in the hydrogen bond's formation. Particularly, this interaction is very important for strong hydrogen bonds where the short H...B distances are observed and the electrostatic interaction does not outweigh the exchange repulsion. For such strong interactions, the term “covalency” is often attributed. For the sample presented here (Table 2), there is also a very good linear correlation between the binding energy and the delocalization interaction energy term because the linear correlation coefficient amounts to 0.987.

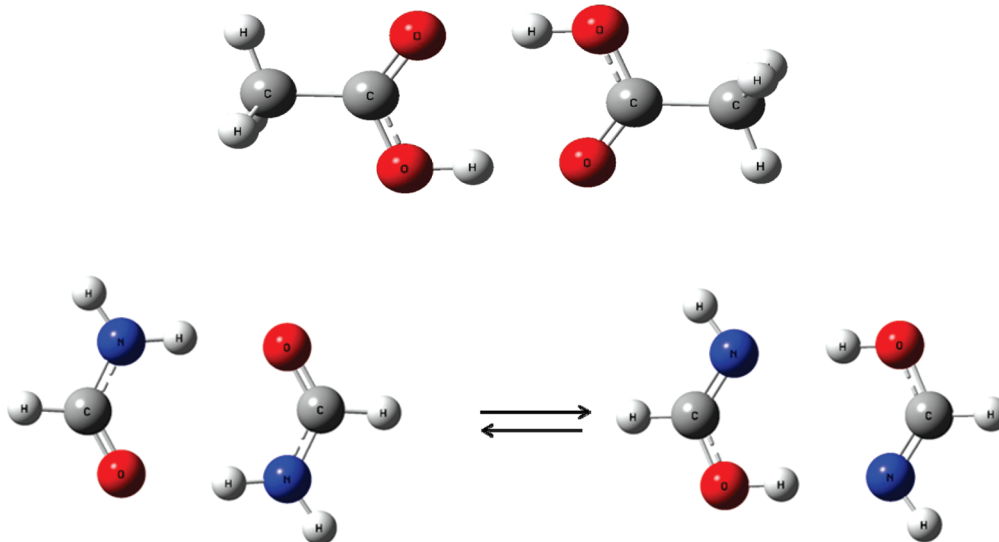
These findings are in line with the other investigations. It was found, using the natural bond orbitals (NBO) analysis, that for numerous hydrogen-bonded systems the charge transfer energy is the major energetic contribution and that the electrostatic attraction is largely canceled by the exchange repulsion.<sup>20</sup> The electrostatic component is a consequence of this charge transfer because if one eliminates CT attraction then stable complexes cannot be formed or they are formed at larger distances between linked monomers.<sup>20</sup> However, one should remember differences between different decomposition schemes.<sup>108–110</sup>



**Table 2.** Decomposition of Interaction Energy for Dimers of Formamide and Its Tautomeric Form as Well as Their Fluoro Derivatives<sup>a</sup>

complex	$E_{\text{H-L}}^{(1)b}$	$E_{\text{ES}}^{(1)}$	$E_{\text{EX}}^{(1)}$	$E_{\text{DEL}}^{(R)}$	$\Delta E^{\text{HF}}$	$E_{\text{CORR}}$	$\Delta E$
N-H...O	-3.6	-23.3	19.7	-8.5	-12.1	0.0	-12.1
N(F)-H...O	-2.5	-22.6	20.1	-9.0	-11.5	0.1	-11.3
N-H...O(C-F)	-4.9	-20.0	15.1	-6.5	-11.4	0.1	-11.3
N(F)-H...O(C-F)	-3.5	-17.3	13.8	-6.1	-9.6	0.3	-9.4
O-H...N	8.8	-45.4	54.2	-26.6	-17.8	-2.7	-20.5
O-H...N(F)	3.6	-32.0	35.6	-17.4	-13.8	-1.9	-15.7
O-H...N(C-F)	13.9	-57.1	71.0	-40.1	-26.2	-3.6	-29.8
O-H...N(F)(C-F)	6.4	-37.7	44.1	-23.8	-17.4	-2.9	-20.3
HCOOH...HCOOH	-0.1	-30.1	30.0	-14.3	-14.4	0.9	-13.6
CH <sub>3</sub> COOH...CH <sub>3</sub> COOH	0.1	-32.2	32.3	-15.2	-15.1	0.5	-14.5
C <sub>4</sub> H <sub>4</sub> NCOOH...C <sub>4</sub> H <sub>4</sub> NCOOH (A)	0.9	-36.7	37.6	-18.6	-17.7	0.6	-17.1
C <sub>4</sub> H <sub>4</sub> NCOOH...C <sub>4</sub> H <sub>4</sub> NCOOH (B)	1.3	-34.8	36.1	-17.3	-16.0	0.3	-15.7
C <sub>4</sub> H <sub>4</sub> NCOOH...C <sub>4</sub> H <sub>4</sub> NCOOH (C)	-3.8	-19.9	16.1	-6.9	-10.7	-1.4	-12.1

<sup>a</sup> The results of studies on dimers of carboxylic acids are included; all energies are in kcal/mol, the MP2/6-311++G(d,p) level of approximation. Results reprinted with permission from ref 121. Copyright 2009 Croatian Chemical Society. N(F): There is fluoro-substituent at nitrogen atom. (C-F): Fluoro-substituent connected with carbon atom. <sup>b</sup> First-order Heitler–London energy term;  $E_{\text{H-L}}^{(1)} = E_{\text{ES}}^{(1)} + E_{\text{EX}}^{(1)}$ .

**Figure 6.** Selected systems of those included in Table 2, acetic acid dimer, formamide dimer, and the dimer of tautomeric form of formamide. Reprinted with permission from ref 121. Copyright 2009 The Croatian Chemical Society.

#### 4. QUANTUM THEORY OF “ATOMS IN MOLECULES” IN ANALYSIS OF HYDROGEN BONDING

The Quantum Theory of “Atoms in Molecules” (QTAIM)<sup>46</sup> is an approach to analyze different intra- and intermolecular interactions,<sup>122</sup> particularly atom–atom interactions such as typical covalent bonds, more or less polarized, but not only, also nonbonded atom–atom contacts, and, what is most important as concerns the present Review, the hydrogen bonds. Briefly speaking, QTAIM is based on the analysis of electron density of any considered system: molecule, ion, more or less complex, ionic pair, complex. Also, greater aggregates and systems may be considered such as biomolecules, particularly proteins, or even crystals.<sup>123,124</sup>

One of the ideas of QTAIM is based on the assumption of transferability of some of the properties of atoms, or groups if they are considered in various systems. However, the other ideas

are also highly inspiring and informative; the more complex and extensive descriptions of QTAIM are presented in the original monographs, chapters, or in reviews.<sup>44–47,125–127</sup>

The analysis of the electron density of the considered system provides the characteristics of various interactions. Hence, the ideas of QTAIM related to the electron density, are roughly presented here. The electron density distribution is mainly affected by interactions between nuclei. The maxima of electron density are attributed to these nuclei (approximately to the atomic positions), and each atom may be described by its boundaries dependent on the balance of forces of the considered system.

The electron density may be considered as a multivariable function of three space coordinates ( $x, y, z$ ); hence, it is not possible to present its view for any system, even a simple one. One can compare the latter situation to a map presentation where on the plane (two dimensions) the third dimension may

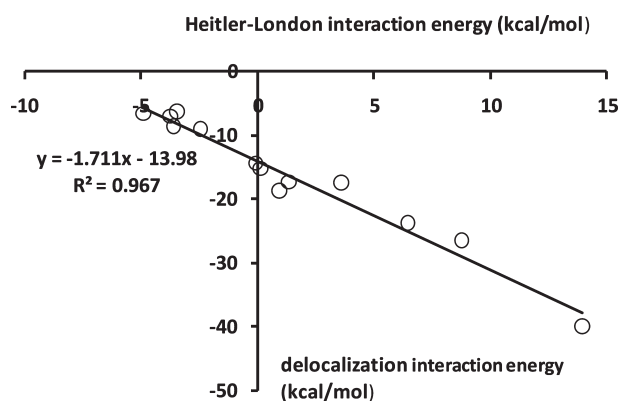


**Figure 7.** The relationship between the Heitler–London interaction energy term and the delocalization energy, both in kcal/mol. Adapted with modifications from ref 121. Copyright 2009 The Croatian Chemical Society.

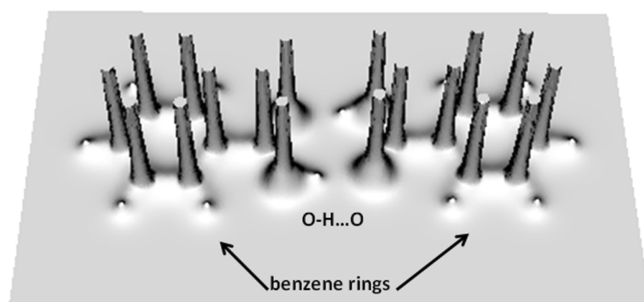


**Figure 8.** The relief map of the electron density of the benzoic acid dimer expressed in the plane of this system. In front, the O–H···O hydrogen bond is visible, and benzene rings are also designated.

be expressed by color, thus indicating, for example, the height of mountains, the sea level, etc. The case of electron density is much more complicated because, being the fourth dimension, it is the function of three coordinates. However, if any plane passes through the considered system (three or even more atoms), then one may consider “in plane electron density” where consequently there is a reduction of one of the dimensions. Thus, for any plane (two dimensions), one can express the electron density (the third dimension) either by color or by applying the so-called relief map. Figure 8 presents the relief map of electron density for the plane passing through benzoic acid dimer. Because the whole system is coplanar or more exactly, nearly so, thus all the maxima of electron density corresponding to the positions of atoms are nicely visible. The maxima corresponding to non-hydrogen atoms are much “higher” than those of hydrogen atoms; thus, the former are cut in the figure at the electron density of 4 au.

There are special points of the considered electron density; these are critical points (CPs), for which the gradient of electron density vanishes (eq 12).

$$\nabla\rho = i\frac{d\rho}{dx} + j\frac{d\rho}{dy} + k\frac{d\rho}{dz} \rightarrow \begin{cases} = \vec{0} & (\text{at critical points and at } \infty) \\ \text{generally } \neq \vec{0} & (\text{at any other point}) \end{cases} \quad (12)$$

The critical points may correspond to the maxima, to the saddle points, or to the local minima. It is possible to distinguish between

various CPs if the second derivatives of the electron density are considered. The nine possible second derivatives of the electron density form the so-called Hessian matrix; if the derivatives are calculated at CP, this matrix may be expressed by eq 13.

$$A(r_c) = \begin{pmatrix} \frac{\partial^2\rho}{\partial x^2} & \frac{\partial^2\rho}{\partial x\partial y} & \frac{\partial^2\rho}{\partial x\partial z} \\ \frac{\partial^2\rho}{\partial y\partial x} & \frac{\partial^2\rho}{\partial y^2} & \frac{\partial^2\rho}{\partial y\partial z} \\ \frac{\partial^2\rho}{\partial z\partial x} & \frac{\partial^2\rho}{\partial z\partial y} & \frac{\partial^2\rho}{\partial z^2} \end{pmatrix}_{r=r_c} \quad (13)$$

The Hessian matrix may be diagonalized via the unitary transformation leading to its diagonal form (eq 14).

$$\Lambda(r_c) = \begin{pmatrix} \frac{\partial^2\rho}{\partial x'^2} & 0 & 0 \\ 0 & \frac{\partial^2\rho}{\partial y'^2} & 0 \\ 0 & 0 & \frac{\partial^2\rho}{\partial z'^2} \end{pmatrix}_{r'=r_c} = \begin{pmatrix} \lambda_1 & 0 & 0 \\ 0 & \lambda_2 & 0 \\ 0 & 0 & \lambda_3 \end{pmatrix} \quad (14)$$

$x'$ ,  $y'$ , and  $z'$  correspond to new coordinates because the unitary transformation may be understood as the rotation of the coordinate system. The diagonal elements of the  $\Lambda$  matrix,  $\lambda_1$ ,  $\lambda_2$ , and  $\lambda_3$ , are named as eigenvalues. The sum of these diagonal elements, the trace of the Hessian matrix of the electron density, expresses the Laplacian (eq 15).

$$\nabla^2\rho(r) = \frac{\partial^2\rho}{\partial x'^2} + \frac{\partial^2\rho}{\partial y'^2} + \frac{\partial^2\rho}{\partial z'^2} = \lambda_1 + \lambda_2 + \lambda_3 \quad (15)$$

Critical points are designated as  $(\omega, \sigma)^{122}$  where  $\omega$  means the rank of CP and  $\sigma$  is its signature. The rank is the number of nonzero eigenvalues of the electron density at the critical point; there are no CPs with rank less than 3 for the equilibrium structure. The signature is the sum of the signs of eigenvalues. There are the following critical points:  $(3, -3)$  corresponds to the local maximum, the attractor;  $(3, -1)$  is the bond critical point (BCP);  $(3, +1)$  is the ring critical point (RCP); and  $(3, +3)$  is the local minimum, that is, the cage critical point (CCP). The analysis of BCP provides information on the nature of interatomic interaction.<sup>128</sup> For shared interactions like covalent and polarized bonds, the Laplacian of electron density is negative because there is concentration of electron density within the atom–atom region. For the interactions between closed-shell systems like van der Waals interactions, ionic ones, and hydrogen bonds, there is the depletion of electron charge within the atom–atom region, and hence the Laplacian is positive. Thus, the sign of the Laplacian may indicate the kind of interaction. There is a very interesting situation in the case of hydrogen bonding where usually the Laplacian is positive; however, for very strong hydrogen bonds like those in  $\text{H}_5\text{O}_2^+$  or  $(\text{FHF})^-$ , the Laplacians are negative, respectively, for both  $\text{H}\cdots\text{O}$  or  $\text{H}\cdots\text{F}$  contacts. This is the strong evidence for the covalent character of hydrogen bonding.

The more detailed descriptions of QTAIM are given in the other studies; for example, Matta and Boyd presented brief descriptions of the basic assumptions of that approach.<sup>125,126</sup> The bond critical point (BCP) is the minimum of electron density on the bond path. For the structure in energetic minimum, the bond path (BP) is the line of maximum electron density connecting two interacting atoms.<sup>122</sup> One may imagine, looking at Figure 8, the summits of two mountains (two attractors of the electron density); somebody would like to climb from one summit to the other choosing the shortest and also “the highest” way. Such climbing is possible through the pass (the line of the greatest electron density). There is a special place, the minimum height on the pass. Similarly, there is the point with the minimum value of electron density on the bond path. This is the bond critical point. The bond paths are usually the straight lines connecting interacting atoms (attractors). However, special cases are known where these connections are strongly curved. The diborane molecule and other boron species are examples of such cases.<sup>129</sup> It is very important that the meaning of the bond path is not the same as that of the bond.<sup>130,131</sup> The BP indicates that two atoms are bonded. The bond paths show the preferable interactions, which may be also bonds in the chemical sense.<sup>130–133</sup>

Similarly, one can imagine the ring critical point, corresponding to a situation of a valley between mountains as the place situated at the lowest height. There are three RCPs for the benzoic acid dimer. Figure 9 presents the molecular graph of that complex where the positions of all critical points are indicated as well as the bond paths between attractors. There are RCPs for benzene rings surrounded by carbon atoms' attractors (six mountains) and one RCP within the eight-member ring of carboxylic groups created due to two equivalent hydrogen bonds. These RCPs are designated by yellow circles in Figure 9.

There are other useful terms derived from the QTAIM approach, for example, gradient paths being the lines of the steepest increase of electron density, and determining interatomic boundaries. The interatomic boundary consists of a bundle of gradient paths originating at infinity and terminating at the critical point. Figure 10 presents the contour map of the electron density for the benzoic acid dimer with gradient paths indicated.

Recently, there are controversies<sup>134,135</sup> and discussions<sup>136–140</sup> concerning the meaning of the bond path. Sometimes, there is the misunderstanding connected with the attributing of BP to any pair of interacting atoms. Popelier explains<sup>122</sup> that the bond path exists for the structure being in an energy minimum; in other cases, the electron density accumulation between nuclei is not sufficient to be bonded. In such a case, the line of the greatest electron density connecting the interacting atoms is named as the atomic interaction line (AIL).

Another problem is the existence of the so-called H–H stabilizing interactions existing for systems being in minima,<sup>126,141,142</sup> for example, for phenanthrene molecule, dibenz[*a,j*]anthracene, or 1-phenyl-0-carborane. There are also other numerous examples of such interactions. It seems that such H–H interactions, different from dihydrogen bonds, exist for the crystal structures of [4-((*E*)-but-1-enyl)-2,6-dimethoxyphenyl] pyridine-3-carboxylate and [4-((*E*)-pent-1-enyl)-2,6-dimethoxyphenyl]pyridine-3-carboxylate as well as for the styrene molecule.<sup>143</sup> Very recently, the concept of H–H stabilizing interactions was criticized, which roused polemics and discussions.<sup>134–136</sup>

It is not the aim of this Review to discuss various concepts and polemics; the recent study of Bader explains clearly the physical meaning of the bond path.<sup>131</sup> There is no doubt that the QTAIM

provides powerful tools and techniques to investigate various interactions. For example, the characteristics of critical points provide additional information on the nature of interactions. The topological criteria of the existence of hydrogen bonding were proposed by Koch and Popelier.<sup>144</sup> They may be summarized as follows:

- (1) There is the bond path between the hydrogen atom and proton acceptor with the bond critical point on it (BCP of H···B contact).
- (2) There should be a relatively high value of the electron density at the H···B BCP ( $\rho_{\text{H}\cdots\text{B}}$ ), in the range 0.002–0.034 au.
- (3) The Laplacian of the electron density at H···B BCP should be within the 0.024–0.139 au range.
- (4) Mutual penetration of the hydrogen and acceptor atoms should be observed upon hydrogen-bonding formation. Such penetration may be evaluated in the following way: the nonbonded radii of both atoms ( $r_{\text{B}}^0, r_{\text{H}}^0$ ) are compared to the corresponding radii within the H-bonded system ( $r_{\text{B}}, r_{\text{H}}$ ). The nonbonded radius  $r^0$  is defined as the distance between the nucleus of the considered atom and a fixed electron density contour; this fixed value is usually assumed to amount to 0.001 au. The radii within H-bonded systems are estimated as distances between the considered positions of nuclei and the position of H···B BCP. Finally, the total penetration may be separated into contributions of hydrogen and acceptor atoms:  $\Delta r_{\text{H}}^0 = r_{\text{H}}^0 - r_{\text{H}}$  and  $\Delta r_{\text{B}}^0 = r_{\text{B}}^0 - r_{\text{B}}$ .
- (5) There is a loss of electron charge of the hydrogen atom.
- (6) One can observe energetic destabilization of the hydrogen atom because there is a positive difference between the total energy of hydrogen atom within the complex and the energy of H-atom not involved in hydrogen bonding.
- (7) The decrease of dipolar polarization of the hydrogen atom is observed as a result of complexation.
- (8) There is a decrease of the hydrogen atom volume after hydrogen-bonding formation.

These criteria may seem to be equivocal. This concerns the ranges of electron density and its Laplacian at H···B BCP,  $\rho_{\text{H}\cdots\text{B}}$  and  $\nabla^2\rho_{\text{H}\cdots\text{B}}$ , respectively. For very strong hydrogen bonds  $\nabla^2\rho_{\text{H}\cdots\text{B}}$  is negative and hence outside the range proposed; the same concerns  $\rho_{\text{H}\cdots\text{B}}$ , which for such interactions is close in values to the values typical for covalent bonds.<sup>83,145–148</sup>

The other characteristics may be applied to describe the considered bond critical point and further the atom–atom interaction. There are well-known relationships between energetic topological parameters and the Laplacian of electron density at critical point (expressed in atomic units, eq 16, virial equation, and eq 17).

$$\frac{1}{4} \nabla^2 \rho = 2G_C + V_C \quad (16)$$

$$H_C = V_C + G_C \quad (17)$$

$G_C$ ,  $V_C$ , and  $H_C$  are the kinetic, potential, and total electron energy densities at critical point, respectively.  $G_C$  is a positive value, whereas  $V_C$  is a negative one. One can see that if the modulus of the potential energy outweighs two times the kinetic energy, then the Laplacian is negative (eq 16). This implies the covalent character of interaction, and, as it was mentioned here, it



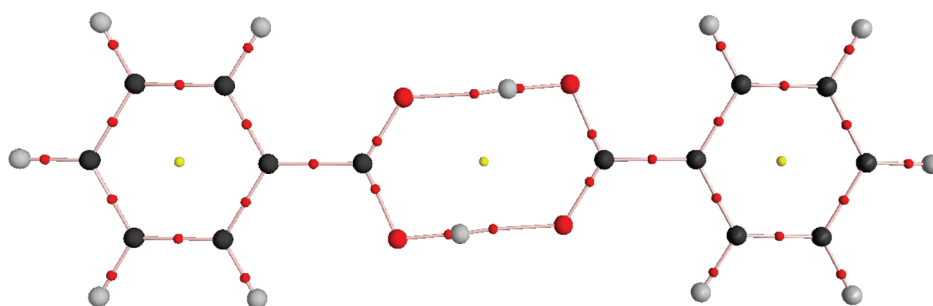


**Figure 9.** Molecular graph of the benzoic acid dimer. All critical points are shown, as are attractors by greater circles: carbon atoms, black; hydrogen atoms, gray; oxygen atoms, red; BCPs, small red circles; RCPs, yellow ones. The bond paths are also shown.

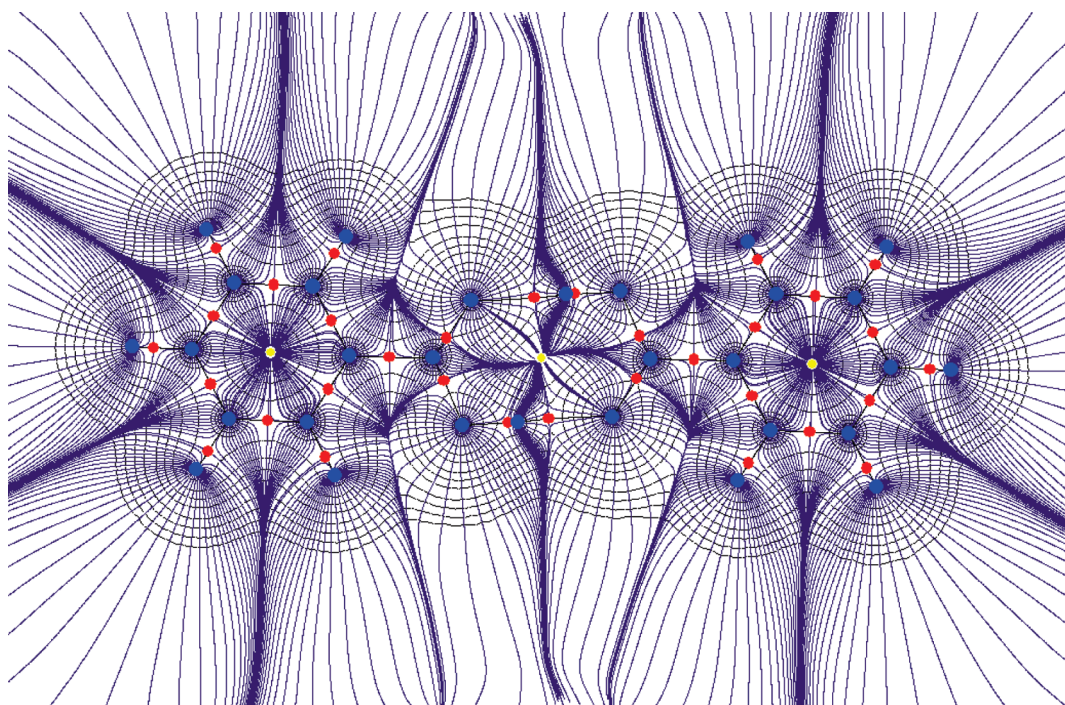


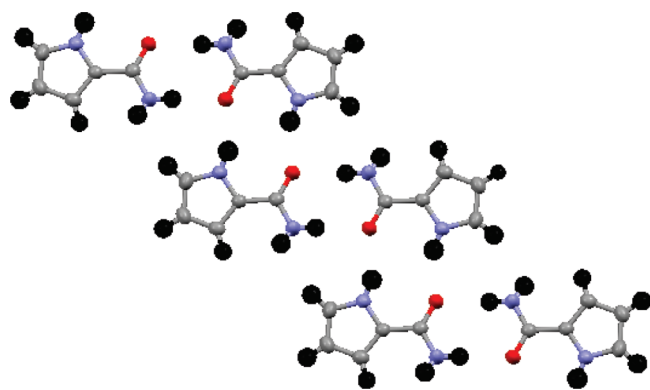
**Figure 10.** The contour electron density map for the benzoic acid dimer; attractors are designated by blue circles, BCPs by small red circles, and RCPs by yellow ones, and the gradient paths are also presented by violet lines. This contour map was obtained for planar geometry of benzoic acid dimer to obtain the picture with visible gradient paths' lines. There is only a slight energy difference between the fully optimized geometry of the dimer and the planar configuration (less than 0.05 kcal/mol for B3LYP/6-311+G(d,p) level of calculations).

may concern covalent bonds as well as very strong hydrogen bonds. However, there are such interactions where the modulus of the potential energy only one time outweighs the kinetic energy; in such a case, the Laplacian is positive, but  $H_C$  is negative (eq 17). Rozas et al. have classified hydrogen bonds on the basis of  $\nabla^2\rho_C$  and  $H_C$  values.<sup>149</sup> Weak and medium in strength hydrogen bonds show both positive  $\nabla^2\rho_C$  and  $H_C$  values. For strong H-bonds,  $\nabla^2\rho_C$  is positive and  $H_C$  is negative. For very strong hydrogen bonds,  $\nabla^2\rho_C$  and consequently  $H_C$  values are negative.

Cremer and Kraka involved the energetic topological parameters into the classification of interactions much earlier.<sup>150</sup> They found positive Laplacian values for covalent double and triple CO bonds. This implies that the condition of the sign of Laplacian to classify any interaction as covalent is not satisfactory. They involved eqs 16 and 17 into their classification. The sign of the total electron energy density at BCP ( $H_C$ ) determines whether or not the local potential or kinetic electron energy density

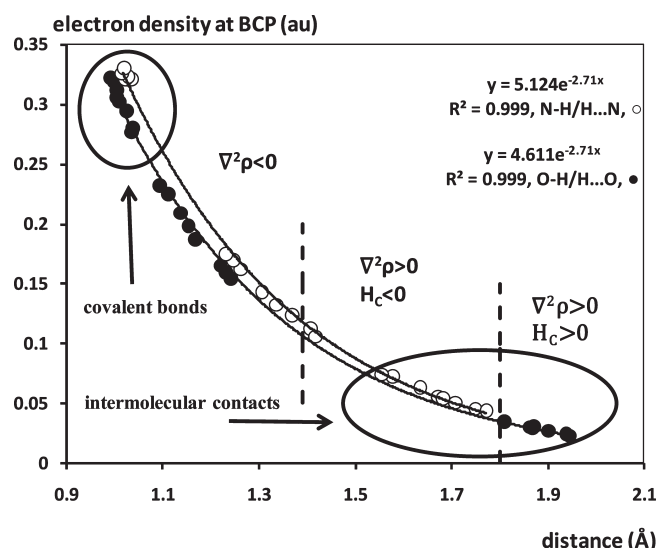
dominates at the considered BCP. If  $H_C$  is negative, then the local potential electron energy dominates and the localization of electron density at BCP has a stabilizing impact on the species; when  $H_C$  is positive, then the electron localization has a destabilizing impact on the system. Thus, Cremer and Kraka stated that any interaction may be covalent for a positive value of the Laplacian, but  $H_C$  has to be negative. This means that if the Rozas et al. classification of hydrogen bonds is considered, then covalency is attributed not only to very strong interactions but also to strong hydrogen bonds ( $H_C$  negative,  $\nabla^2\rho_C$  positive). Some of the authors claim that the latter case corresponds to partial covalency of the interaction.<sup>151,152</sup>

Numerous correlations and dependencies between the energetic parameters derived from the Bader theory (eqs 16 and 17) and the other parameters of the analyzed systems were found.<sup>153–165</sup> For example, metal–oxide interactions were analyzed, and the monotonic changes of  $H_C$ ,  $G_C$ , and  $V_C$  were found if the oxygen–metal distance is changing.<sup>166</sup>



**Figure 11.** Fragment of the crystal structure of pyrrole-2-carboxamide (PyCa) determined by single-crystal X-ray diffraction; one can observe dimers of PyCa connected through  $\text{N-H}\cdots\text{O}$  hydrogen bonds.

There are relationships between different parameters if dimers of amides are analyzed. Recently, the crystal and molecular structure of pyrrole-2-carboxamide (PyCa) was determined by single crystal X-ray diffraction.<sup>167</sup> It was found that PyCa molecules form centrosymmetric dimers in crystals (Figure 11) with two equivalent  $\text{N-H}\cdots\text{O}$  hydrogen bonds existing between amide groups because the eight-member pseudo ring is formed with the inversion center within. One can see that *s-cis* conformers exist in the crystal structure of PyCa. For the *s-cis* conformer, the  $\text{C=O}$  carbonyl group is at the same side as the  $\text{N-H}$  bond of the pyrrole ring (Figure 11); for the *s-trans* conformer, the  $\text{C=O}$  group is at the opposite side of the  $\text{N-H}$  bond of the pyrrole ring. The  $^1\text{H}$  and  $^{13}\text{C}$  NMR spectra of pyrrole-2-carboxamide indicate the existence of both conformers in DMSO solution. The population of these forms was calculated from the integral intensity of carbon signals in the  $^{13}\text{C}$  NMR spectra. It was found that *s-cis* pyrrole-2-carboxamide is the dominant form (70%). Also, the IR spectrum confirms the existence of both forms in the DMSO solution. Hence, the appropriate B3LYP/6-311++G(d,p) calculations were performed for centrosymmetric dimers of both forms. Optimizations of the dimers were carried out with symmetry constraints to keep the inversion center within the eight-member ring mentioned above. The optimized species correspond to minima because no imaginary frequencies are observed. Similar calculations were performed for the derivatives of PyCa, where the  $-\text{NFH}$  group is inserted instead of the  $-\text{NH}_2$ ; two related dimers with the same symmetry constraints as for the source systems were analyzed. The calculations for the simple formamide dimer (Figure 6) and its fluorine centrosymmetric analogs were also carried out.<sup>120,121</sup> For all these dimers, PyCa, formamide, and their fluorine derivatives, the double proton transfer  $\text{N-H}\cdots\text{O} \rightleftharpoons \text{N}\cdots\text{H}-\text{O}$  reaction was considered. This means that the same type of calculations was performed for the centrosymmetric conformations with two equivalent  $\text{O-H}\cdots\text{N}$  hydrogen bonds. Figure 6 shows formamide dimer with  $\text{N-H}\cdots\text{O}$  hydrogen bonds and its centrosymmetric analogue possessing  $\text{O-H}\cdots\text{N}$  interactions. For all systems and their analogues, the transition states (TSs) were found, and for each TS, the imaginary frequency corresponding to the double proton transfer process was detected. For the sample of dimers described here, numerous relationships were found between geometrical, topological, and energetic characteristics of hydrogen bonding.



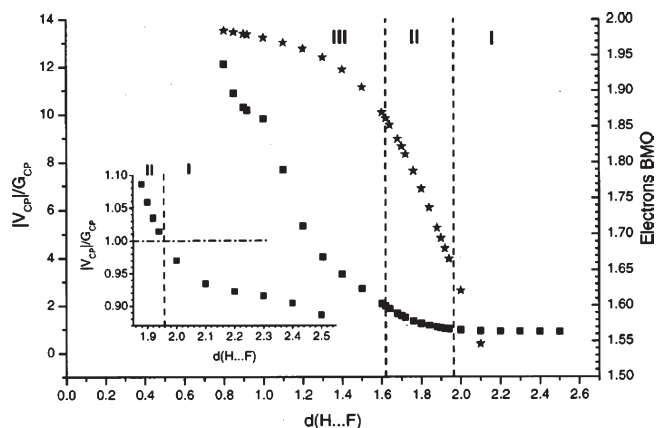
**Figure 12.** Dependence between the atom–atom distance (in Å),  $\text{H}\cdots\text{N}$  ( $\text{N-H}$ ) or  $\text{H}\cdots\text{O}$  ( $\text{O-H}$ ), and electron density at the corresponding BCP (in au). Solid circles correspond to the  $\text{O,H}$  pair of interacting atoms, and the open circles correspond to the  $\text{N,H}$  pair.

Figure 12 presents the relationship between the atom–atom distance and the electron density at the corresponding BCP. This concerns the above-described amides' dimers and their analogues. Two kinds of atom–atom pairs are taken into account,  $\text{H/N}$  and  $\text{H/O}$ . For both pairs, the following interactions within the  $\text{N-H}\cdots\text{O}$  and  $\text{O-H}\cdots\text{N}$  hydrogen bridges are considered: typical covalent bonds,  $\text{O-H}$  and  $\text{N-H}$  as well as intermolecular contacts, and  $\text{H}\cdots\text{N}$  and  $\text{H}\cdots\text{O}$ . Additionally, the interactions of transition states are included. For both pairs of atoms, the exponential relationships were found (Figure 12). It reflects the exponential dependence between the distance and the interaction energy because the electron density at BCP is usually a good description of the strength of interaction. The correlations between the binding energy and  $\rho_{\text{C}}$  were presented in numerous studies.<sup>84,155,157</sup> Generally better correlations are detected for homogeneous samples of species. For example,  $\text{R-C}\equiv\text{N}\cdots\text{H-F}$  and  $\text{R-C}\equiv\text{N}\cdots\text{H-Cl}$  complexes were analyzed with numerous  $\text{R}$ -substituents.<sup>168</sup> Two linear correlations for two samples differing in the proton donor system ( $\text{HF}$  or  $\text{HCl}$ ) were found for the dependence between proton–acceptor distance and the binding energy. If the dependence between the  $\text{H}\cdots\text{B}$  distance and electron density is considered, then a linear correlation is found for all complexes (both  $\text{HF}$  and  $\text{HCl}$  donors). This means that the topological parameters (in this case, the electron density at BCP) are better descriptors of H-bond strength than the binding energy because the former may be applied to heterogeneous samples of complexes. For this  $\text{H}\cdots\text{B}$  versus  $\rho_{\text{C}}$  relationship, the linear correlation was detected inasmuch the narrow range of  $\text{H}\cdots\text{B}$  distances is considered with the same kind of acceptor center, nitrogen. However, Figure 12 presents the dependences for a wide range of  $\text{H}\cdots\text{B}$  distances concerning typical covalent bonds, intermolecular contacts, and contacts for transition states. Hence, two nonlinear exponential relationships were found for  $\text{N}$  and  $\text{O}$  centers. Ellipsoidal shapes in Figure 12 indicate the regions of covalent bonds ( $\text{NH}$  and  $\text{OH}$ ) and intermolecular interactions ( $\text{H}\cdots\text{O}$  and  $\text{H}\cdots\text{N}$ ). The remaining results represent all contacts of transition states. The results presented in this figure are interesting because the division into

three regions, covalent bonds, TS-contacts, and intermolecular interactions, includes the division into regions connected with QTAIM parameters. For example, for both positive  $\nabla^2\rho_C$  and  $H_C$  values, we have all  $H\cdots O$  intermolecular interactions of  $N-H\cdots O$  hydrogen bridges. For  $\nabla^2\rho_C$  positive and  $H_C$  negative, the interactions are at least partially covalent in nature. The latter ones are all  $H\cdots N$  interactions of  $O-H\cdots N$  hydrogen bonds and also two  $H\cdots N$  interactions of transition states. One can see negative values of Laplacians for the remaining covalent  $H\cdots N$  and  $H\cdots O$  interactions. Summarizing, almost all hydrogen bonds' contacts of transition states are covalent ones because they have negative Laplacians. What is most interesting, for  $O-H\cdots N$  hydrogen bonds for all  $H\cdots N$  BCPs there are negative values of  $H_C$ ; this indicates that these hydrogen bonds are at least partially covalent. Another interesting observation is that all  $O-H\cdots N$  hydrogen bonds are stronger than the  $N-H\cdots O$  counterparts, while hydrogen bonds of transition states are the strongest ones. If one considers total energies of the corresponding species, then the amides' dimers with  $N-H\cdots O$  hydrogen bonds are characterized by the lowest energies, their counterparts with  $O-H\cdots N$  hydrogen bonds have higher total energies, and it is well-known that transition states are characterized by the highest total energies. This is in agreement with the Leffler–Hammond postulate<sup>169,170</sup> because hydrogen bonds are stronger for systems being closer to the transition state. A similar analysis was performed for the intramolecular  $N-H\cdots O$  resonance-assisted hydrogen bonds, and the results being in line with the Leffler–Hammond postulate were found.<sup>171–174</sup> The enhancement of hydrogen bonds by  $\pi$ -electron delocalization is observed for such complexes as carboxylic acid dimers,<sup>119,175,176</sup> malonaldehyde derivatives,<sup>30,31,177–180</sup> and the other systems<sup>181,182</sup> where short  $H\cdots B$  (proton–acceptor) distances were found, relatively high values of the electron density at the corresponding BCP, and very often negative values of Laplacians or at least negative  $H_C$  values. Some of these species are often classified as resonance assisted hydrogen bonds (RAHBs), especially malonaldehyde derivatives, but also carboxylic acid dimers are sometimes assigned to intermolecular RAHB systems.<sup>175</sup>

The other indices derived from the Bader theory were introduced to systematize various interactions, particularly to estimate the degree of covalency. For example, Espinosa and co-workers analyzed a wide range of  $H\cdots F$  interactions,<sup>183</sup> from short ones usually attributed to covalent bonds to longer  $H\cdots F$  distances of hydrogen bonds, or even much weaker van der Waals interactions. Figure 13 shows the relationship between  $H\cdots F$  distance and the parameter defined as  $|V_C|/G_C$ . According to eqs 16 and 17, the latter ratio is positive because the modulus of  $V_C$  is considered and  $G_C$  is always positive. This ratio is greater than 2 for negative values of the Laplacian ( $\nabla^2\rho_C$ ) attributed to covalent bonds (region III, Figure 13); it is in the range (1,2) for positive Laplacians and negative  $H_C$  values, which corresponds to partially covalent bonds (region II, Figure 13); and the ratio is smaller than 1 (region I, Figure 13) for weak closed-shell interactions where both  $\nabla^2\rho_C$  and  $H_C$  are positive. The borderline between covalent and partially covalent systems occurs for the  $H\cdots F$  distance of 1.62 Å, whereas the border between the latter systems and the weakest interactions is for 1.96 Å.

There is another parameter presented in Figure 13, bond molecular orbital (BMO) electrons calculated from the Natural Bond Orbitals (NBO) method.<sup>20</sup> The BMO electrons for  $F\cdots H$  interactions were calculated in the following way.<sup>183</sup> One may



**Figure 13.** Relationship between  $H\cdots F$  distance (Å) and the  $|V_C|/G_C$  parameter (■); the dependence between  $H\cdots F$  distance and BMO electrons (★) is also included. The data corresponding to the 1.85–2.55 Å range of the  $H\cdots F$  distance are focused. Reprinted with permission from ref 183. Copyright 2002 American Institute of Physics.

assume that the interaction is along the Z-axis. Five molecular orbitals (MOs) are created for  $F\cdots H$  interaction. Four MOs are built only from the fluorine atomic orbitals, and each molecular orbital is occupied by two electrons coming from  $1s(F)$ ,  $2p_y(F)$ ,  $2p_x(F)$  orbitals and a hybrid of  $2s(F)$  and  $2p_z(F)$ . One bonding molecular orbital (BMO) positioned according to the Z-direction is built from  $2s(F)$ ,  $2p_z(F)$ , and  $1s(H)$  atomic orbitals. Hence,  $1\sigma$  and  $2\sigma$   $H-F$  bonding orbitals are created from  $1s(F)$  atomic and mixing of  $2s(F)$ ,  $2p_z(F)$ , and  $1s(H)$  atomic orbitals, respectively. BMO electrons are those participating in the formation of the  $H-F$  bond. Figure 13 shows that the number of BMO electrons is equal to 2 for the  $F\cdots H$  distance corresponding to the  $H-F$  bond length of hydrogen fluoride molecule. The BMO electrons' number decreases if the  $H\cdots F$  distance increases, but even for the distance equal to 2 Å it is greater than 1.6.

One can also observe (Figure 13) the negative values of the Laplacian ( $|V_C|/G_C$  ratio greater than 2) for  $H\cdots F$  distances being far from the  $H-F$  bond length (distances shorter than 1.62 Å). If negativity of  $H_C$  is attributed to covalency, then the latter characteristic arises for  $H\cdots F$  distances as only slightly shorter than 2 Å. These findings show that the covalency is connected not only with very strong hydrogen bonds and short  $H\cdots B$  distances, but it covers a wide range of interactions.

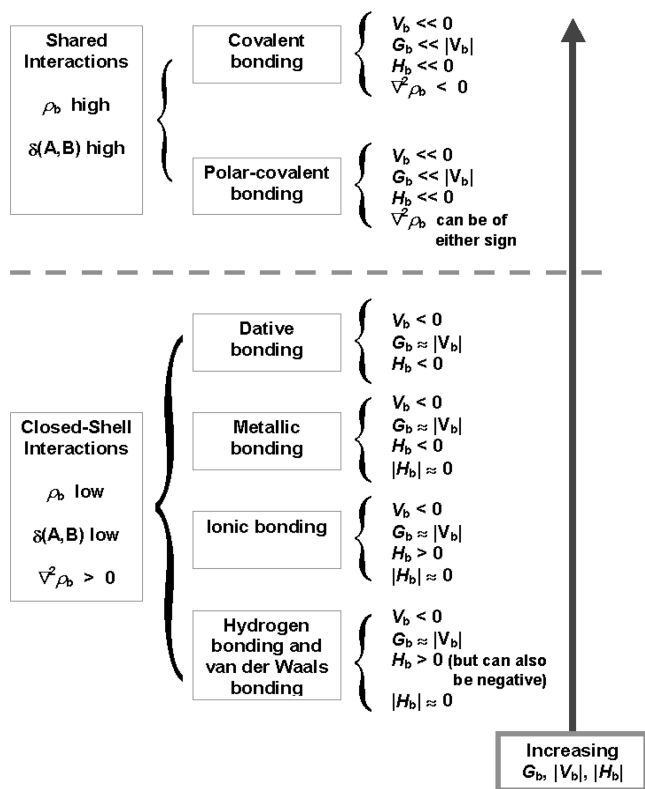
The use of localization  $\lambda(A)$  (eq 18) and delocalization  $\delta(A, B)$  (eq 19) indices<sup>184,185</sup> may provide additional information on the nature of interactions.

$$\lambda(A) = - \int_A (2\Gamma(r_1, r_2) - \rho(r_1)\rho(r_2)) dr_1 dr_2 \quad (18)$$

$$\delta(A, B) = - 2 \int_{A, B} (2\Gamma(r_1, r_2) - \rho(r_1)\rho(r_2)) dr_1 dr_2 \quad (19)$$

$\rho(r)$  and  $\Gamma(r_1, r_2)$  are one- and two-electron densities, respectively, and the integrations are performed through one or two atomic basins. Briefly speaking, the localization index  $\lambda(A)$  corresponds to the number of electrons that are localized in one atom, while the delocalization index  $\delta(A, B)$  measures the number of electrons delocalized between two atoms (A and B). In other words, the latter parameter may be treated as being related to the degree of covalency or directly as the number of



Chart 2.<sup>a</sup>

<sup>a</sup>Reprinted with permission from ref 126. Copyright 2006 Springer. Reprinted with permission from ref 189. Copyright 2000 American Chemical Society.

shared electrons. However, for the sample of various H-bonded systems (for a nonhomogeneous sample), a few relationships between the delocalization index and the parameters corresponding to hydrogen bond strength were analyzed, and such correlations appeared rather poor.<sup>186</sup>

The evidence of the covalent character of hydrogen bonding was detected not only from results of calculations. The QTAIM analyses on experimental electron densities were performed for different crystal structures. It was found in several structures that for A–H···B hydrogen bonds for both A–H and H···B interactions the Laplacian of electron density at the corresponding bond critical points was negative. That was found for the intramolecular O–H···O hydrogen bond of benzylacetone,<sup>48,187</sup> or for N–H···N systems of some of proton sponges.<sup>188</sup>

Chart 2 shows the classification of interactions based<sup>126,189</sup> on the QTAIM parameters: the electron density at BCP and its Laplacian, the total electron energy density at BCP, the delocalization index, etc. (the subscript “b” is applied in the chart instead of the “C” subscript occurring in this Review). Different types of interactions, among them hydrogen bonds, are presented (Chart 2). The characteristics collected in Chart 2 correspond to the medium in strength hydrogen bonds because strong and particularly very strong hydrogen bonds often have the characteristics of covalent bonds.

One can see that the Bader theory provides additional parameters, which allow one to characterize interactions, among them hydrogen bonds. Traditional investigations were based on analyses of geometrical parameters such as the A–H bond

length, H···B and A···B distances, and also A–H···B angle, which may be calculated if the latter distances are known. Chart 3 presents the molecular graph of the FH···NH<sub>3</sub> complex where a few parameters useful to describe hydrogen bonding are indicated. It is shown that BCP’s characteristics of the H···B contact as well as of the proton-donating A–H bond may be taken into account. The characteristics of H···B BCP were earlier described in this Review. However, the A–H bond critical point properties may also be considered. Because A–H is a covalent bond, thus its elongation as a result of H-bond formation is connected with a decrease of electron density at A–H BCP. Similarly, there is an increase of the Laplacian (a decrease of its modulus) and consequently a decrease of  $|V_C|$  and  $G_C$ .

A measure of the hydrogen-bonding strength, named as a “complex parameter”, based on geometrical and topological parameters of the A–H proton-donating bond, was introduced and calculated for a sample of different hydrogen-bonded complexes.<sup>84,190</sup>

$$\Delta_{\text{com}} = \left\{ \left[ \frac{(r_{\text{A-H}} - r_{\text{A-H}}^0)/r_{\text{A-H}}^0}{\rho_{\text{A-H}}^0} \right]^2 + \left[ \frac{(\rho_{\text{A-H}}^0 - \rho_{\text{A-H}})/\rho_{\text{A-H}}^0}{\nabla^2 \rho_{\text{A-H}}^0} \right]^2 + \left[ \frac{(\nabla^2 \rho_{\text{A-H}} - \nabla^2 \rho_{\text{A-H}}^0)/\nabla^2 \rho_{\text{A-H}}^0}{\rho_{\text{A-H}}^0} \right]^2 \right\}^{1/2} \quad (20)$$

where  $r_{\text{A-H}}$ ,  $\rho_{\text{A-H}}$ , and  $\nabla^2 \rho_{\text{A-H}}$  correspond to the proton-donating bond involved in H-bonding, the bond length, electronic density at A–H bond critical point, and the Laplacian of this density, respectively;  $r_{\text{A-H}}^0$ ,  $\rho_{\text{A-H}}^0$ , and  $\nabla^2 \rho_{\text{A-H}}^0$  correspond to the same parameters of the A–H bond not involved in H-bond formation or any other nonbonded interaction. It seems that the  $\Delta_{\text{com}}$  parameter may be useful because the normalization of the characteristics of the proton-donating bond in relation to the same characteristics of the uninvolved in additional interactions and thus undisturbed proton-donating bond allows one to consider samples of heterogeneous systems. Figure 14 presents the relationship between the complex parameter  $\Delta_{\text{com}}$  and the binding energy for a sample of various complexes. The following complexes were taken into account: (FHF)<sup>−</sup> (with covalent hydrogen bonding,  $\nabla^2 \rho_C < 0$  for both H···F contacts), the interactions where  $H_C$  is negative and which are often classified as partially covalent: (FHC1)<sup>−</sup>, F–H···H–Li (dihydrogen bond), H<sub>2</sub>CO···HF, H<sub>2</sub>O···HF, H<sub>3</sub>N···HF, (HCOOH)<sub>2</sub>, H<sub>3</sub>N···H<sub>2</sub>O; for the other complexes there are weaker hydrogen bonds with positive values of  $H_C$ , these are (H<sub>2</sub>O)<sub>2</sub>, (C<sub>2</sub>H<sub>2</sub>)<sub>2</sub>, C<sub>2</sub>H<sub>2</sub>···HF, H<sub>2</sub>O···HCCH, C<sub>2</sub>H<sub>2</sub>···H<sub>2</sub>O, and HCCH···HLi. The calculations for these complexes were performed at MP2/6-311++G(d,p) level of approximation. There is a good linear correlation between the complex parameter and the binding energy (the linear correlation coefficient  $R = 0.98$ ). Figure 14 presents this dependence where the (FHF)<sup>−</sup> is excluded because it is far from the range of the other species. Despite this exclusion,  $R$  is still high and even has the same value ( $R = 0.98$ ). There is the border designated within Figure 14 between hydrogen bonds possessing the characteristics of covalent interaction and rather weak closed-shell interactions.

The complex parameter expresses the covalency of hydrogen-bonding interaction because the higher values of  $\Delta_{\text{com}}$  simply correspond to a greater lengthening of the proton donating bond, which corresponds to shorter proton–acceptor distances (see previous section). This is shown in Figure 14: the higher are  $\Delta_{\text{com}}$  values, the greater are binding energies and negative values of the total electron energy density at the H···B BCP,  $H_C$ .

Chart 3

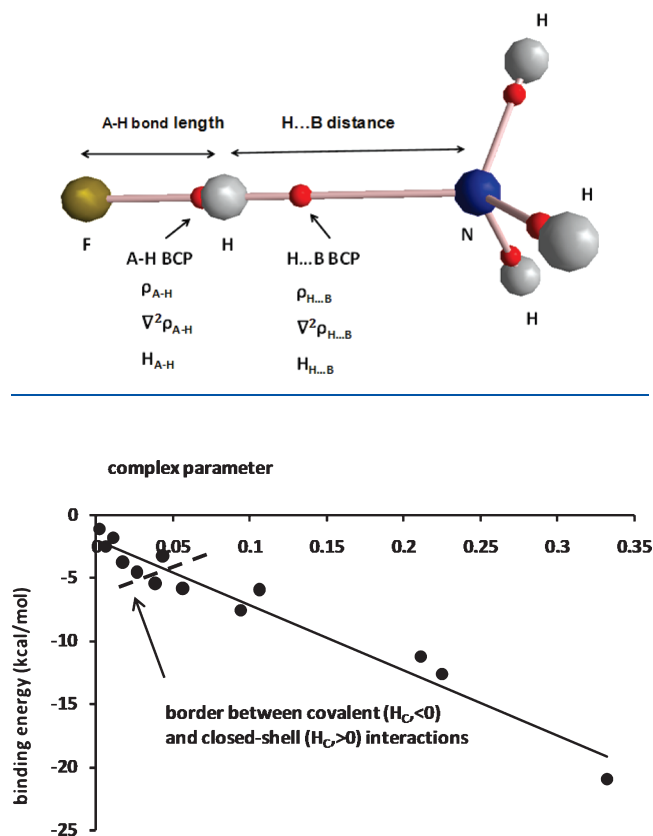


**Figure 14.** The relationship between the complex parameter  $\Delta_{\text{com}}$  and the binding energy (kcal/mol).

One can see that the square of expression 20 may be divided into three terms; the first one is connected with geometrical parameters, the second one is connected with electron densities, and the third one is based on Laplacians. It was shown that if only one term is taken into account, then it still expresses the strength of hydrogen bonding. A good linear correlation was found between the binding energy and the term that corresponds to the lengthening of the proton-donating bond (eq 21) for a sample of complexes bound by  $\text{F}-\text{H}\cdots\text{N}\equiv\text{C}-\text{R}$  and  $\text{Cl}-\text{H}\cdots\text{N}\equiv\text{C}-\text{R}$  hydrogen bonds, where R is a simple substituent.<sup>168</sup>

$$\Delta_{\text{geo}} = (r_{\text{A-H}} - r_{\text{A-H}}^0)/r_{\text{A-H}}^0 \quad (21)$$

In some cases,  $\Delta_{\text{com}}$  cannot be applied because there are certain systems, which, although classified as hydrogen bonds, do not possess their typical characteristics. There are the so-called blue-shifting hydrogen bonds<sup>191–198</sup> where there occurs a contraction of the proton-donating A–H bond as a result of complexation. For these interactions, a decrease of the stretching vibration frequency is observed (the blue-shift) as compared to the noninteracting species. It seems that for such interactions the use of the complex parameter is not justified.

Apart from QTAIM, there is another topological approach based on the electron localization function (ELF). This is a local scalar function related to the Fermi hole curvature, proposed by Becke and Edgecombe and usually denoted by  $\eta(r)$ .<sup>199</sup> The ELF measures the excess kinetic energy density due to the Pauli repulsion,<sup>200</sup>

and it is close to unity if such repulsion is weak, which corresponds to the single electron or opposite spin-pair. If the probability to find the same-spin electrons close together is high, thus the ELF tends to zero. Because ELF is a scalar, thus its gradient field may be performed to locate its attractors (maxima) as well as the corresponding basins.<sup>201</sup> There are two types of basins: the core basins designated by C with the atom symbol in parentheses (the nuclei with  $Z > 2$  may be taken into account) and the valence basins designated by V with the list of atoms in parentheses. The latter ones are characterized by the synaptic order, that is, the number of core basins with which they share a common boundary; a proton as a formal core increases the synaptic order by one. The idea of the localization domains directly connected with basins is also very important for this approach.<sup>202,203</sup> The picture of molecule provided by ELF approach is in agreement with the Lewis valence theory.

Different kinds of hydrogen bonds and related interactions were analyzed by ELF.<sup>204,205</sup> Figure 15 presents  $\eta(r)$  localization domains for selected systems. For diborane,  $\text{B}_2\text{H}_6$ , the  $\text{V}(\text{B},\text{H},\text{B})$  basins link two boron centers belonging to the atomic valence shell of boron atoms, and thus it is not hydrogen-bonding interaction. In  $\text{FH}\cdots\text{N}_2$ ,  $\text{V}(\text{F},\text{H})$  basin belongs to the fluorine valence shell sharing a boundary with  $\text{V}(\text{N})$  basin, which is typical for hydrogen bonding; the similar situation occurs for malonaldehyde,  $\text{C}_3\text{H}_4\text{O}_2$ , where there are  $\text{V}(\text{O},\text{H})$  and  $\text{V}(\text{O})$  basins.  $\text{ClH}\cdots\text{H}_3\text{CH}$  complex is an example of so-called bifurcated dihydrogen bond because there is one  $\text{Cl}-\text{H}$  proton-donating bond and three acceptor centers of methane molecule. Thus, there is  $\text{V}(\text{Cl},\text{H})$  basin sharing a boundary with three  $\text{V}(\text{C},\text{H})$  basins. For two complexes with strong hydrogen bonds,  $\text{H}_5\text{O}_2^+$  and  $\text{C}_2\text{H}_2\cdots\text{H}^+\cdots\text{C}_2\text{H}_2$ , there is the monosynaptic basin  $\text{V}(\text{H})$ , which does not belong to any heavy atom valence shell. In  $\text{H}_5\text{O}_2^+$ ,  $\text{V}(\text{H})$  is linked to each  $\text{V}(\text{O})$  of oxygen atom, while in  $\text{C}_2\text{H}_2\cdots\text{H}^+\cdots\text{C}_2\text{H}_2$ , there are two  $\text{V}(\text{C},\text{C})$  basins for each acetylene molecule, and thus  $\text{V}(\text{H})$  is linked to four such basins. One can see that monosynaptic  $\text{V}(\text{H})$  basins occur for very strong hydrogen bonds, while for weaker  $\text{A}-\text{H}\cdots\text{B}$  interactions there are  $\text{V}(\text{A},\text{H})$  disynaptic basins. The ELF topological classification of hydrogen bonds was performed by Fuster and Silvi.<sup>204</sup>

The ELF indicator of hydrogen-bonding strength was also introduced, the core–valence bifurcation (CVB) index,  $I_{\text{CVB}}$ ,<sup>204,205</sup> which is the difference of  $\eta(r_{\text{cv}})$ , the lowest value of the ELF for which all the core basins are separated from the valence, and  $\eta(r_{\text{AHB}})$ , the value of the saddle link of  $\text{V}(\text{A},\text{H})$  and  $\text{V}(\text{B})$  basins. The  $I_{\text{CVB}}$  is positive for weak hydrogen bond, and it decreases if the strength of this interaction increases; usually this index is negative for strong hydrogen bonds. Figure 15 presents the  $I_{\text{CVB}}$  values for hydrogen-bonded systems (except for  $\text{B}_2\text{H}_6$  species). The lowest values of the index are observed for  $\text{H}_5\text{O}_2^+$  and  $\text{C}_2\text{H}_2\cdots\text{H}^+\cdots\text{C}_2\text{H}_2$ ,  $-0.579$  and  $-0.443$ , respectively. The latter complexes correspond to “the proton bound homodimers” described earlier here, where the proton is situated in the midpoint of the donor–acceptor distance, or nearly so. For such a case, the bond number of both  $\text{A}\cdots\text{H}$  and  $\text{H}\cdots\text{B}$  interactions is equal to 0.5 or very close to such a value.

## 5. INTERRELATIONS BETWEEN QTAIM AND THE INTERACTION ENERGY COMPONENTS

The delocalization interaction energy (or charge transfer) is usually attributed to the covalency of interaction considered.

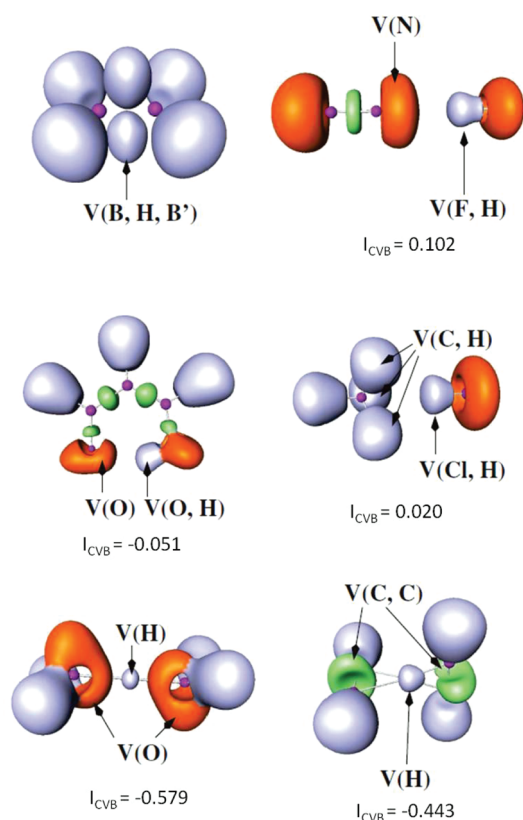


**Figure 15.**  $\eta(r)$  localization domains of  $B_2H_6$  (top left),  $FH \cdots N_2$  (top right),  $C_3H_4O_2$  (center left),  $ClH \cdots CH_4$  (center right),  $H_5O_2^+$  (bottom left), and  $C_2H_2 \cdots H^+ \cdots C_2H_2$  (bottom right); the core valence bifurcation indices ( $I_{CVB}$ 's) are also included. Reprinted with permission from ref 205. Copyright 2005 Springer.

Similarly, the negative value of Laplacian of the electron density at the bond critical point or at least the negative value of the total electron energy density at BCP is treated as the evidence of the covalency of interaction. Hence, the interrelations between the energy terms derived from the partitioning scheme and the QTAIM characteristics seem to be interesting.<sup>206</sup> Various relationships were analyzed for a wide range of hydrogen-bonded complexes<sup>101,206</sup> and also for a narrow range of specific hydrogen bonds, as, for example, for dihydrogen bonds.<sup>207</sup>

Figure 16 presents the relationship between the proton–acceptor distance and the ratio of delocalization and electrostatic energy.<sup>29</sup> Different complexes are taken into account here: systems with very strong hydrogen bonds, such as  $(FHF)^-$ , and the other charge-assisted hydrogen bonds, interactions enhanced by  $\pi$ -electron delocalization, complexes bound through dihydrogen bond, systems with  $\pi$ -electrons as the proton acceptors, and the other ones. For strong hydrogen bonds, this ratio is greater than for the other weaker interactions. This indicates the meaningful covalency contribution. For weak hydrogen bonds, the electrostatic energy is the most important attractive term, and the ratio is not high. Because different types of acceptors are considered, then this dependence (Figure 16) is only a rough one. However, one can observe three regions of hydrogen-bonding interactions. There are hydrogen bonds with very short  $H \cdots B$  distances, shorter than 1.2 Å, with a negative  $\nabla^2\rho_{H \cdots B}$  and a high value of the ratio  $E_{DEL}^{(R)}/E_{ES}^{(1)}$  (see eq 11).  $(FHF)^-$  ion is representative of this subsample; however,

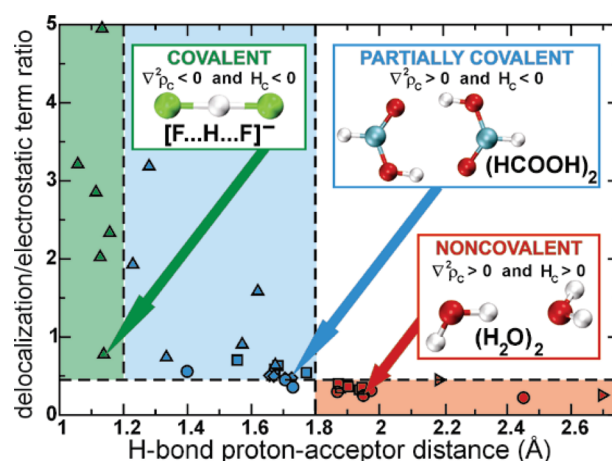


**Figure 16.** Relationship between the proton–acceptor distance (Å) and the ratio of delocalization and electrostatic energy. Three regions are designated: green color corresponds to the strongest H-bonds with negative  $\nabla^2\rho_{H \cdots B}$  values, blue region is of the partially covalent interactions with positive  $\nabla^2\rho_{H \cdots B}$  values but negative  $H_C$ 's, and red color designates the weakest interactions with positive  $H_C$  values. Reprinted with permission from ref 29. Copyright 2006 American Chemical Society.

there are also other species, the charge-assisted dihydrogen bonds. The next subsample is situated in  $\{1.2; 1.8\}$  Å range of  $H \cdots B$  distances; here,  $\nabla^2\rho_{H \cdots B}$  is positive but  $H_C$  is negative. These interactions are partially covalent in nature. The formic acid dimer represents this subsample, and the  $E_{DEL}^{(R)}/E_{ES}^{(1)}$  ratio is still high here. The last subsample concerns the weakest hydrogen bonds where both  $\nabla^2\rho_{H \cdots B}$  and  $H_C$  are positive; here, the electrostatic interaction is the dominant attractive interaction, and thus the energy ratio is low. The trans-linear water dimer represents such an interaction. Figure 16 shows the horizontal broken line for  $E_{DEL}^{(R)}/E_{ES}^{(1)}$  ratio equal to 0.45; this is the borderline between closed-shell interactions and partially covalent interactions for which  $H_C$  is negative. Figure 16 shows the interrelations between the geometrical ( $H \cdots B$  distance), energetic ( $E_{DEL}^{(R)}/E_{ES}^{(1)}$  ratio), and topological ( $\nabla^2\rho_{H \cdots B}$  and  $H_C$ ) characteristics. The same sample of complexes as the one applied in Figure 16 was used to analyze the dependence between electron density at  $H \cdots B$  BCP,  $\rho_{H \cdots B}$ , and the delocalization interaction energy term,  $E_{DEL}^{(R)}$ . This is the second-order polynomial correlation (Figure 17). It is important that the correlation concerns various unrelated systems.  $\rho_{H \cdots B}$  is the well-known and frequently applied descriptor of hydrogen-bonding strength, whereas  $E_{DEL}^{(R)}$  is responsible for the covalent character of interaction. It was shown earlier here (Table 2) that the latter term correlates well with the binding energy.

The results of the Natural Bond Orbitals (NBO) method<sup>20,42</sup> are in line with the latter relationships. According to the NBO approach, the  $n_B \rightarrow \sigma_{AH}^*$  interaction is responsible for the hydrogen-bonding formation. This interaction is connected with the maximum  $n_B \rightarrow \sigma_{AH}^*$  overlap, which leads to a linear, or nearly so,  $A-H \cdots B$  arrangement.  $n_B$  designates the lone electron pair of the proton acceptor (electron donor). The hydrogen-bond formation leads to an increase of the occupancy of the  $\sigma_{AH}^*$  antibond orbital and hence the weakening and lengthening of the  $A-H$  bond. This leads to the red-shifted  $\nu_{AH}$  stretching frequency. The  $n_B \sigma_{AH}^*$  interaction may be estimated by



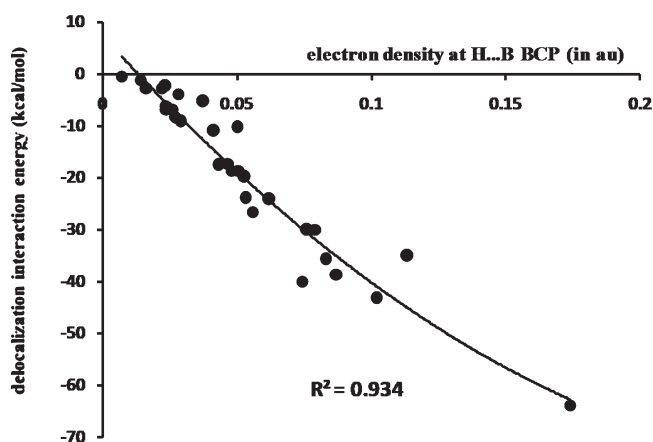


Figure 17. Relationship between  $\rho_{H\cdots B}$  (in au) and the delocalization interaction energy term,  $E_{\text{DEL}}^{(R)}$  (in kcal/mol), using the same sample as that of Figure 16.

second-order perturbation theory (eq 22).

$$\Delta E(n_B \rightarrow \sigma_{AH}^*) = -2\langle n_B | F | \sigma_{AH}^* \rangle^2 / (\varepsilon(\sigma_{AH}^*) - \varepsilon(n_B)) \quad (22)$$

$\langle n_B | F | \sigma_{AH}^* \rangle$  is the Fock matrix element, while  $\varepsilon(\sigma_{AH}^*) - \varepsilon(n_B)$  is the orbital energy difference (the difference of diagonal Fock matrix elements). The decomposition of the interaction energy ( $\Delta E$ ) within the NBO approach may be briefly presented by eq 23.

$$\begin{aligned} \Delta E &= E(\text{complex}) - E(\text{monomer 1}) - E(\text{monomer 2}) \\ &= \Delta E_{\text{NCT}} + \Delta E_{\text{CT}} \end{aligned} \quad (23)$$

$\Delta E_{\text{NCT}}$  and  $\Delta E_{\text{CT}}$  are noncharge transfer and charge transfer energies, respectively. Charge transfer interaction is connected within NBO scheme with the shift of occupancy from the manifold of filled orbitals of one monomer to the unfilled orbitals of the other. This energy may be calculated within the Hartree–Fock theory by deleting Fock matrix elements connecting the mentioned manifolds and further expressing the change in energy.

$\Delta E(n_B \rightarrow \sigma_{AH}^*)$  energy expresses the delocalization of electrons within the system considered. Table 3 presents the results concerning various complexes where different types of hydrogen bonds exist;<sup>20</sup> the  $\Delta E(n_B \rightarrow \sigma_{AH}^*)$  energy is great for  $\text{FH}\cdots\text{F}^-$ ,  $\text{H}_2\text{OH}^+\cdots\text{OH}_2$ , and  $\text{HOH}\cdots\text{OH}^-$  Lewis acid–Lewis base interactions, and it is equal to 166.2, 168.4, and 63.4 kcal/mol, respectively. The corresponding  $\text{H}\cdots\text{B}$  bond orders for the latter complexes are equal to 0.5, 0.5, and 0.365, indicating the meaningful covalent character of these interactions. For the other weaker H-bonded complexes like, for example,  $\text{H}_3\text{CH}\cdots\text{OH}_2$ ,  $\text{H}_2\text{NH}\cdots\text{OH}_2$ , and  $\text{HOH}\cdots\text{OH}_2$ , this energy amounts to 0.9, 3.1, and 7.5 kcal/mol, respectively. The bond orders for the corresponding  $\text{H}\cdots\text{B}$  contacts, that is, (C)H $\cdots$ O, (N)H $\cdots$ O, and (O)H $\cdots$ O, are equal to 0.001, 0.008, and 0.030. These bond orders are much less than those of the charge-assisted hydrogen bonds. Thus, if the bond order is a measure of covalent character of any interaction, then the  $\Delta E(n_B \rightarrow \sigma_{AH}^*)$  energy also clearly expresses such a character.

Table 3 contains the results concerning neutral hydrogen bonds as well as the results for charge-assisted hydrogen bonds. One can see that the latter interactions are stronger than the former ones. There are the binding energies,  $\Delta E$ 's, as well as the net charge transfers from the acceptors of proton to the

Table 3. Complexes with Various Kinds of Hydrogen Bonds<sup>a</sup>

Lewis base, B	Lewis acid, AH	charge	$\Delta E$	$\Delta E_{n_B \rightarrow \sigma_{AH}^*}$	$Q_{B \rightarrow AH}$	$b_{A-H}$	$b_{B \cdots H}$
H <sub>2</sub> O	HCH <sub>3</sub>	0	0.4	0.9	2.0	0.999	0.001
HF	HNH <sub>2</sub>	0	1.1	0.6	1.2	1.000	0.000
H <sub>2</sub> CO	HNH <sub>2</sub>	0	1.4	1.2	2.6	0.921	0.071
CO	HF	0	1.8	1.5	28.0	0.988	0.009
H <sub>2</sub> O	HNH <sub>2</sub>	0	2.7	3.1	3.4	0.990	0.008
OC	HF	0	3.6	10.4	28.0	0.941	0.059
HF	HF	0	5.1	6.7	12.4	0.967	0.026
H <sub>2</sub> O	HOH	0	5.8	7.5	13.8	0.969	0.030
HO <sup>-</sup>	HCH <sub>3</sub>	−	6.5	10.9	40.0	0.957	0.043
H <sub>3</sub> N	HOH	0	7.3	12.6	26.9	0.951	0.049
H <sub>2</sub> O	HF	0	10.1	18.0	33.9	0.902	0.074
HF	HNH <sub>3</sub> <sup>+</sup>	+	12.9	8.9	19.8	0.957	0.034
H <sub>3</sub> N	HF	0	14.3	34.9	72.1	0.826	0.164
OH <sup>-</sup>	HNH <sub>2</sub>	−	17.1	31.1	85.9	0.856	0.143
H <sub>2</sub> O	HNH <sub>3</sub> <sup>+</sup>	+	22.0	30.1	64.4	0.868	0.117
H <sub>3</sub> N	HNH <sub>3</sub> <sup>+</sup>	+	28.2	75.6	169.1	0.685	0.306
HO <sup>-</sup>	HOH	−	29.4	63.4	188.6	0.634	0.365
H <sub>2</sub> O	HOH <sub>2</sub> <sup>+</sup>	+	36.7	168.4	236.5	0.500	0.500
F <sup>-</sup>	HF	−	46.5	166.2	233.6	0.500	0.500

<sup>a</sup> The binding,  $\Delta E$ , and the charge transfer,  $\Delta E_{n_B \rightarrow \sigma_{AH}^*}$ , energies (in kcal/mol) are given, as well as the net transfer charge,  $Q_{B \rightarrow AH}$  (in milli-electrons), and bond orders of the A–H bond and B $\cdots$ H intermolecular contact,  $b_{A-H}$  and  $b_{B \cdots H}$ , respectively. This table is reprinted with permission from ref 20. Copyright 2005 Cambridge University Press.

proton-donating systems ( $Q_{B \rightarrow AH}$ 's), and bond orders of A–H bonds and H $\cdots$ B contacts. Various correlations for the results of Table 3 were reported earlier;<sup>20</sup> one can see that an increase in binding energy is connected with an increase of  $\Delta E(n_B \rightarrow \sigma_{AH}^*)$  and  $Q_{B \rightarrow AH}$ , a decrease of A–H bond order, and an increase of the H $\cdots$ B bond order. Figure 18 presents the relationship between A–H and B $\cdots$ H bond orders and  $\Delta E(n_B \rightarrow \sigma_{AH}^*)$  energy.

The calculations showing the importance of the charge transfer energy for hydrogen-bonded systems were performed.<sup>20</sup> The binding energies were evaluated for various complexes, and later the calculations were performed for the same complexes but with deleting all intermolecular charge transfer interactions. In other words, the reoptimizations of these complexes were carried out with the exclusion of the charge transfer interaction energy. It was found that these “CT-deleted” structures were characterized by much less hydrogen-bonding energies than the true such energies. Additionally, the intermolecular distances for “CT-deleted” complexes are more than 1 Å beyond those of the true hydrogen-bonded complexes. The “CT-deleted” H $\cdots$ B distances are usually much greater than the corresponding sums of van der Waals radii. Table 4 contains the corresponding results for a few complexes.

The charge transfer, CT, energy for hydrogen-bonded systems within NBO scheme is connected with the electron flow from the proton acceptor to the proton donor.<sup>20</sup> This is the Lewis base–Lewis acid interaction, that is, the electron donor–electron acceptor interaction. Such donors and acceptors may be classified according to the type of orbitals donating and accepting electrons. There are the following orbitals donating electrons,  $\sigma$ ,  $\pi$ , or  $n$  (nonbonding orbitals), and orbitals accepting electrons,  $\sigma$ ,  $\pi$ , or  $\nu$  (vacant orbitals). It was pointed out that the charge-transfer  $n \rightarrow \nu$  complexes are the strongest, whereas the  $\pi \rightarrow \pi^*$  type

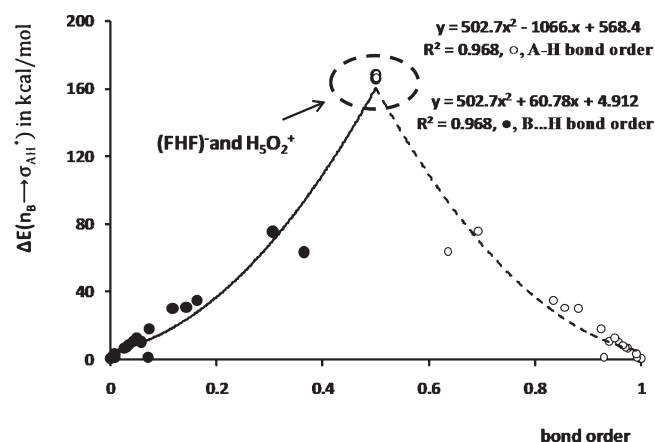


**Figure 18.** Relationship between A–H and B···H bond orders and  $\Delta E_{n_B \rightarrow \sigma^*_{AH}}$  energy (in kcal/mol); the sample presented in Table 3 is considered here.

**Table 4.** Binding energies,  $\Delta E$  (in kcal/mol), B···H Distances,  $R_{H \cdots B}$  (in Å), and the Corresponding Sum of van der Waals Radii,  $R_{H \cdots B}^{vdW}$  (in Å)<sup>a</sup>

species	$\Delta E$	$\Delta E^c$	$R_{H \cdots B}$	$R_{H \cdots B}^c$	$R_{H \cdots B}^{vdW}$
H <sub>3</sub> N···HOH	7.27	0.16	1.96	5.80	3.05
HF···HF	5.05	0.84	1.83	3.65	2.69
H <sub>2</sub> CO···HNH <sub>2</sub>	1.41	0.14	2.35	6.72	2.88
HO <sup>−</sup> ···HF <sup>b</sup>	52.18	12.5	1.06	2.32	2.88
HO <sup>−</sup> ···HOH	29.39	5.5	1.363	2.68	2.88
HO <sup>−</sup> ···HNH <sub>2</sub>	17.09	1.6	1.685	6.76	2.88
HO <sup>−</sup> ···HCH <sub>3</sub>	6.48	0.2	1.979	2.71	2.88

<sup>a</sup> This table is based on tables taken from ref 20, table 5.1 (p 598), table 5.4 (p 603), table 5.7 (p 609), and table 5.10 (p 614). Copyright 2005 Cambridge University Press. <sup>b</sup> Binding energy and H···B distance with respect to HO<sup>−</sup> and HF in the HOH···F<sup>−</sup> complex. <sup>c</sup> Concerns the “CT-deleted” complexes.

interactions are the weakest ones.<sup>208</sup> The typical hydrogen-bonding interaction being in agreement with the Pauling definition may be classified as the electron donor–electron acceptor interaction of the type  $n \rightarrow \sigma^*$ .

## 6. COVALENCY OF DIFFERENT TYPES OF HYDROGEN BONDS

It was described in the previous section that the charge transfer interaction is very important for the stability of hydrogen-bonded systems.<sup>20</sup> However, it is also postulated in the literature from time to time that the electrostatic forces sufficiently describe the hydrogen-bonding interaction. For example, the simple electrostatic model may properly describe numerous complexes connected through hydrogen bonds. For such a model,<sup>209–211</sup> the electrostatic interaction between monomers is calculated with the use of point multipoles located on atoms and bond centers; the hard spheres are also modeled on heavy atoms to mimic the repulsive interactions. The multipoles were obtained from SCF and SCF/MP calculations performed on individual monomers. The hard spheres correspond to the van der Waals radii proposed by Pauling. The geometry of the complex corresponds to the minimum of electrostatic interaction between monomers. This model predicts properly the geometries of hydrogen-bonded

species; for example, the following complexes were considered: H<sub>3</sub>N···HF, N<sub>2</sub>···HF, (HF)<sub>2</sub>, (HCl)<sub>2</sub>, H<sub>2</sub>CO···HF, but also the systems with  $\pi$ -electrons as a proton acceptor were analyzed, like, for example, acetylene–HF or ethylene–HCl.<sup>211</sup> The considered complexes are not characterized by very strong interactions, and thus the systems where the covalent nature is clearly manifested were not taken into account.

The other approach, the Electrostatic-Covalent H-Bond Model (ECHBM), connects various former ideas.<sup>30,31</sup> Both aspects of the interaction, the covalency and the electrostatic character, are taken into account here. There are following the assumptions of that model: weak hydrogen bonds are electrostatic interactions, and they become more covalent if their strength increases; very strong hydrogen bonds are three-center–four-electron covalent bonds; very strong hydrogen bonds are homonuclear and symmetrical because two VB structures (for example, I and II; see Figure 19) are in such a case isoenergetic and equally contribute to the real structure of hydrogen bonding.

According to Gilli et al., there are three ways to enhance the hydrogen-bonding strength: by adding an electron, by withdrawing an electron, or by resonance. Hence, the following types of strong and covalent in nature hydrogen bonds are possible: charge-assisted hydrogen bond, (−)CAHB or (+)CAHB, and the resonance-assisted hydrogen bond, RAHB (Figure 19).

The (FHF)<sup>−</sup> is an example of (−)CAHB, H<sub>5</sub>O<sub>2</sub><sup>+</sup> is an example of (+)CAHB, and the malonaldehyde having the intramolecular hydrogen bonding is an example of the RAHB system. The idea of the RAHB type of interaction was questioned in both earlier<sup>212,213</sup> and recent studies.<sup>214,215</sup> It was found that neither the coupling constants nor the proton chemical shifts for the species with intramolecular O–H···O and N–H···N hydrogen bonds in malonaldehyde and its diaza derivative, respectively, showed the existence of the resonance-assisted stabilization.<sup>212,213</sup> The authors found that for the latter systems there are stronger H-bonds than for their saturated analogues. In their opinion, it is connected with the  $\sigma$ -skeletons of unsaturated molecules containing  $\pi$ -electrons because the skeleton structural requirements allow the donor and the acceptor atoms to be closer than in the corresponding saturated systems.

The so-called resonance-assisted hydrogen bonds (RAHBs) are sometimes given different names. For example, the name resonance-assisted binding (RAB) was suggested recently.<sup>176</sup> It seems that despite controversies over some of the statements of RAHB model, the  $\pi$ -electron delocalization is certainly typical of such hydrogen bonds. As it was pointed out by Gilli et al.,<sup>30,31</sup> one of the main characteristics of RAHBs is the existence of conjugated single and double bonds, which leads to the  $\pi$ -electron delocalization, the equalization of bonds, and finally to the enhancement of H-bond strength. This is in force for malonaldehyde and its derivatives (Chart 4) where equalization of CO bonds (d1 and d4) can be observed, on the one hand, and also equalization of CC bonds (d2 and d3), on the other. It was proven that at least 20–30% of the hydrogen-bond energy for malonaldehyde and its simple chloro and fluoro derivatives is connected with  $\pi$ -electron delocalization.<sup>216</sup> However, it was also found that the equalization of CO and CC bonds for such species is not always connected with the enhancement of hydrogen-bonding strength. For example, the external agents, like strong Lewis acids interacting with carbonyl oxygen center, lead to such an equalization and to a weakening of the intramolecular hydrogen bond.<sup>217,218</sup>

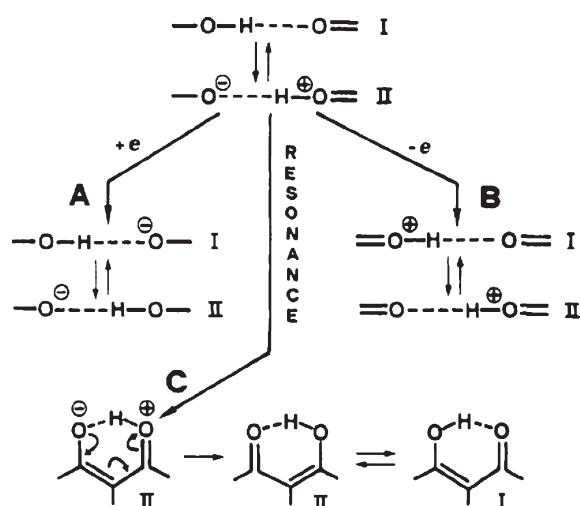
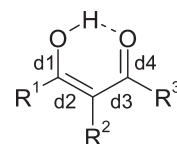


**Figure 19.** The model of enhancement of hydrogen bonding, through addition of an electron, (−)CAHB; through withdrawing an electron, (+)CAHB; and through the resonance, RAHB. Reprinted with permission from ref 30. Copyright 1994 American Chemical Society.

A similar  $\pi$ -electron delocalization as for malonaldehyde and its derivatives can be observed for the intermolecular hydrogen bonds in dimers of carboxylic acids<sup>119</sup> and amides.<sup>120,167</sup> For these complexes, there occurs equalization of CO bonds of the carboxylic group, whereas for amides there occurs the shortening of C–N bond and the lengthening of C=O bond within the amide group. These changes may lead to the strengthening of hydrogen bonding. It was also found that, similarly as for intramolecular hydrogen bonds, the external agents may cause the  $\pi$ -electron delocalization and the weakening of hydrogen bonding.<sup>219</sup> However, the systems where the  $\pi$ -electron delocalization enhances the strength of hydrogen bond are classified as rather strong hydrogen bonds. The formic acid dimer is characterized by a negative  $H_C$  of the  $H\cdots O$  (proton  $\cdots$  acceptor) bond critical point (Figure 16). This shows the covalent character of the  $H\cdots O$  intermolecular interaction.<sup>29</sup> The results of calculations performed on a few dimers of amides and carboxylic acids are summarized in Table 2, and such systems were analyzed in the previous section.

According to Gilli et al. (see Figure 19), the  $\pi$ -electron delocalization in homonuclear RAHBs systems leads to the situation that two VB resonance structures  $X-H\cdots X$  and  $X\cdots H-X$  are isoenergetic (or their energies are close to each other) and can mix to the greatest extent.<sup>171,172</sup> Similarly, adding an electron or withdrawing an electron leads to the same energies of I and II VB structures (Figure 19) for (−)CAHBs and (+)CAHBs, respectively. It seems that the statement about the same energy of VB structures is equivalent with the principle of equality of proton affinities of the donor and acceptor ( $\Delta PA = 0$ ).<sup>220</sup> It is also equivalent with the principle of equality of  $pK_a$  values of  $B^+-H$  and  $A-H$  ( $\Delta pK_a = 0$ ). The latter parameter introduced by Huyskens and Zeegers-Huyskens to analyze the proton transfer process in hydrogen-bonded systems<sup>221</sup> was later applied and described in numerous studies.<sup>222–224</sup> There are theoretical and experimental investigations that show linear relationships between  $\Delta pK_a$  and the hydrogen-bonding strength.<sup>225–229</sup> This means that the former value decreases if the strength of interaction increases. The latter relationship is only approximately linear, and the deviations from

**Chart 4**



linearity increase if the donor and acceptor of proton become different. Besides, it was pointed out that the hydrogen bonds fulfilling the  $\Delta pK_a = 0$  principle are not characterized by the same strength.<sup>230</sup> The dependencies mentioned above were analyzed in detail very recently.<sup>231</sup>

These rules,  $\Delta pK_a = 0$ ,  $\Delta PA = 0$ , and the same energy of the proton donor ( $A^-$ ) and the proton acceptor ( $B$ ), roughly refer to the identity or at least similarity of the donor and acceptor of proton. This is in line with the early concept of Latimer and Rodebush<sup>16</sup> that “the hydrogen nucleus held between 2 octets constitutes a weak ‘bond’.” If there are the same systems and the hydrogen nucleus is inserted between, then the above rules concerning the donor and acceptor may be fulfilled. Also, all categories of “assisted” hydrogen bonds (Figure 19) are in line with the latter statements. For example, the proton inserted between two octets of water molecules leads to the  $H_5O_2^+$  system where the proton is situated in the center of the whole system,<sup>232–234</sup> or nearly so; both water molecules are characterized by the same  $pK_a$ 's, and this is the case of (+)CAHB. Similarly, if the proton is in the middle of  $F^-\cdots F^-$  and  $Cl^-\cdots Cl^-$  distances for  $(FHF)^-$  and  $(ClHCl)^-$  systems,<sup>235–237</sup> respectively, they are classified as (−)CAHB interactions. In the case of the RAHB systems,  $\pi$ -electron delocalization leads to a decrease of  $\Delta pK_a$  and  $\Delta PA$  values; in other words, the proton donor and the proton acceptor become similar in nature. Because additional effects are needed to equalize the acceptor and donor properties, it is difficult to find the system belonging to the RAHB class of interactions with the proton situated exactly in the middle of the donor–acceptor distance. A few examples of the neutral species are known from crystal structures where the proton is situated approximately in the middle of the donor–acceptor distance. These are, for example, benzylacetone<sup>187</sup> and nitromalonamide<sup>238</sup> crystal structures.

The principles of  $\Delta pK_a$  and  $\Delta PA = 0$  require the same donor and acceptor, and if they are symmetrically positioned then this may lead to a single-well potential hydrogen bond with the proton in the center. For example, in the case of  $H_5O_2^+$  the proton lies exactly on the inversion center or nearly so, as different studies present various pictures. Such a situation was also observed for the  $(XYO\cdots H\cdots OXY)^+$  ( $X, Y = H, F, Cl$ ) systems where in almost all cases the proton is situated exactly in the middle of the  $O\cdots O$  distance.<sup>232</sup> These are (+)CAHB systems. It seems that such symmetric species are characterized by the greatest possible covalency of hydrogen bonding. In fact, the bond orders for them are equal to 0.5, similarly as for the  $(FHF)^-$  and  $H_5O_2^+$  species presented in Table 3.

However, the  $\Delta PA = 0$  principle and the requirements of symmetry described above are not sufficient to have the proton situated exactly in the middle of the donor–acceptor distance. Chan et al.<sup>239</sup> analyzed proton-bound  $(Y\cdots H^+\cdots Y)$  homodimers. According to them, the proton is shared equally between two moieties for  $Y = Ne, O$ , and  $F$ ;  $O$  is the Lewis base center of water, and  $F^-$  ion is considered in these studies. Such equal sharing is not the case for  $N$ . For example, for the  $NH_4^+\cdots NH_3$  complex, the proton is closer to one of the nitrogen centers.



Generally, it was found for a series of  $(Y \cdots H^+ \cdots Y)$  homodimers that the binding energies neither decrease nor increase monotonically with the increasing proton affinity of  $Y$ . However, there are recent interesting studies on  $H_3O_2^-$  and  $N_2H_7^+$  systems,<sup>240</sup> which were analyzed with the use of the multi-component density functional theory (MC-DFT)<sup>241</sup> and the gauge-including atomic orbital (GIAO) or continuous set of gauge transformation (CSGT) techniques. In the case of classical nuclei, the asymmetric  $O-H \cdots O$  structure was found for  $H_3O_2^-$ ; however, for quantum protons and quantum deuterons, the symmetric structures exist corresponding to the single potential well with respect to the H(D) coordinate. In the case of the  $N_2H_7^+$  system, the single well with symmetrical  $N \cdots H \cdots N$  was found only for quantum proton. The latter result seems to be surprising because the previous studies never showed the symmetric  $N_2H_7^+$  system being in the energetic minimum.

A similar situation may be found for proton sponges where the proton is situated between lone electron pairs of nitrogen atoms.<sup>242,243</sup>  $N-H \cdots N$  proton sponges exist most frequently, but other types of proton sponges are also possible, for example,  $P-H \cdots P$  interactions.<sup>244</sup> For the  $N \cdots H^+ \cdots N$  systems, the proton may be positioned in the middle of  $N \cdots N$  distance or nearly so, but also the cases with proton attached exactly to one of the nitrogen centers are known. The position of the proton depends on the character of species where hydrogen bond exists, on the environment, and also on steric effects. The latter ones may be important because the short  $N \cdots N$  distance is often forced by molecular constraints. Figure 20 presents the case of the crystal structure of an adduct of 1,8-bis(dimethylamino)2,7-dimethoxynaphthalene  $((CH_3O)_2 \cdot DMAN)^{245}$  where the studies revealed a symmetric and planar  $DMAN \cdot H^+$  cation with a short  $N \cdots H^+ \cdots N$  hydrogen bond ( $N \cdots N$  distance equal to 2.567(3) Å). The X-ray diffraction results show the central position of the proton within  $N \cdots H^+ \cdots N$ , which is reflected by symmetry requirements. However, DFT and MP2 calculations show two potential minima for the proton position with the zero point energy level close to the proton transfer barrier height. Hence, the calculations show there is the low barrier hydrogen bond (LBHB) in this case.

There is another case of strong hydrogen bonds analyzed earlier. Jeffrey analyzed the effect of cooperativity in crystal structures.<sup>2</sup> It is connected with  $\sigma$ -bonds, which interrelate in a chain or a cycle. The chain of molecules interacting through OH bonds is an example, like within  $[(R)OH \cdots (R)OH \cdots (R)OH \cdots]$ . It can be expected that such a situation often occurs in crystals where the translational symmetry exists and it requires a subsystem reduplicated within a chain, often through hydrogen-bonding interactions. Hence, there is strong experimental evidence of the importance of this kind of cooperativity. However, not only crystal structures provide the evidence in this respect. For example, the cooperative effect was also investigated by the microwave and ab initio techniques for  $H_3N \cdots HF$  and  $H_3N \cdots HF \cdots HF$  complexes.<sup>246</sup> It was found that for the  $H_3N \cdots HF \cdots HF$  complex the  $H \cdots N$  distance is by 0.21(6) Å shorter than such a distance for the complex containing one HF molecule. There are also other studies on the cooperativity effect.<sup>247</sup> For example, the cooperativity effects in  $C-H \cdots O$  and  $OH \cdots O$  hydrogen bonds were compared.<sup>248</sup> It was found that the enhancement of H-bond strength occurs for the  $O-H \cdots O$  interaction; one can observe a decrease of covalent nature of the proton-donating  $O-H$  bond revealed by its

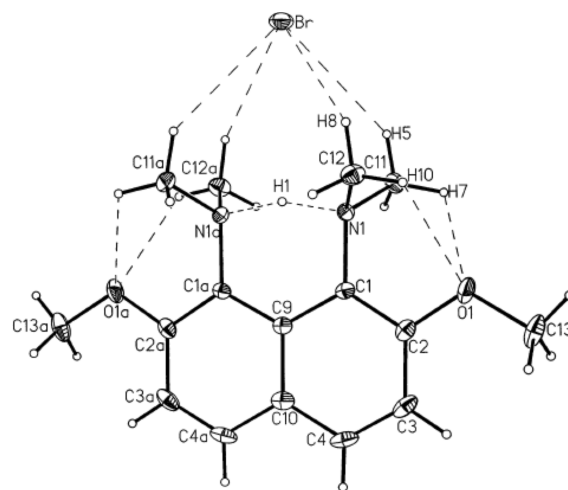
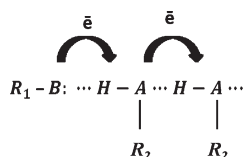


**Figure 20.** Crystal structure of an adduct of 1,8-bis-(dimethylamino)2,7-dimethoxynaphthalene  $((CH_3O)_2 \cdot DMAN)$ , and the 40% probability displacement ellipsoid with atom numbering. Reprinted with permission from ref 245. Copyright 2005 American Chemical Society.

elongation and the red-shift of the corresponding stretching mode. In the case of  $C-H \cdots O$  interaction, the blue-shifting is observed for H-bonds in  $(H_2CO)_n$  and  $(HFCO)_n$  systems. The cooperativity for the other types of H-bonds was also investigated, for example, for  $CH \cdots F$  hydrogen bonding, where an increase of blue-shift was observed as a result of cooperativity.<sup>249</sup> Another interesting example involves the so-called  $\pi$ H-bonded interactions analyzed at the MP2/6-311++(2d,2p) level of approximation.<sup>250</sup> There are numerous studies on cooperativity effect where the enhancement of hydrogen-bonding strength is observed.<sup>251–254</sup> However, it was also found that the weakening of hydrogen bonding may be possible if any species acts simultaneously as the proton donor and the proton acceptor.<sup>255</sup> Thus, the positive cooperativity is attributed to the strengthening of hydrogen bonding and the negative cooperativity if the weakening of that interaction is observed. The cooperativity term is not strictly defined; however, very often it is understood as the enhancement (or diminution) of hydrogen bond if the additional species interacts either with the proton donor or with the proton acceptor forming the next hydrogen bonding.<sup>254,256,257</sup>

In the case of positive cooperativity, the enhancement of any  $H \cdots B$  interaction within the  $A-H \cdots B$  system may be explained in the following way (Chart 5). The A-center acts as the proton donor for  $A-H \cdots B$  interaction, on the one hand, and also as the proton acceptor for the additional  $A-H \cdots A$  interaction, on the other. Such an additional interaction causes greater polarization of the  $A-H$  bond and finally the enhancement of the  $H \cdots B$  interaction. This explains the relationship between the proton donating bond length and the proton-acceptor distance. The cooperativity effect expressed by the additional  $A-H \cdots A$  interactions (see Chart 5) weakens the  $A-H$  proton-donating bond and enhances  $H \cdots B$  interaction; this is also in line with the bond number conservation rule (see the previous section)<sup>55</sup> because the lowering of the  $A-H$  bond number has to be connected with the increase of bond number of  $H \cdots B$  contact. Chart 5 shows that the enhancement of polarization of the  $A-H$  proton-donating bond is connected with the electron charge transfer, from B to  $A-H$  and next from A to  $A-H$ , and so on,

Chart 5



within the chain of  $\sigma$ -bonds and the proton–acceptor contacts ( $B \cdots H$ ,  $A-H$ , and  $H \cdots A$ ).

The cooperativity effect was analyzed recently for complexes of  $H_2CO$  with HF molecules.<sup>258</sup> Full optimizations were performed for the  $H_2CO \cdots HF$ ,  $H_2CO \cdots HF \cdots HF$ , and  $H_2CO \cdots HF \cdots HF \cdots HF$  systems. The results of these optimizations correspond to energy minima because no imaginary frequencies were found. Additionally,  $C_{2v}$  symmetry  $H_2CO \cdots (HF)_n$  systems were considered ( $C=O \cdots (HF)_n$  atoms are situated on the same line) with the number of HF molecules ranging from 1 to 9. The calculations were carried out using MP2 method; the Pople style 6-311++G(d,p) basis set was applied as well as the Dunning type basis sets: aug-cc-pVDZ and aug-cc-pVTZ.

Figure 21 presents the relationship between  $H \cdots O$  distance and the ratio of the interaction energy terms (delocalization and electrostatic); the linear systems of  $C_{2v}$  symmetry and fully optimized complexes are included. One can observe that a decrease of the  $H \cdots O$  distance is connected with an increase of the delocalization interaction energy term. In other words, if the proton–acceptor distance roughly reflects the strength of interaction and the delocalization energy corresponds to the covalency, then one can observe that cooperativity effect increases the covalent character of the interaction. Figure 21 shows that cooperativity is stronger for the fully optimized, nonlinear systems (molecular graphs of two such complexes are presented) and for the greater number of HF molecules. Closed circles (Figure 21) correspond to linear systems; the number of HF molecules is not indicated for linear systems. However, this number increases if  $H \cdots O$  distance decreases. The other parameters of hydrogen bond such as the binding energy and the topological characteristics also correlate with the  $H \cdots O$  distance. Figure 21 shows that for two nonlinear systems containing two and three HF molecules, the  $H \cdots O$  interaction possesses the characteristics of covalent interaction because the total electron energy density ( $H_C$ ) for  $H \cdots O$  BCP is negative.

There are interactions classified as hydrogen bonds where  $\pi$ -electrons play the role of Lewis base and the acceptor of proton; they are designated as  $X-H \cdots \pi$  (or as  $X-H/\pi$ ).<sup>3,259–261</sup> The question arises: what is the nature of such interactions? The early studies show that they are common in crystal structures<sup>3</sup> and are rather weak because very often the  $X-H \cdots \pi$  hydrogen-bond energy is of about 2 kcal/mol.<sup>262</sup> However, stronger interactions also occur; for example, for the T-shaped  $FH \cdots C_2H_2$  complex, the binding energy calculated at the MP2/6-311++G(d,p) level of approximation amounts to 3.1 kcal/mol (BSSE correction included).<sup>262</sup> The decomposition of the interaction energy performed within the Kitaura–Morokuma scheme<sup>22</sup> (eq 9) shows the following energy contributions:  $E_{ES}$  (−6.4 kcal/mol),  $E_{EX}$  (+6.3 kcal/mol),  $E_{PL}$  (−1.5 kcal/mol),  $E_{CT}$  (−2.2 kcal/mol), and the correlation energy calculated as the difference between MP2 and SCF binding energies is equal to −0.4 kcal/mol. One can see that the Heitler–London energy ( $E_{ES} + E_{EX}$ ) is close to

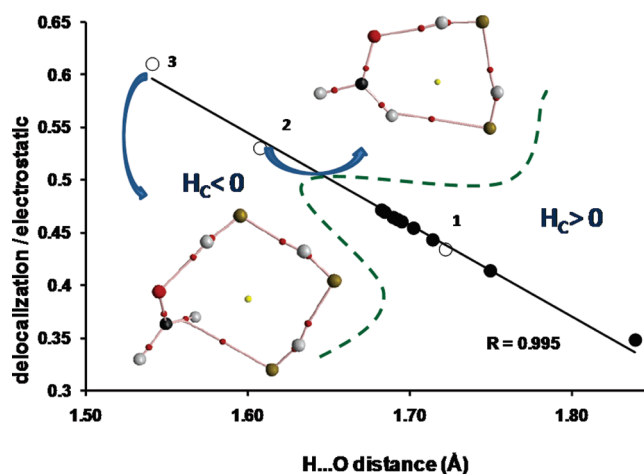


**Figure 21.** Linear relationship between  $H \cdots O$  distance (Å) and the ratio of the interaction energy terms (electrostatic and delocalization). Solid circles correspond to linear systems, while the open ones correspond to those fully optimized; numbers 1, 2, and 3 correspond to complexes fully optimized and containing one, two, and three HF molecules, respectively. The decomposition scheme is according to eq 11, MP2/aug-cc-pVDZ level of approximation. The molecular graphs of  $H_2CO \cdots (HF)_2$  and  $H_2CO \cdots (HF)_3$  complexes are included. The regions with positive and negative values of the total electron energy density ( $H_C$ ) at  $H \cdots O$  BCP are shown.

zero because the electrostatic ( $E_{ES}$ ) attractive term is balanced by the positive exchange energy ( $E_{EX}$ ). Hence, the polarization and charge transfer energies ( $E_{PL}$  and  $E_{CT}$ ) are responsible for the stability of that complex for relatively short distance between HF and  $C_2H_2$  ( $\sim 2.19$  Å is distance separating bridging H from the center of  $C \equiv C$  bond). For the  $C_2H_2 \cdots H_3O^+$  complex calculated at the MP2/6-311++G(d,p) level of approximation,<sup>263</sup> the following energy contributions were found:  $E_{ES}$  (−19.1 kcal/mol),  $E_{EX}$  (+25.4 kcal/mol),  $E_{PL}$  (−15.3 kcal/mol),  $E_{CT}$  (−16.3 kcal/mol),  $E_{MIX}$  (+6.9 kcal/mol), and the correlation energy is equal to −3.5 kcal/mol. The  $O-H \cdots \pi$  hydrogen bonding is much stronger here than  $F-H \cdots \pi$  in the case of  $C_2H_2 \cdots HF$  T-shaped complex. However, the former  $O-H \cdots \pi$  interaction may be classified as the charge-assisted hydrogen bonding, CAHB(+), where both polarization and charge transfer interaction energies are much more important than the electrostatic one. Hence, one may expect that for some of the  $X-H \cdots \pi$  interactions the covalent character of  $H \cdots \pi$  interaction may be detected.

The  $\sigma$ -electrons may also act as the proton acceptor in  $X-H \cdots \sigma$  interactions. For example, the calculations were performed on  $NH_4^+ \cdots H_2$  complex<sup>264</sup> and further on the other complexes such as  $PH_4^+ \cdots H_2$ ,  $AsH_4^+ \cdots H_2$ ,  $SbH_4^+ \cdots H_2$ , and  $BiH_4^+ \cdots H_2$ ; the systems containing the greater number of molecular hydrogen molecules were also considered.<sup>265</sup> These complexes may be classified as charge-assisted ones. However, also the neutral  $X-H \cdots \sigma$  interactions were investigated,  $HCCH \cdots H_2$  and  $FCCH \cdots H_2$  complexes, for which the calculations were carried out up to the MP2/6-311++G-(3df,3pd) level of approximation showing the binding energies for both complexes of −0.3 kcal/mol.<sup>266</sup> The  $F-H \cdots H_2$  T-shaped complex is another example, as it was analyzed up to the MP2/aug-cc-pVSZ level of approximation showing the binding energy of −0.99 kcal/mol.<sup>267</sup>

**Table 5. Topological Parameters (in au) of the Complexes with Acetylene and Hydrogen as Lewis Bases<sup>a</sup>**

C <sub>2</sub> H <sub>2</sub> Lewis base	$\rho_C$	$\nabla^2\rho_C$	$G_C$	$V_C$	$H_C$	$\Delta E$
H <sup>+</sup> ...C <sub>2</sub> H <sub>2</sub>	0.2059	-0.3220	0.0776	-0.2357	-0.1581	-154.45
Li <sup>+</sup> ...C <sub>2</sub> H <sub>2</sub>	0.0192	0.0907	0.0198	-0.0169	0.0029	-19.68
Na <sup>+</sup> ...C <sub>2</sub> H <sub>2</sub>	0.0124	0.0581	0.0118	-0.0091	0.0027	-12.16
FH...C <sub>2</sub> H <sub>2</sub>	0.0199	0.0532	0.0127	-0.0122	0.0005	-3.91
C <sub>2</sub> H <sub>2</sub> ...C <sub>2</sub> H <sub>2</sub> <sup>b</sup>	0.0077	0.0235	0.0047	-0.0036	0.0011	-1.43
NH <sub>4</sub> <sup>+</sup> ...C <sub>2</sub> H <sub>2</sub>	0.0251	0.0554	0.0147	-0.0156	-0.0009	-10.74
H <sub>3</sub> O <sup>+</sup> ...C <sub>2</sub> H <sub>2</sub>	0.0534	0.0278	0.0265	-0.0461	-0.0196	-19.39
C <sub>2</sub> H <sub>2</sub> ...H <sup>+</sup> ...C <sub>2</sub> H <sub>2</sub>	0.0651	0.0126	0.0289	-0.0546	-0.0257	-15.46

H <sub>2</sub> Lewis base	$\rho_C$	$\nabla^2\rho_C$	$G_C$	$V_C$	$H_C$	$\Delta E$
H <sup>+</sup> ...H <sub>2</sub>	0.1380	-0.2458	0.0021	-0.0656	-0.0635	-105.74
Li <sup>+</sup> ...H <sub>2</sub>	0.0126	0.0685	0.0141	-0.0110	0.0031	-5.68
Na <sup>+</sup> ...H <sub>2</sub>	0.0075	0.0401	0.0079	-0.0058	0.0021	-2.94
FH...H <sub>2</sub> <sup>b</sup>	0.0109	0.0079	0.0381	-0.0062	0.0319	-0.84
C <sub>2</sub> H <sub>2</sub> ...H <sub>2</sub> <sup>b</sup>	0.0033	0.0124	0.0024	-0.0016	0.0008	-0.28
NH <sub>4</sub> <sup>+</sup> ...H <sub>2</sub>	0.0131	0.0406	0.0088	-0.0074	0.0014	-2.34
H <sub>3</sub> O <sup>+</sup> ...H <sub>2</sub>	0.0307	0.0536	0.0185	-0.0235	-0.005	-5.19
C <sub>2</sub> H <sub>2</sub> ...H <sup>+</sup> ...H <sub>2</sub>	0.0167	0.0428	0.0100	-0.0094	0.0006	-2.76

<sup>a</sup> The characteristics of H<sup>+</sup>(Li<sup>+</sup>, Na<sup>+</sup>)... $\pi$  ( $\sigma$ ) BCP: the electron density at BCP ( $\rho_C$ ), its Laplacian ( $\nabla^2\rho_C$ ), the potential electron energy density ( $V_C$ ), the kinetic electron energy density ( $G_C$ ), and the total electron energy density at BCP ( $H_C$ ). The binding energies ( $\Delta E$ 's) corrected for BSSE (kcal/mol) are also included. The results obtained at MP2/6-311++G(3df,3pd) level of approximation. Results reprinted with permission from ref 268. Copyright 2007 American Chemical Society. <sup>b</sup> T-shaped complex.

Table 5 summarizes the results of investigations on complexes where acetylene or molecular hydrogen act as Lewis bases<sup>268</sup> and there are different Lewis acids; some of the complexes may be treated as connected through hydrogen bonds. For the NH<sub>4</sub><sup>+</sup>...C<sub>2</sub>H<sub>2</sub>, H<sub>2</sub>OH<sup>+</sup>...C<sub>2</sub>H<sub>2</sub>, and C<sub>2</sub>H<sub>3</sub><sup>+</sup>...C<sub>2</sub>H<sub>2</sub> complexes, there are negative  $H_C$  values for H<sup>+</sup>... $\pi$  BCPs, indicating that they may be treated as partially covalent interactions. Similarly, for the H<sub>2</sub>OH<sup>+</sup>...H<sub>2</sub> complex, the value of  $H_C$  is negative.

These are the N-H... $\pi$ , O-H... $\pi$ , and  $\pi$ -H... $\pi$  hydrogen bonds (Table 5). The latter type of interaction was analyzed earlier for two complexes of C<sub>2</sub>H<sub>3</sub><sup>+</sup>...C<sub>2</sub>H<sub>2</sub> and C<sub>2</sub>H<sub>5</sub><sup>+</sup>...C<sub>2</sub>H<sub>2</sub>;<sup>269</sup> these are the systems of two molecules of acetylene and the proton inserted between them, and the ethylene and acetylene molecules with the proton between  $\pi$ -electron systems.

Figure 22 shows examples of complexes presented in Table 5; for all of them there are H<sup>+</sup>... $\pi$ ( $\sigma$ ) interactions, relatively strong because the  $H_C$  values are negative. The H<sub>3</sub>O<sup>+</sup>...H<sub>2</sub> complex is very interesting; despite the weak Lewis base (molecular hydrogen), the binding energy of 5.2 kcal/mol outweighs such values for the typical H-bonded system, dimer of water, where the binding energy is of about 4.5–5 kcal/mol, depending on the level of approximation used in calculations.<sup>270</sup> The C<sub>2</sub>H<sub>3</sub><sup>+</sup>...C<sub>2</sub>H<sub>2</sub> complex presented in Figure 22 contains two H<sup>+</sup>... $\pi$  interactions; for the shorter H<sup>+</sup>... $\pi$  contact, the Laplacian of electron density at the corresponding BCP is negative as for a typical covalent bond, and this interaction may be classified as the multicenter covalent bond. The second H<sup>+</sup>... $\pi$  contact is slightly longer and may be treated as the proton-acceptor interaction within this unusual  $\pi$ -H... $\pi$  hydrogen bonding. However, for the C<sub>2</sub>H<sub>3</sub><sup>+</sup>...C<sub>2</sub>H<sub>2</sub> complex,

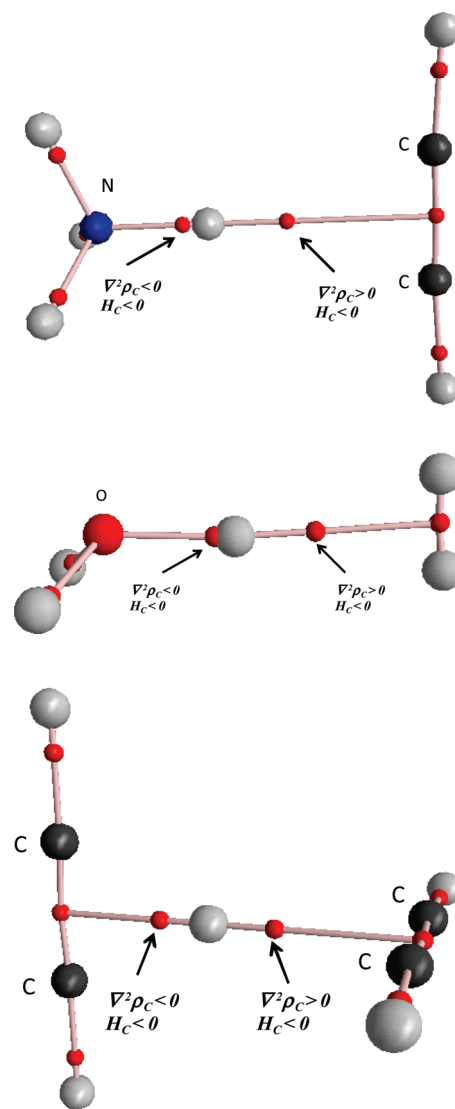


**Figure 22.** Molecular graphs of selected complexes presented in Table 5. For all of them, there are H<sup>+</sup>... $\pi$ ( $\sigma$ ) interactions; big circles correspond to the attractors (all gray circles correspond to hydrogen atoms), and small circles correspond to critical points. The following molecular graphs are presented: NH<sub>4</sub><sup>+</sup>...C<sub>2</sub>H<sub>2</sub>, H<sub>2</sub>OH<sup>+</sup>...H<sub>2</sub>, and C<sub>2</sub>H<sub>3</sub><sup>+</sup>...C<sub>2</sub>H<sub>2</sub>. Adapted with modifications from ref 268. Copyright 2007 American Chemical Society.

the energy difference between the transition state of the proton transfer reaction and the form corresponding to the local minimum amounts to 0.1 kcal/mol (MP2/6-311++G(3df,3pd) level of approximation);<sup>271</sup> thus, the zero-point energy along the proton transfer coordinate places the proton above this barrier in the symmetric position. It is in agreement with the later experimental and theoretical studies on this species and related systems.<sup>272</sup>

Table 5 also presents the interactions of Li<sup>+</sup> and Na<sup>+</sup> ions with acetylene or molecular hydrogen; the topological parameters clearly indicate that these are the closed-shell interactions. There are the H<sup>+</sup>...C<sub>2</sub>H<sub>2</sub> and H<sup>+</sup>...H<sub>2</sub> complexes, protonated acetylene (C<sub>2</sub>H<sub>3</sub><sup>+</sup>) and protonated hydrogen (H<sub>3</sub><sup>+</sup>), respectively. These are the multicenter  $\pi$ -H and  $\sigma$ -H covalent bonds. The binding energies for them are much higher than for the remaining systems and do correspond to typical covalent bonds' energies. Thus, the one-center and multicenter proton



Table 6. Classification of Hydrogen Bonds<sup>a</sup>

A—H···B H-bond	more detailed characterization	examples
one-center proton donor and one-center acceptor	Pauling type H-bond (3c–4e)	O—H···O, N—H···O, N—H···N
	nonelectronegative A (3c–4e)	C—H···O, C—H···N, C—H···S
	nonelectronegative B	O—H···C, N—H···C
	nonelectronegative A and B	C—H···C
	A—H···H—B (dihydrogen bond)	N—H···H—Re, C—H···H—C, O—H···H—Be
multicenter A or/and B	multicenter proton acceptor	X—H··· $\pi$ , X—H··· $\sigma$
	multicenter proton donor and proton acceptor	$\pi$ —H··· $\pi$ , $\pi$ —H··· $\sigma$ , $\sigma$ —H··· $\sigma$
	multicenter proton donor	$\pi$ —H···O

<sup>a</sup> Table reprinted with permission from ref <sup>271</sup>. Copyright 2007 American Chemical Society.

donors and acceptors are possible. Such systems were analyzed recently,<sup>273</sup> and a new classification of hydrogen bonds was proposed (Table 6).<sup>271</sup>

Among the different types of hydrogen bonds collected in Table 6 there is the dihydrogen bond (DHB). DHB may be designated as A—H···H—B, where A—H is the typical proton-donating bond with the excess of positive charge on hydrogen atom, and the second hydrogen connected with B plays the role of the proton acceptor and it is negatively charged. DHBs have been investigated since the mid-1990s by experimental<sup>34,35,274–278</sup> as well as theoretical methods.<sup>36,37,279–287</sup> It was proven that these interactions are a subclass of hydrogen bonds because they have the characteristics typical of hydrogen-bond interactions.<sup>288</sup>

Very recently, a large sample of various dihydrogen-bonded complexes was analyzed at the MP2/6-311++G(d,p) level of approximation.<sup>207</sup> Figure 23 presents molecular graphs of representatives of that sample. The  $\text{NH}_4^+ \cdots \text{HBeH}$ ,  $\text{H}_2\text{OH}^+ \cdots \text{HBeH}$ , and  $\text{HCCH} \cdots \text{HLi}$  complexes are presented; for the first two species, the H···H interactions belong to strong ones (9.6 and 19.5 kcal/mol, respectively), while for the last complex, the interaction is of medium strength (4.2 kcal/mol). It was found that a wide range of H···H interactions exist,<sup>207</sup> from van der Waals contacts, through stronger interactions, and finally to covalent bonds. Figure 24 presents the relationship between the H···H distance and the interaction energy components obtained from the decomposition scheme expressed by eq 11. Three regions of interactions can be seen: closed-shell interactions, those classified as partially covalent because the  $H_C$  values for H···H BCPs are negative there, and the strongest H···H interactions classified as covalent ones. For closed-shell interactions, the electrostatic interaction energy is the most important attractive term; for the other, stronger interactions (with at least  $H_C$  negative values), the delocalization interaction energy is the most important attractive factor. For these two subclasses, the H···H distance versus exchange energy dependences may be clearly separated. Besides, one can see that for the whole sample there is a nonlinear relationship between the H···H distance and the delocalization interaction energy, whereas no such dependence can be found between the H···H distance and the electrostatic energy. This may mean that the delocalization interaction is the driving attractive force for a wide range of interactions from van der Waals to very strong interactions possessing the covalent character.

Chart 1 presents various Lewis acid–Lewis base interactions.<sup>40</sup> All contain hydrogen atom situated between the other atoms; halogen bonding is the only exception. There are numerous studies and discussions on the C—Hal···B halogen bonding where C—Hal acts as the Lewis acid and B is the Lewis base

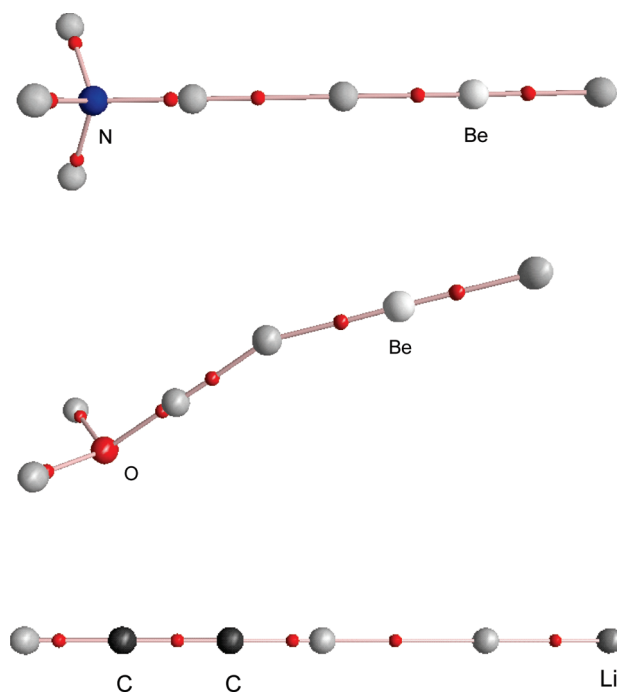


**Figure 23.** Molecular graphs of representatives of a sample of complexes bound through dihydrogen bond. The following complexes are presented:  $\text{NH}_4^+ \cdots \text{HBeH}$ ,  $\text{H}_2\text{OH}^+ \cdots \text{HBeH}$ , and  $\text{HCCH} \cdots \text{HLi}$  complexes. Big circles correspond to the attractors (gray circles correspond to hydrogen atoms), and small circles correspond to critical points. Reprinted with permission from ref 207. Copyright 2007 Elsevier.

center, and Hal designates Cl, Br, or I halogen atom (fluorine is rarely accepted as the atom involved in halogen bonding).<sup>289–293</sup>

The nature of halogen bonding is out of the scope of this Review. As concerns hydrogen bonding, it is stated in numerous definitions of this interaction that the hydrogen atom is positively charged and positioned between the other negatively charged centers; this may be treated as Brønsted acid–Brønsted base interaction<sup>41</sup> or at least as the Lewis acid–Lewis base interaction.<sup>40</sup> The hydride bonding is not in line with such definitions because the hydrogen atom is a negatively charged Lewis base center,<sup>39</sup> and a similar situation occurs for the halogen–hydride bonding.<sup>40</sup> It was also proved that an agostic interaction is the special case of hydride bonding;<sup>39</sup> thus, it could not be classified as hydrogen bonding.

The results presented in this Review show that different types of hydrogen bonding, among them dihydrogen bonding, reveal the covalent character of the interaction. The question arises if the covalent character may be also attributed to the blue-shifting

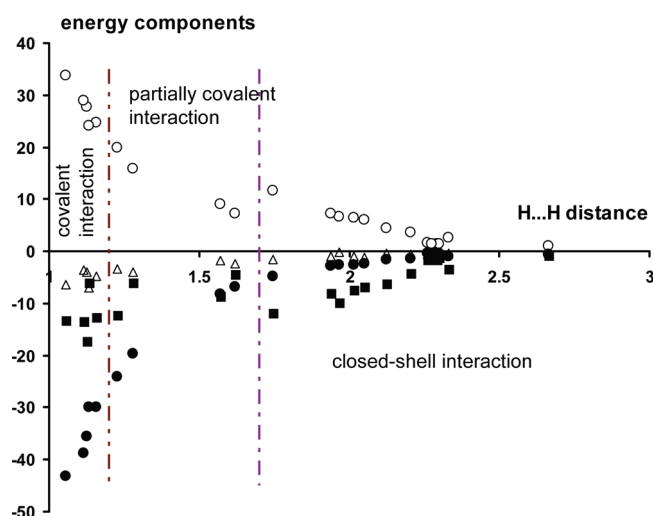


**Figure 24.** Relationship between the H...H distance (Å) and the interaction energy components obtained from the decomposition scheme expressed by eq 11. ○, exchange energy; △, correlation energy; ■, electrostatic energy; ●, delocalization energy. Three regions of interactions are designated; covalent interactions correspond to the strongest H-bonds with negative  $\nabla^2\rho_{H...B}$  values, partially covalent interactions with positive  $\nabla^2\rho_{H...B}$  values but negative  $H_C$ 's, and closed-shell interactions are the weakest ones with positive  $H_C$  values. Reprinted with permission from ref 207. Copyright 2007 Elsevier.

hydrogen bonding. There are different explanations of the nature of the latter type of interaction.<sup>195–198,294–296</sup> However, briefly speaking, the contraction of the proton-donating A–H bond as a result of complexation is characteristic for this interaction. This is not in line with the bond number conservation rule (eq 3) because the bond number for A–H in blue-shifting A–H...B interaction (most often this is C–H...B interaction) exceeds unity. On the other hand, any H...B contact may be described by the corresponding bond number, and hence it possesses the covalent character.

It was stated that for the hydrogen-bonding formation there are two effects: hyperconjugation leading to the weakening and elongation of the proton-donating bond, and the rehybridization that promoted the strengthening and shortening of that bond.<sup>297</sup> If the latter effect outweighs hyperconjugation, thus it is the blue-shift hydrogen bonding. However, it was also found<sup>297</sup> that for the sample of blue-shifting hydrogen bonds, there is the increase of the hyperconjugative energy expressed by eq 22 if the H...B distance decreases. It proves that also the blue-shifting hydrogen bonds are the covalent in nature interactions.

Both effects, hyperconjugation and rehybridization, are general for all types of hydrogen bonds; thus, there are no fundamental differences between blue-shifting and red-shifting hydrogen bond.<sup>297</sup> The rehybridization is connected with the strengthening of A–H proton-donating bond and an increase in s-character of A hybrid orbital in this bond; such an increase is greater for the shorter (A)H...B distances.<sup>297</sup> The increase of the s-character of hybrid orbital is in line with the Bent rule.<sup>298</sup> The latter states that the s-character of A-atom hybrid orbital increases if this orbital is aimed toward electropositive substituent; if this orbital is aimed toward the electronegative orbital, thus its p-character increases. The formation of A–H...B hydrogen bonding is connected with the increase of the electropositivity of H-atom and hence with the increase of the s-character of A hybrid orbital.

## 7. SUMMARY

What is specific to the hydrogen-bonding interaction? Such a question is sometimes asked, and the usual answers involve two concepts. The first one says that it is mainly electrostatic interaction. The second concept, while appreciating the electrostatic interaction, holds that some other kinds of interaction energy terms are also important, mainly charge transfer and dispersive energies. However, many lines of evidence converge on recognition of the unique importance of covalency (charge transfer) in the general H-bonding phenomenon. Remaining disagreements can be traced to discordant definitions of charge transfer, which naturally depend on how atomic charge density is assigned to each atomic center. Because “atomic boundary” is understood quite differently in QTAIM-based versus NBO-based methods, one might have expected these methods to yield quite different charge assignments. However, QTAIM and NBO-based descriptors of H-bonding are actually found to exhibit reasonably consistent patterns. Much deeper disagreements separate the overlap-dependent energy decomposition schemes of Morokuma type from the NBO-based NEDA method. For reasons discussed previously in this Review and in earlier studies,<sup>20,42,43,108–110</sup> one can believe that apparent conclusions drawn from such overlap-dependent analysis are misleading.

The covalent character is connected with those terms of interaction that concern the redistribution of electronic charge as an effect of complexation. According to the NBO approach, this is the energy connected with electron charge transfer from the lone pair of acceptor to the antibonding  $\sigma^*$  orbital of the proton-donating bond;<sup>20</sup> it was shown here that this may be any other transfer from the acceptor orbital to  $\sigma^*$  orbital. Because for all hydrogen bonds the stabilizing role of charge transfer interaction may be found, thus one may state that all hydrogen bonds are in any way covalent in nature.

The Quantum Theory of “Atoms in Molecules” (QTAIM)<sup>45</sup> provides the characteristics of critical points, for example, of H...B critical points. The negative value of the Laplacian of electron density at H...B bond critical point proves the electron charge concentration in the H...B region and the covalent character of the interaction. There is substantial theoretical and experimental evidence of the existence of hydrogen bonds, which are covalent in nature, because Laplacians of the electron density at H...B BCP are negative or at least the total electron energy density at H...B BCP is negative.

There is abundant evidence that covalency is attributed to hydrogen bond as a kind of interaction, not only to short and strong interactions. The covalency is the driving force of hydrogen bond determining its characteristics. The following evidence of the covalent nature of hydrogen bond can be mentioned.

- (1) The delocalization interaction energy (or any other related energy, charge transfer, polarization, etc.) correlates with the proton–acceptor distance for a wide range of hydrogen-bond interactions; this correlation is much better than for any other term of interaction energy (electrostatic, exchange, etc.).
- (2) The delocalization interaction energy correlates with the binding energy.
- (3) The so-called “CT-deleted” structures, that is, those where the charge transfer interaction energy is rejected and the complex stability is based on the remaining interaction energy terms. They form intermolecular links at much greater distances between monomers; in other words, the

formation of hydrogen bonds in such cases is problematic, or the H-bonded complexes are not formed at all.

- (4) This is in line with the third statement; for numerous hydrogen-bonded complexes, the exchange energy term cancels the electrostatic interaction energy, and hence the other attractive energy terms, mainly delocalization energy, are responsible for the stability of the system at a relatively short distance between linked monomers.
- (5) The potential electron energy density at  $H \cdots B$  BCP,  $V_C$ , decreases (its modulus increases) monotonically if the  $H \cdots B$  distance decreases; this topological parameter derived from QTAIM correlates with the other measures of the hydrogen-bond strength. Because the negative value of  $V_C$  determines the sign of the “indicators” of covalency,  $H_C$  and  $\nabla^2 \rho_{H \cdots B}$  values, one can see that  $V_C$  fulfills the similar role as the delocalization interaction energy term within any energy partitioning scheme. It was shown that the total electron energy density at the proton  $\cdots$  acceptor BCP ( $H_C$ ) is negative if the Heitler–London energy is positive.

## AUTHOR INFORMATION

### Corresponding Author

\*E-mail: s.grabowski@ikerbasque.org.

## BIOGRAPHY

Sławomir Janusz Grabowski was born in Warsaw, Poland (1956) and received his M.Sc. degree (1981) and his Ph.D. (1986) at the University of Warsaw. He received his D.Sc. (habilitation, 1998) at the Technical University of Łódź, Poland. Since 1986, he has been working at the University of Białystok, and since 2002 he has been at the University of Łódź (the full professor position since 2005), Poland. He was employed in different universities as PostDoc or professor: ETH Zentrum, Zürich, Switzerland (1987), University of Uppsala, Sweden (1988), University of Grenoble, France (1992), Jackson State University, Jackson, MS (during summers in 2003–2008), and Fukuoka University, Japan (2009, awarded by Japan Society for the Promotion of Science). In 2009, he moved to San Sebastian and currently is employed as the Ikerbasque Research Professor at the University of the Basque Country, Spain. Dr. Grabowski has authored or coauthored about 130 papers and 10 book chapters, and he has edited a book on hydrogen bonding. His work encompasses the analysis of hydrogen bonding, halogen bonding, and the other Lewis acid–Lewis base interactions in the gas phase as well as in crystals.



## ACKNOWLEDGMENT

Technical and human support provided by IZO-SGI SGiker (UPV/EHU, MICINN, GV/EJ, ESF) is gratefully acknowledged.

I wish to thank reviewers for their comments and suggestions, which helped to improve the manuscript significantly. Especially, the comments of one of the reviewers on the decomposition of interaction energy influenced positively numerous parts of the text.

## REFERENCES

- (1) Jeffrey, G. A.; Saenger, W. *Hydrogen Bonding in Biological Structures*; Springer-Verlag: Berlin, 1991.
- (2) Jeffrey, G. A. *An Introduction to Hydrogen Bonding*; Oxford University Press: New York, 1997.
- (3) Desiraju, G. R.; Steiner, T. *The Weak Hydrogen Bond in Structural Chemistry and Biology*; Oxford University Press Inc.: New York, 1999.
- (4) *Hydrogen Bonding – New Insights*; Grabowski, S. J., Ed. In *Series Challenges and Advances in Computational Chemistry and Physics*; Leszczynski, J., Ed.; Springer: New York, 2006.
- (5) Gerlt, J. A.; Kreevoy, M. M.; Cleland, W. W.; Frey, P. A. *Chem. Biol.* **1997**, *4*, 259.
- (6) Perrin, C. L.; Nielson, J. B. *Annu. Rev. Phys. Chem.* **1997**, *48*, 511.
- (7) Leiserowitz, L. *Acta Crystallogr.* **1976**, *B32*, 775.
- (8) Bernstein, J.; Etter, M. C.; Leiserowitz, L. In *The Role of Hydrogen Bonding in Molecular Assemblies, in Structure Correlation*; Bürgi, H.-B., Dunitz, J. D., Eds.; VCH: Weinheim, 1994.
- (9) Desiraju, G. R. *Crystal Engineering. The Design of Organic Solids*; Elsevier: Amsterdam, 1989.
- (10) Zundel, G. In *Advances in Chemical Physics*; Prigogine, I., Rice, S. A., Eds.; J. Wiley: New York, 2000; Vol. 111.
- (11) *Hydrogen-Transfer Reactions*; Hynes, J. T., Klinman, J. P., Limbach, H.-H., Schowen, R. L., Eds.; Wiley-VCH Verlag GmbH & Co. KGaA: Weinheim, 2007.
- (12) Lehn, J.-M. *Angew. Chem., Int. Ed. Engl.* **1990**, *29*, 1304.
- (13) Lehn, J.-M. *Supramolecular Chemistry*; Verlag-Chemie: Weinheim, 1995.
- (14) Pauling, L. *The Nature of the Chemical Bond*, 3rd ed.; Cornell University Press: Ithaca, NY, 1960.
- (15) Lewis, G. N. *Valence and the Structure of Atoms and Molecules*; Chemical Catalog Co.: New York, 1923.
- (16) Latimer, W. M.; Rodebush, W. H. *J. Am. Chem. Soc.* **1920**, *42*, 1419.
- (17) Chan, B.; Del Bene, J. E.; Radom, L. *Mol. Phys.* **2009**, *107*, 1095.
- (18) Grabowski, S. J.; Ugalde, J. M. *Chem. Phys. Lett.* **2010**, *493*, 37.
- (19) Lee, H. M.; Kumar, A.; Kołaski, M.; Kim, D. Y.; Lee, E. C.; Min, S. K.; Park, M.; Choi, Y. C.; Kim, K. S. *Phys. Chem. Chem. Phys.* **2010**, *12*, 6278.
- (20) Weinhold, F.; Landis, C. *Valency and Bonding. A Natural Bond Orbital Donor – Acceptor Perspective*; Cambridge University Press: New York, 2005.
- (21) Pimentel, G. C.; McClellan, A. L. *The Hydrogen Bond*; W.H. Freeman and Co.: San Francisco and London, 1960.
- (22) Morokuma, K.; Kitaura, K. In *Molecular Interactions*; Ratajczak, H., Orville-Thomas, W. J., Eds.; John Wiley and Sons Ltd.: New York, 1980; Vol. 1, pp 21–66.
- (23) Jensen, F. *Introduction to Computational Chemistry*; John Wiley & Sons: Chichester, England, 1999.
- (24) Cramer, C. J. *Essentials of Computational Chemistry*; John Wiley & Sons: Chichester, England, 2004.
- (25) Chałasiński, G.; Szczęśniak, M. M. *Chem. Rev.* **1994**, *94*, 1723.
- (26) Umeyama, H.; Morokuma, K. *J. Am. Chem. Soc.* **1977**, *99*, 1316.
- (27) Scheiner, S. *Hydrogen Bonding: A Theoretical Perspective*; Oxford University Press: New York, 1997.
- (28) Desiraju, G. R. *Acc. Chem. Res.* **2002**, *35*, 565.
- (29) Grabowski, S. J.; Sokalski, W. A.; Dyguda, E.; Leszczynski, J. *J. Phys. Chem. B* **2006**, *110*, 6444.



- (30) Gilli, P.; Bertolasi, V.; Ferretti, V.; Gilli, G. *J. Am. Chem. Soc.* **1994**, *116*, 909.
- (31) Gilli, G.; Gilli, P. *J. Mol. Struct.* **2000**, *552*, 1.
- (32) Suttor, D. J. *J. Chem. Soc.* **1963**, 1105.
- (33) Taylor, R.; Kennard, O. *J. Am. Chem. Soc.* **1982**, *104*, 5063.
- (34) Wessel, J.; Lee, J. C., Jr.; Peris, E.; Yap, G. P. A.; Fortin, J. B.; Ricci, J. S.; Sini, G.; Albinati, A.; Koetzle, T. F.; Eisenstein, O.; Rheingold, A. L.; Crabtree, R. H. *Angew. Chem., Int. Ed. Engl.* **1995**, *34*, 2507.
- (35) Crabtree, R. H.; Siegbahn, P. E. M.; Eisenstein, O.; Rheingold, A. L.; Koetzle, T. F. *Acc. Chem. Res.* **1996**, *29*, 348.
- (36) Liu, Q.; Hoffman, R. *J. Am. Chem. Soc.* **1995**, *117*, 10108.
- (37) Alkorta, I.; Elguero, J.; Foces-Foces, C. *Chem. Commun.* **1996**, 1633.
- (38) Rozas, I.; Alkorta, I.; Elguero, J. *J. Phys. Chem. A* **1997**, *101*, 4236.
- (39) Grabowski, S. J.; Sokalski, W. A.; Leszczynski, J. *Chem. Phys. Lett.* **2006**, *422*, 334.
- (40) Lipkowski, P.; Grabowski, S. J.; Leszczynski, S. J. *J. Phys. Chem. A* **2006**, *110*, 10296.
- (41) Huyskens, P.; Tzeegers-Huyskens, T. *J. Chim. Phys.* **1964**, *61*, 84.
- (42) Reed, A. E.; Curtiss, L. A.; Weinhold, F. *Chem. Rev.* **1988**, *88*, 899.
- (43) Weinhold, F. *J. Mol. Struct. (THEOCHEM)* **1997**, *398–399*, 181.
- (44) Bader, R. F. W. *Acc. Chem. Res.* **1985**, *18*, 9.
- (45) Bader, R. F. W. *Chem. Rev.* **1991**, *91*, 893.
- (46) Bader, R. F. W. *Atoms in Molecules, A Quantum Theory*; Oxford University Press, Oxford, 1990.
- (47) *Quantum Theory of Atoms in Molecules: Recent Progress in Theory and Application*; Matta, C., Boyd, R. J., Eds.; Wiley-VCH: New York, 2007.
- (48) Madsen, G. K. H.; Iversen, B. B.; Larsen, F. K.; Kapon, M.; Reisner, G. M.; Herbstein, F. H. *J. Am. Chem. Soc.* **1998**, *120*, 10040.
- (49) Cleland, W. W.; Kreevoy, M. M. *Science* **1994**, *264*, 1887.
- (50) Isaacs, E. D.; Shukla, A.; Platzman, P. M.; Hamann, D. R.; Barbiellini, B.; Tulk, C. A. *Phys. Rev. Lett.* **1999**, *82*, 600.
- (51) Grabowski, S. J. *J. Phys. Org. Chem.* **2004**, *17*, 18.
- (52) McWeeny, R. *Coulson's Valence*; Oxford University Press: New York, 1979.
- (53) Wiberg, K. *Tetrahedron* **1968**, *24*, 1083.
- (54) Pauling, L. *J. Am. Chem. Soc.* **1947**, *69*, 542.
- (55) Dunitz, J. D. *X-Ray Analysis and the Structure of Organic Molecules*; Cornell University Press: Ithaca, 1979.
- (56) Bürgi, H.-B. *Angew. Chem., Int. Ed. Engl.* **1975**, *14*, 460.
- (57) Johnston, H. S. *Adv. Chem. Phys.* **1960**, *3*, 131.
- (58) Johnston, H. S.; Parr, Ch. *J. Am. Chem. Soc.* **1963**, *85*, 2544.
- (59) Grabowski, S. J. *Croat. Chem. Acta* **1988**, *61*, 815.
- (60) Lippincott, E. R.; Schroeder, R. *J. Chem. Phys.* **1955**, *23*, 1099.
- (61) Lippincott, E. R.; Schroeder, R. *J. Phys. Chem.* **1957**, *61*, 921.
- (62) Reid, C. *J. Chem. Phys.* **1959**, *30*, 182.
- (63) Steiner, T. *J. Phys. Chem. A* **1998**, *102*, 7041.
- (64) Olovsson, I.; Jönsson, P.-G. In *The Hydrogen Bond, Recent Developments in Theory and Experiments*; Schuster, P., Zundel, G., Sandorfy, C., Eds.; North-Holland: Amsterdam, 1976; pp 394–455.
- (65) Chiari, G.; Ferraris, G. *Acta Crystallogr.* **1982**, *B38*, 2331.
- (66) Steiner, T.; Saenger, W. *J. Am. Chem. Soc.* **1992**, *114*, 7123.
- (67) Grabowski, S. J. *J. Mol. Struct.* **2000**, *552*, 153.
- (68) Allen, F. H.; Davies, J. E.; Galloy, J. E.; Johnson, J. J.; Kennard, O.; Macrae, C. F.; Mitchel, E. M.; Smith, J. M.; Watson, D. G. *J. Chem. Inf. Comput. Sci.* **1991**, *31*, 187.
- (69) Sequeira, A.; Berkebile, C. A.; Hamilton, W. C. *J. Mol. Struct.* **1968**, *1*, 283.
- (70) Currie, M.; Speakman, J. C.; Kanters, J. A.; Kroon, J. J. *Chem. Soc., Perkin Trans. 2* **1975**, 1549.
- (71) Brown, I. D. *Acta Crystallogr.* **1977**, *B33*, 1305.
- (72) Brown, I. D. *Chem. Soc. Rev.* **1978**, *7*, 359.
- (73) Brown, I. D. *Chem. Rev.* **2009**, *109*, 6858.
- (74) Steiner, T. *J. Chem. Soc., Perkin Trans. 2* **1995**, 1315.
- (75) Grabowski, S. J.; Krygowski, T. M. *Tetrahedron* **1998**, *54*, 5683.
- (76) Grabowski, S. J. *Tetrahedron* **1998**, *54*, 10153.
- (77) Cieplak, A. S. In *Organic Addition and Elimination Reactions; Transformation Paths of Carbonyl Derivatives, in Structure Correlation*; Bürgi, H.-B., Dunitz, J. D., Eds.; VCH Verlagsgesellschaft mbH: Weinheim, 1994.
- (78) Auf der Heyde, T. In *Structure Correlation*; Bürgi, H.-B., Dunitz, J. D., Eds.; VCH Verlagsgesellschaft mbH: Weinheim, 1994.
- (79) Bürgi, H.-B.; Shklover, V. In *Structure Correlation*; Bürgi, H.-B., Dunitz, J. D., Eds.; VCH Verlagsgesellschaft mbH: Weinheim, 1994.
- (80) Benedict, H.; Limbach, H. H.; Wehlan, M.; Fehlhammer, W. P.; Golubev, N. S.; Janoschek, R. *J. Am. Chem. Soc.* **1998**, *120*, 2939.
- (81) Smirnov, S. S.; Benedict, H.; Golubev, N. S.; Denisov, G. S.; Kreevoy, M. M.; Schowen, L. R.; Limbach, H. H. *Can. J. Chem.* **1999**, *77*, 943.
- (82) Grabowski, S. J.; Krygowski, T. M. *Chem. Phys. Lett.* **1999**, *305*, 247.
- (83) Sobczyk, L.; Grabowski, S. J.; Krygowski, T. M. *Chem. Rev.* **2005**, *105*, 3513.
- (84) Grabowski, S. J. *J. Phys. Chem. A* **2001**, *105*, 10739.
- (85) Schuster, P. In *Intermolecular Interactions: From Diatomics to Biopolymers*; Pullman, B., Ed.; J. Wiley: New York, 1978; Chapter 4, pp 363–430.
- (86) Negative values for different H-bonds are presented in figures and tables in this Review. However, for the convenience of discussion and presentation, the ( $-\Delta E$ ) positive values are given in the text. Sometimes, the H-bond formation energy is defined similarly as in eq 4, but there are inverse signs in the right-hand side of this equation, and thus such defined energy is positive; for example, such positive values of hydrogen-bonding energies are presented in: Gordon, M. S.; Jensen, J. H. *Acc. Chem. Res.* **1996**, *29*, 536.
- (87) Grabowski, S. J. *Annu. Rep. Prog. Chem., Sect. C: Phys. Chem.* **2006**, *102*, 131.
- (88) Grabowski, S. J.; Sadlej, A. J.; Sokalski, W. A.; Leszczynski, J. *Chem. Phys.* **2006**, *327*, 151.
- (89) van Lenthe, J. H.; van Duijneveldt-van de Rijdt, J. C. G. M.; van Duijneveldt, F. B. *Adv. Chem. Phys.* **1987**, *69*, 521.
- (90) Piel, L. *Ideas of Quantum Chemistry*; Elsevier Science Publishers: Amsterdam, 2007.
- (91) Boys, S. F.; Bernardi, F. *Mol. Phys.* **1970**, *19*, 553.
- (92) van Duijneveldt, F. B.; van Duijneveldt-van de Rijdt, J. C. G. M.; van Lenthe, J. H. *Chem. Rev.* **1994**, *94*, 1873.
- (93) Simon, S.; Duran, M.; Dannenberg, J. J. *J. Chem. Phys.* **1996**, *105*, 11024.
- (94) Simon, S.; Duran, M.; Dannenberg, J. J. *J. Phys. Chem. A* **1999**, *103*, 1640.
- (95) Simon, S.; Duran, M.; Dannenberg, J. J. *J. Chem. Phys.* **2000**, *113*, 5666.
- (96) Simon, S.; Bertran, J.; Sodupe, M. *J. Phys. Chem. A* **2001**, *105*, 4359.
- (97) Tuma, Ch.; Boese, A. D.; Handy, N. C. *Phys. Chem. Chem. Phys.* **1999**, *1*, 3939.
- (98) Buemi, G. . In *Hydrogen Bonding – New Insights*; Grabowski, S. J., Ed.; Springer: New York, 2006; Chapter 2.
- (99) Emsley, J.; Hoyte, O. P. A.; Overill, R. E. *J. Am. Chem. Soc.* **1978**, *100*, 3303.
- (100) Turi, L.; Dannenberg, J. J. *J. Phys. Chem.* **1993**, *97*, 2488.
- (101) Grabowski, S. J.; Sokalski, W. A. *J. Phys. Org. Chem.* **2005**, *18*, 779.
- (102) Kollman, P. A.; Allen, L. C. *Theor. Chim. Acta* **1970**, *18*, 399.
- (103) Kollman, P. A.; Allen, L. C. *Chem. Rev.* **1972**, *72*, 283.
- (104) Kitaura, K.; Morokuma, K. *Int. J. Quantum Chem.* **1976**, *10*, 325.
- (105) Morokuma, K. *Acc. Chem. Res.* **1977**, *10*, 294.
- (106) Sokalski, W. A.; Roszak, S.; Pecul, K. *Chem. Phys. Lett.* **1988**, *153*, 153.
- (107) Sokalski, W. A.; Roszak, S. *J. Mol. Struct. (THEOCHEM)* **1991**, *234*, 387.

- (108) Corcoran, C. T.; Weinhold, F. *J. Chem. Phys.* **1980**, *72*, 2866.
- (109) Weinhold, F.; Carpenter, J. E. *J. Mol. Struct. (THEOCHEM)* **1988**, *165*, 189.
- (110) Weinhold, F. *Angew. Chem., Int. Ed.* **2003**, *42*, 4188.
- (111) Ziegler, T.; Rauk, A. *Inorg. Chem.* **1979**, *18*, 1558.
- (112) Bickelhaupt, F. M.; Baerends, E. J. *Rev. Comput. Chem.* **2000**, *15*, 1.
- (113) Esterhuysen, C.; Frenking, G. *Theor. Chem. Acc.* **2004**, *111*, 381.
- (114) Mo, Y.; Peyerimhoff, S. D. *J. Chem. Phys.* **2000**, *112*, 5530.
- (115) Mo, Y.; Song, L.; Lin, Y. *J. Phys. Chem. A* **2007**, *111*, 8291.
- (116) Nakashima, K.; Zhang, X.; Xiang, M.; Lin, Y.; Lin, M.; Mo, Y. *J. Theor. Chem. Comput.* **2008**, *7*, 639.
- (117) Khaliullin, R. Z.; Lochan, R.; Cobar, E.; Bell, A. T.; Head-Gordon, M. *J. Phys. Chem. A* **2007**, *111*, 8753.
- (118) Khaliullin, R. Z.; Bell, A. T.; Head-Gordon, M. *Chem.-Eur. J.* **2008**, *15*, 851.
- (119) Gora, R. W.; Grabowski, S. J.; Leszczynski, J. *J. Phys. Chem. A* **2005**, *109*, 6397.
- (120) Grabowski, S. J.; Sokalski, W. A.; Leszczynski, J. *J. Phys. Chem. A* **2006**, *110*, 4772.
- (121) Grabowski, S. J. *Croat. Chem. Acta* **2009**, *185*, 82.
- (122) Popelier, P. *Atoms in Molecules. An Introduction*; Prentice Hall, Pearson Education Limited: New York, 2000.
- (123) Koritsansky, T. S.; Coppens, P. *Chem. Rev.* **2001**, *101*, 1583.
- (124) Coppens, P. *X-Ray Charge Densities and Chemical Bonding*; IUCr, Oxford University Press: New York, 1997.
- (125) Matta, C. J.; Boyd, R. J. In *Quantum Theory of Atoms in Molecules: Recent Progress in Theory and Application*; Matta, C. J., Boyd, R. J., Eds.; Wiley-VCH: New York, 2007; Chapter 1.
- (126) Matta, C. F. In *Hydrogen Bonding – New Insights*; Grabowski, S. J., Ed.; Springer: New York, 2006; Chapter 9.
- (127) Bader, R. F. W. *Monatsh. Chem.* **2005**, *126*, 819.
- (128) Bader, R. F. W.; Essen, H. *J. Chem. Phys.* **1984**, *80*, 1943.
- (129) Bader, R. F. W.; Nguyen-Dang, T.; Tal, Y. *Rep. Prog. Phys.* **1981**, *44*, 893.
- (130) Bader, R. F. W. *J. Phys. Chem. A* **1998**, *102*, 7314.
- (131) Bader, R. F. W. *J. Phys. Chem. A* **2009**, *113*, 10391.
- (132) Grabowski, S. J.; Ugalde, J. M. *J. Phys. Chem. A* **2010**, *114*, 7223.
- (133) Grabowski, S. J.; Ugalde, J. M. *Can. J. Chem.* **2010**, *88*, 769.
- (134) Poater, J.; Solà, M.; Bickelhaupt, F. M. *Chem.-Eur. J.* **2006**, *12*, 2889.
- (135) Poater, J.; Solà, M.; Bickelhaupt, F. M. *Chem.-Eur. J.* **2006**, *12*, 2902.
- (136) Bader, R. F. W. *Chem.-Eur. J.* **2006**, *12*, 2896.
- (137) Bader, R. F. W.; Fang, D.-C. *J. Chem. Theory Comput.* **2005**, *1*, 403.
- (138) Bader, R. F. W.; Matta, C. F.; Cortés-Guzmán, F. *Organometallics* **2004**, *23*, 6253.
- (139) Matta, C. F.; Bader, R. F. W. *J. Phys. Chem. A* **2006**, *110*, 6365.
- (140) Krapp, A.; Frenking, G. *Chem.-Eur. J.* **2007**, *13*, 8256.
- (141) Matta, C. F.; Hernández-Trujillo, J.; Tang, T.-H.; Bader, R. F. W. *Chem.-Eur. J.* **2003**, *9*, 1940.
- (142) Wolstenholme, D. J.; Matta, C. F.; Cameron, T. S. *J. Phys. Chem. A* **2007**, *111*, 8803.
- (143) Grabowski, S. J.; Pfitzner, A.; Zabel, M.; Dubis, A. T.; Palusiak, M. *J. Phys. Chem. B* **2004**, *108*, 1831.
- (144) Koch, U.; Popelier, P. L. A. *J. Phys. Chem.* **1995**, *99*, 9747.
- (145) Pacios, L. F.; Gálvez, O.; Gómez, P. C. *J. Chem. Phys.* **2005**, *122*, 214307.
- (146) Vener, M. V.; Manaev, A. V.; Egorova, A. N.; Tsirelson, V. G. *J. Phys. Chem. A* **2007**, *111*, 1155.
- (147) Gatti, C.; Cargnoni, F.; Bertini, L. *J. Chem. Phys.* **2003**, *24*, 422.
- (148) Mariam, Y. H.; Musin, R. *J. Phys. Chem. A* **2008**, *112*, 134.
- (149) Rozas, I.; Alkorta, I.; Elguero, J. *J. Am. Chem. Soc.* **2000**, *122*, 11154.
- (150) Cremer, D.; Kraka, E. *Croat. Chem. Acta* **1984**, *57*, 1259.
- (151) Jenkins, S.; Morrison, I. *Chem. Phys. Lett.* **2000**, *317*, 97.
- (152) Arnold, W. D.; Oldfield, E. *J. Am. Chem. Soc.* **2000**, *122*, 12835.
- (153) Carrol, M. T.; Chang, C.; Bader, R. F. W. *Mol. Phys.* **1988**, *63*, 387.
- (154) Carrol, M. T.; Bader, R. F. W. *Mol. Phys.* **1988**, *65*, 695.
- (155) Mó, O.; Yáñez, M.; Elguero, J. *J. Chem. Phys.* **1992**, *97*, 6628.
- (156) Mó, O.; Yáñez, M.; Elguero, J. *J. Mol. Struct. (THEOCHEM)* **1994**, *314*, 73.
- (157) Espinosa, E.; Molins, E.; Lecomte, C. *Chem. Phys. Lett.* **1998**, *285*, 170.
- (158) Galvez, O.; Gomez, P. C.; Pacios, L. F. *Chem. Phys. Lett.* **2001**, *337*, 263.
- (159) Galvez, O.; Gomez, P. C.; Pacios, L. F. *J. Chem. Phys.* **2001**, *115*, 11166.
- (160) Galvez, O.; Gomez, P. C.; Pacios, L. F. *J. Chem. Phys.* **2003**, *118*, 4878.
- (161) Pacios, L. F. *J. Phys. Chem. A* **2004**, *108*, 1177.
- (162) Pacios, L. F. *Struct. Chem.* **2005**, *16*, 223.
- (163) Knop, O.; Rankin, K. N.; Boyd, R. J. *J. Phys. Chem. A* **2001**, *105*, 6552.
- (164) Knop, O.; Rankin, K. N.; Boyd, R. J. *J. Phys. Chem. A* **2003**, *107*, 272.
- (165) Parthasarathi, R.; Subramanian, V.; Sathyamurthy, N. *J. Phys. Chem. A* **2006**, *110*, 3349.
- (166) Gibbs, G. V.; Cox, D. F.; Crawford, T. D.; Rosso, K. M.; Ross, N. L.; Downs, R. T. *J. Chem. Phys.* **2006**, *14*, 084704.
- (167) Grabowski, S. J.; Dubis, A. T.; Palusiak, M.; Leszczynski, J. *J. Phys. Chem. B* **2006**, *110*, 5875.
- (168) Grabowski, S. J. *J. Mol. Struct.* **2002**, *615*, 239.
- (169) Leffler, J. E. *Science* **1953**, *117*, 340.
- (170) Hammond, G. S. *J. Am. Chem. Soc.* **1955**, *77*, 334.
- (171) Gilli, P.; Bertolasi, V.; Pretto, L.; Lyčka, A.; Gilli, G. *J. Am. Chem. Soc.* **2002**, *124*, 13554.
- (172) Gilli, P.; Bertolasi, V.; Pretto, L.; Ferretti, V.; Gilli, G. *J. Am. Chem. Soc.* **2004**, *126*, 3845.
- (173) Gilli, P.; Bertolasi, V.; Pretto, L.; Antonov, L.; Gilli, G. *J. Am. Chem. Soc.* **2005**, *127*, 4943.
- (174) Grabowski, S. J.; Małecka, M. *J. Phys. Chem. A* **2006**, *110*, 11847.
- (175) Gilli, G.; Bellucci, F.; Ferretti, V.; Bertolasi, V. *J. Am. Chem. Soc.* **1989**, *111*, 1023.
- (176) Beck, J. F.; Mo, Y. *J. Comput. Chem.* **2006**, *28*, 455–466.
- (177) Grabowski, S. J. *J. Mol. Struct.* **2001**, *562*, 137.
- (178) Pichierri, F. *Chem. Phys. Lett.* **2003**, *376*, 781.
- (179) Srinivasan, R. S.; Feenstra, J. S.; Park, S. T.; Xu, S.; Zewail, A. H. *J. Am. Chem. Soc.* **2004**, *126*, 2266.
- (180) Palusiak, M.; Simon, S.; Solà, M. *Chem. Phys.* **2007**, *342*, 43.
- (181) Guerra, C. F.; Bickelhaupt, F. M.; Snijders, J. G.; Baerends, E. J. *Chem.-Eur. J.* **1999**, *5*, 3581.
- (182) Palusiak, M.; Simon, S.; Solà, M. *J. Org. Chem.* **2006**, *71*, 5241.
- (183) Espinosa, E.; Alkorta, I.; Elguero, J.; Molins, E. *J. Chem. Phys.* **2002**, *117*, 5529.
- (184) Fradera, X.; Austen, M. A.; Bader, R. F. W. *J. Phys. Chem. A* **1999**, *103*, 304.
- (185) Fradera, X.; Poater, J.; Simon, S.; Duran, M.; Solà, M. *Theor. Chem. Acc.* **2002**, *107*, 362.
- (186) Poater, J.; Fradera, X.; Solà, M.; Duran, M.; Simon, S. *Chem. Phys. Lett.* **2003**, *369*, 248.
- (187) Madsen, G. K. H.; McIntyre, G. J.; Schiøtt, B.; Larsen, F. K. *Chem.-Eur. J.* **2007**, *13*, 5539.
- (188) Mallison, P. R.; Woźniak, K.; Smith, G. T.; McCormack, K. L.; Yufit, D. S. *J. Am. Chem. Soc.* **1997**, *119*, 11502.
- (189) Bianchi, R.; Gervasio, G.; Marabello, D. *Inorg. Chem.* **2000**, *39*, 2360.
- (190) Grabowski, S. J. *Chem. Phys. Lett.* **2001**, *338*, 361.
- (191) Pinchas, S. *Anal. Chem.* **1955**, *27*, 2.
- (192) Trudeau, G.; Dumas, J. M.; Dupuis, P.; Guerin, M.; Sandorfy, C. *Top. Curr. Chem.* **1980**, *93*, 91.

- (193) Hobza, P.; Havlas, Z. *Chem. Rev.* **2000**, *100*, 4253 (and references cited therein).
- (194) Hermansson, K. *J. Phys. Chem.* **2002**, *106*, 4695.
- (195) Scheiner, S.; Kar, T. *J. Phys. Chem. A* **2002**, *106*, 1784.
- (196) Li, X.; Liu, L.; Schlegel, B. *J. Am. Chem. Soc.* **2002**, *124*, 9639.
- (197) Karpfen, A.; Kryachko, E. S. *J. Phys. Chem. A* **2003**, *107*, 9724.
- (198) Kryachko, E. S. In *Hydrogen Bonding – New Insights*; Grabowski, S. J., Ed.; Springer: New York, 2006; Chapter 8.
- (199) Becke, A. D.; Edgecombe, K. E. *J. Chem. Phys.* **1990**, *92*, 5397.
- (200) Savin, A.; Becke, A. D.; Flad, J.; Nesper, R.; Preuss, H.; von Schnering, H. G. *Angew. Chem., Int. Ed. Engl.* **1991**, *30*, 409.
- (201) Silvi, B.; Gillespie, R. J. In *Quantum Theory of Atoms in Molecules: Recent Progress in Theory and Application*; Matta, C. J., Boyd, R. J., Eds.; Wiley-VCH: New York, 2007; Chapter VI.
- (202) Savin, A.; Silvi, B.; Colonna, F. *Can. J. Chem.* **1996**, *74*, 1088.
- (203) Silvi, B.; Fourré, I.; Alikhani, M. E. *Monatsh. Chem.* **2005**, *136*, 855.
- (204) Fuster, F.; Silvi, B. *Theor. Chem. Acc.* **2000**, *104*, 13.
- (205) Alikhani, M. E.; Fuster, F.; Silvi, B. *Struct. Chem.* **2005**, *16*, 203.
- (206) Grabowski, S. J. In *Quantum Theory of Atoms in Molecules: Recent Progress in Theory and Application*; Matta, C. J., Boyd, R. J., Eds.; Wiley-VCH: New York, 2007; Chapter 17, p 453.
- (207) Grabowski, S. J.; Sokalski, W. A.; Leszczynski, J. *Chem. Phys.* **2007**, *337*, 68.
- (208) Müller-Dethlefs, K.; Hobza, P. *Chem. Rev.* **2000**, *100*, 143.
- (209) Buckingham, A. D.; Fowler, P. W. *J. Chem. Phys.* **1983**, *79*, 6426.
- (210) Buckingham, A. D.; Fowler, P. W. *Can. J. Chem.* **1985**, *63*, 2018.
- (211) Buckingham, A. D.; Fowler, P. W.; Hutson, J. M. *Chem. Rev.* **1988**, *88*, 963.
- (212) Alkorta, I.; Elguero, J.; Mó, O.; Yáñez, M.; del Bene, J. E. *Mol. Phys.* **2004**, *102*, 2563.
- (213) Alkorta, I.; Elguero, J.; Mó, O.; Yáñez, M.; del Bene, J. E. *Chem. Phys. Lett.* **2002**, *411*, 411.
- (214) Sanz, P.; Alkorta, I.; Mó, O.; Yáñez, M.; Elguero, J. *Chem-PhysChem* **2007**, *8*, 1950.
- (215) Sanz, P.; Mó, O.; Yáñez, M.; Elguero, J. *Chem.-Eur. J.* **2008**, *14*, 4225.
- (216) Grabowski, S. J. *J. Phys. Org. Chem.* **2003**, *16*, 797.
- (217) Grabowski, S. J. *Pol. J. Chem.* **2007**, *81*, 799.
- (218) Grabowski, S. J. *J. Mol. Struct. (THEOCHEM)* **2007**, *811*, 61.
- (219) Grabowski, S. J. *J. Phys. Org. Chem.* **2008**, *21*, 694.
- (220) Reinhardt, L. A.; Sacksteder, K. A.; Cleland, W. W. *J. Am. Chem. Soc.* **1998**, *120*, 13366.
- (221) Huyskens, P.; Zeegers-Huyskens, T. *J. Chim. Phys.* **1964**, *61*, 84.
- (222) Meot-Ner (Mautner), M. *J. Am. Chem. Soc.* **1984**, *106*, 1257.
- (223) Malarski, Z.; Rospenk, M.; Sobczyk, L.; Grech, E. *J. Phys. Chem.* **1982**, *86*, 401.
- (224) Sobczyk, L. *Ber. Bunsen-Ges. Phys. Chem.* **1998**, *102*, 377.
- (225) Shan, S.; Loh, S.; Herschlag, D. *Science* **1996**, *272*, 97.
- (226) Shan, S.; Herschlag, D. *Proc. Natl. Acad. Sci. U.S.A.* **1996**, *93*, 14474.
- (227) McAllister, M. A. *Can. J. Chem.* **1997**, *75*, 1195.
- (228) Pan, Y.; McAllister, M. A. *J. Am. Chem. Soc.* **1998**, *120*, 166.
- (229) Chen, J. C.; McAllister, M. A.; Lee, J. K.; Houk, K. N. *J. Org. Chem.* **1998**, *63*, 4611.
- (230) Remer, R. C.; Jensen, J. H. *J. Phys. Chem. A* **2000**, *104*, 9266.
- (231) Gilli, P.; Pretto, L.; Bertolasi, V.; Gilli, G. *Acc. Chem. Res.* **2009**, *42*, 33.
- (232) Chandra, A. K.; Zeegers-Huyskens, T. *J. Mol. Struct. (THEOCHEM)* **2004**, *706*, 75.
- (233) Krokidis, X.; Vuilleumier, R.; Borgis, D.; Silvi, B. *Mol. Phys.* **1999**, *96*, 265.
- (234) Dahlke, E. E.; Orthmeyer, M. A.; Truhlar, D. G. *J. Phys. Chem. B* **2008**, *112*, 2372.
- (235) Panich, A. M. *Chem. Phys.* **1995**, *196*, 511.
- (236) Berski, S.; Latajka, Z. *Int. J. Quantum Chem.* **2002**, *90*, 1108.
- (237) Latajka, Z.; Bouteller, Y.; Scheiner, S. *Chem. Phys. Lett.* **1995**, *234*, 159.
- (238) Madsen, G. K. H.; Wilson, C.; Nymand, T.; McIntyre, G. J.; Larsen, F. K. *J. Phys. Chem. A* **1999**, *103*, 8684.
- (239) Chan, B.; Del Bene, J. E.; Radom, L. *J. Am. Chem. Soc.* **2007**, *129*, 12197.
- (240) Kita, Y.; Udagawa, T.; Tachikawa, M. *Chem. Lett.* **2009**, *38*, 1156.
- (241) Udagawa, F.; Tachikawa, M. *J. Chem. Phys.* **2006**, *125*, 244105.
- (242) Lau, Y. K.; Saluja, P. P. S.; Kebarle, P.; Alder, R. W. *J. Am. Chem. Soc.* **1978**, *100*, 7328.
- (243) Howard, S. T. *J. Am. Chem. Soc.* **1996**, *118*, 10269.
- (244) Reiter, S. A.; Nogai, S. D.; Karaghiosoff, K.; Schmidbaur, H. *J. Am. Chem. Soc.* **2004**, *126*, 15833.
- (245) Ozeryanskii, V. A.; Pozharskii, A. F.; Bieńko, A. J.; Sawka-Dobrowolska, W.; Sobczyk, L. *J. Phys. Chem. A* **2005**, *109*, 1637.
- (246) Hunt, S. W.; Higgins, K. J.; Craddock, M. B.; Brauer, C. S.; Leopold, K. R. *J. Am. Chem. Soc.* **2003**, *125*, 13850.
- (247) Kar, T.; Scheiner, S. *J. Chem. Phys.* **2003**, *119*, 1473.
- (248) Kar, T.; Scheiner, S. *J. Phys. Chem. A* **2004**, *108*, 9161.
- (249) Karpfen, A.; Kryachko, E. S. *J. Phys. Chem. A* **2003**, *118*, 10593.
- (250) DuPré, D. B.; Yappert, C. *J. Phys. Chem. A* **2002**, *106*, 567.
- (251) Parra, R. D.; Bulusu, S.; Zeng, X. C. *J. Chem. Phys.* **2003**, *118*, 3499.
- (252) Wieczorek, R.; Dannenberg, J. J. *J. Am. Chem. Soc.* **2003**, *125*, 8124.
- (253) Parra, R. D.; Ohlssen, J. *J. Phys. Chem. A* **2008**, *112*, 3492.
- (254) Mó, O.; Yáñez, M.; del Bene, J. E.; Alkorta, I.; Elguero, J. *ChemPhysChem* **2005**, *6*, 1411.
- (255) Kar, T.; Scheiner, S. *Int. J. Quantum Chem.* **2006**, *106*, 843.
- (256) Del Bene, J.; Pople, J. A. *Chem. Phys. Lett.* **1969**, *4*, 426.
- (257) Kollman, P. *J. Am. Chem. Soc.* **1977**, *99*, 4875.
- (258) Ziolkowski, M.; Grabowski, S. J.; Leszczynski, J. *J. Phys. Chem. A* **2006**, *110*, 6514.
- (259) Nishio, M.; Hirota, M.; Umezawa, Y. *The CH/π Interaction, Evidence, Nature, and Consequences*; Wiley-VCH: New York, 1998.
- (260) Kim, K. S.; Tarakeshwar, P.; Lee, J. Y. *Chem. Rev.* **2000**, *100*, 4145.
- (261) Stoyanov, E. S.; Hoffmann, S. P.; Kim, K.-C.; Tham, F. S.; Reed, C. A. *J. Am. Chem. Soc.* **2005**, *127*, 7664.
- (262) Scheiner, S.; Grabowski, S. J. *J. Mol. Struct.* **2002**, *615*, 209.
- (263) Domagała, M.; Grabowski, S. J. *Chem. Phys.* **2009**, *363*, 42.
- (264) Urban, J.; Roszak, S.; Leszczynski, J. *Chem. Phys. Lett.* **2001**, *346*, 512.
- (265) Szymczak, J. J.; Grabowski, S. J.; Roszak, S.; Leszczynski, J. *Chem. Phys. Lett.* **2004**, *393*, 81.
- (266) Grabowski, S. J.; Sokalski, W. A.; Leszczynski, J. *J. Phys. Chem. A* **2004**, *108*, 5823.
- (267) Grabowski, S. J.; Sokalski, W. A.; Leszczynski, J. *Chem. Phys. Lett.* **2006**, *432*, 33.
- (268) Grabowski, S. J. *J. Phys. Chem. A* **2007**, *111*, 3387.
- (269) Grabowski, S. J.; Sokalski, W. A.; Leszczynski, J. *J. Phys. Chem. A* **2004**, *108*, 1806.
- (270) Scheiner, S. *Annu. Rev. Phys. Chem.* **1994**, *45*, 23.
- (271) Grabowski, S. J. *J. Phys. Chem. A* **2007**, *111*, 13537.
- (272) Douberly, G. E.; Ricks, A. M.; Ticknor, B. W.; McKee, W. C.; Schleyer, P. v. R.; Duncan, M. A. *J. Phys. Chem. A* **2008**, *112*, 1897.
- (273) Grabowski, S. J. *Chem. Phys. Lett.* **2007**, *436*, 63.
- (274) Richardson, T. B.; Koetzle, T. F.; Crabtree, R. H. *Inorg. Chim. Acta* **1996**, *250*, 69.
- (275) Cramer, C. J.; Gladfelder, W. L. *Inorg. Chem.* **1997**, *36*, 5358.
- (276) Calhorda, M. J.; Costa, P. J. *CrystEngComm* **2002**, *4*, 368.
- (277) Custelcean, R.; Jackson, J. E. *Chem. Rev.* **2001**, *101*, 1963.
- (278) Epstein, L. M.; Shubina, E. S. *Coord. Chem. Rev.* **2002**, *231*, 165.
- (279) Remko, M. *Mol. Phys.* **1998**, *94*, 839.
- (280) Braga, D.; DeLeonardis, P.; Grepioni, F.; Tedesco, E.; Calhorda, M. J. *Inorg. Chem.* **1998**, *37*, 3337.



- (281) Kulkarni, S. A. *J. Phys. Chem. A* **1998**, *102*, 7704.
- (282) Kulkarni, S. A. *J. Phys. Chem. A* **1999**, *103*, 9330.
- (283) Kulkarni, S. A.; Srivastava, A. K. *J. Phys. Chem. A* **1999**, *103*, 2836.
- (284) Orlova, G.; Scheiner, S. *J. Phys. Chem.* **1998**, *102*, 260.
- (285) Orlova, G.; Scheiner, S. *J. Phys. Chem.* **1998**, *102*, 4813.
- (286) Grabowski, S. J. *Chem. Phys. Lett.* **1999**, *312*, 542.
- (287) Grabowski, S. J. *J. Phys. Chem. A* **2000**, *104*, 5551.
- (288) Cybulski, H.; Pecul, M.; Sadlej, J. *J. Chem. Phys.* **2003**, *119*, 5094.
- (289) Dumas, J. M.; Gomel, L.; Guérin, M. *Molecular Interactions Involving Organic Halides. The Chemistry of Functional Groups*, supplement D; Wiley: New York, 1983; pp 983–1020.
- (290) Legon, A. C. *Angew. Chem., Int. Ed.* **1999**, *38*, 2686.
- (291) Metrangolo, P.; Resnati, G. *Chem.-Eur. J.* **2001**, *7*, 2511.
- (292) Zordan, F.; Brammer, L.; Sherwood, P. *J. Am. Chem. Soc.* **2005**, *127*, 5979.
- (293) Grabowski, S. J.; Bilewicz, E. *Chem. Phys. Lett.* **2006**, *427*, 51.
- (294) Qian, W.; Krimm, S. *J. Phys. Chem. A* **2002**, *106*, 6628.
- (295) Rodziewicz, P.; Rutkowski, K. S.; Melikova, S. M.; Koll, A. *ChemPhysChem* **2005**, *6*, 1282.
- (296) Domagała, M.; Grabowski, S. J. *Chem. Phys.* **2010**, *367*, 1.
- (297) Alabugin, I. V.; Manoharan, M.; Peabody, S.; Weinhold, F. *J. Am. Chem. Soc.* **2003**, *125*, 5973.
- (298) Bent, H. A. *Chem. Rev.* **1961**, *61*, 275.